UNIVERSITÀ DEGLI STUDI DI TRIESTE

UNIVERSITÀ CA' FOSCARI DI VENEZIA

XXXIII CICLO DEL DOTTORATO DI RICERCA IN

CHIMICA

DOTTORATO IN COLLABORAZIONE CON ISTITUTO ITALIANO DI TECNOLOGIA

PROTECTIVE TREATMENTS IN FABRICS CONSERVATION

Settore scientifico-disciplinare: CHIM/12 - CHIMICA DELL'AMBIENTE E DEI BENI CULTURALI

DOTTORANDA
GIULIA MAZZON

COORDINATORE
PROF. ENZO ALESSIO

SUPERVISORI DI TESI
PROF. ELISABETTA ZENDRI
DR. ATHANASSIA ATHANASSIOU
DR. ILKER S. BAYER

ANNO ACCADEMICO 2019/2020

Acknowledgments

This thesis is the result of a fruitful collaboration, and it would not have been possible without the contribution and support of many people.

First of all, I would like to thank Professor Elisabetta Zendri for being my mentor, from my first day at Ca' Foscari, through my experiences abroad, to the end of my PhD. Nine years passed, and she was always an encouraging and enthusiastic supervisor. Thank you, Prof. Zendri, for being such an inspiring woman.

I would sincerely like to thank my supervisors Dr. Athanassia Athanassiou and Dr. Ilker Bayer for the kindness and support they always offered to me. Thank you for motivating me to work hard, to push my limits and to help me to become the scientist I am now.

I would love to thank my parents for their loving care, for reminding me where I come from, for being my roots. Thank you, mum and dad, for the patience in dealing with this nomad daughter.

I would love to thank my brother Antonio and my sister Anna with Giacomo with the new lovely entry Federico. Thank you for supporting me wherever I went, for the sincere chats and for the great time we spend together each and every time we meet.

Thanks to the grandmas, Elma and Carla, for always welcoming me with a cup of tea or a glass of gingerino. Thank you for the time spent sharing your memories about the past with me.

I would love to thank Leonardo, for his bravery, determination and love. Thank you, Leo, for encouraging me, and believing in what I do, from scientific research to ski touring. Also, thanks to sweet Federica, it is always wonderful receiving her long hugs.

Thanks to the girls who started this PhD adventure with me: Ana, Federica, Giulia, and Maria Elena. I was very lucky to meet you. You made my years better, here in Genova, but also in Andalusia, Sicily and Marche. We started all together, willing to share work and fun. We ended up being great friends. I am sure we will stay in touch, meet again and create new amazing memories.

Thanks to Margherita, who trusted me when I suggested her to apply for a PhD at IIT. I still believe you took the best decision! Thank you for creating with me the “conservation-team”, for dealing with me when I am stressed and for being always in when it’s time to have a break, cheer and chill. Of course, thanks to Alessio, the greatest fan of Margherita. He became to me a great friend and camper buddy.

Thanks to Gabriele and Giorgia, Luca Ph., Francesco, Edoardo, Luca R. for standing Generale Mazzon. It has been fun to hike to rifugio Pratorotondo with you, I promise. Dinners and aperitivi were less stressful, though.

I want to thank Dr. Muhammad Zahid, who welcomed me in IIT when I was just an inexperienced Master’s student, dedicated a lot of time introducing me to textiles technology and became a great friend.

Thanks to Dr. Marco Contardi. At first, your Sicilian slang was very difficult for me to understand, but once I got it, we could work (and eat) perfectly together.

Thanks to all friends I met in Smart Materials: Margherita, Amir, Anitha, Arek, Aurelio, Dagmara, Danila, Despina, Evie, Fabrizio, Gabriele, Giacomo, Giovanni, Giulia, Jasim, Laura, Lia, Maedeh, Marco, Maria Laura, Marta, Martina, Nga, Sara, Siew, Taimoor, Uttam and Valentina. It has been a pleasure and fun to work with you.

Thanks to all the friends I met in IIT: Roodra, Anthony, Arrfou, Alperen. Thanks for all the coffee breaks and the stories about different cultures.

Thanks to all the scientist and technicians who supported me during my PhD: Eleonora, Lara, Giorgio e Luca.

Thanks to my friends in Schio: Anna and Giacomo with Martino, Betty and Silva, Sara, Daniele, Marta and Elly. It is always lovely to come back home, get updated about each other’s lives, share chats and aperitivi.

Thanks to Angelina, Fernanda, Michael, Emma, Rachel, Jirka, Chiara, David, Febaio and the whole Erasmus family. We were in Malta in 2015 and, still, we are willing to stay in touch, travel together and spend quality time together.

Thanks to Cristian, Viviana and Chiara. You are my Italian family in Germany, and you strongly motivated me to start this PhD. Thanks to Elena, Simon, Georg and Michael for welcoming me at DBM in Bochum and enhancing my passion about conservation of cultural heritage.

A special thanks to Margherita Donnici. Even if we worked in two different institutes, we always supported and motivated each other, both about research and personal issues.

Thank you all relatives: Luli and Alberto, Giovanna and Leone, Marta, Stefano, Leonardo and Tommaso, Marco, Alessio, Lorenzo, Elena, Annalisa and Gianni, Cinzia and Dario. I know I can always rely on your support and love.

Thanks to my scout friends, who always welcomed me when I came back home.

Contents

Synopsis

The aim of this thesis is to develop protective formulations for the conservation of cellulose fabrics, using sustainable products and application techniques. In fact, a wide range of Cultural Heritage objects is composed of cellulose, such as painted canvases, costumes, tapestries, and design objects. The stability of these artworks is threatened by several factors, among which the most dangerous are the presence of water, biodeterioration and polluting agents.

This study was possible thanks to the collaboration of the Smart Materials group of Istituto Italiano di Tecnologia (IIT) in Genova, the research group of Dipartimento di Scienze Ambientali, Informatica e Statistica (DAIS) in Università Ca' Foscari of Venezia, and Univeristà degli Studi di Trieste.

Polymeric manufacturing and fabrics treatment know-how, in addition to several chemical, physical, and mechanical characterization techniques of Smart Materials group (IIT) were involved in the fruitful collaboration. Ca' Foscari team contributed with long-standing conservation science knowledge and awareness of the delicate equilibrium between conservation actions and safeguard of the original artifacts. Trieste University offered several educational events and opportunities for dialogue and confrontation.

The promising results obtained thanks to the collaboration are summarized and illustrated in this thesis, which has been structured in four chapters:

- The first part is dedicated to explain the extent presence of cellulose fabrics in Cultural Heritage, their components, structure and properties. After explaining the possible degradation phenomena, the chapter illustrates the protective treatments found in literature and explains the need for innovative conservation treatments. In this chapter, a summary of accelerated aging methods and tests for the durability of treatments is also reported. Finally, in light of all these elements, the scope of the research is illustrated in details.

- In the second part, a transparent, hydrophobic and breathable treatment for cotton fabric was developed from the synergic action of siloxane and polyurethane polymers. The preparation of the fluorine-free polymeric emulsion and its effective application is

described, as well as the effectiveness of the treatment, in terms of wettability, breathability, stability to aging, color change and mechanical properties.

- The third part focuses on a multifunctional coating, which aims to propose a double layer treatment able to protect the cellulose fabric from water-linked deterioration reactions, and to make it withstand oxidative aging environment. Cotton fabrics were developed using polycaprolactone added with butylated hydroxytoluene, and dimethylsiloxane. This resulted in an effective fluorine-free, environmental friendly approach.

- The last part summarizes the results obtained throughout this study and outlines possible future developments and applications of this research.

1. Introduction

Cellulosic materials have been widely used in past and present by artist and artisans for artistic production. The most well-known application of fabrics is probably the painted canvases, which were introduced around the XV century as an alternative to the more heavy and rigid painting on wood. Moreover, in museums and historical buildings a wide range of art containing textile components are present, *e.g.*, flags, curtains, tapestries, carpets, blankets, laces, macramé, liturgical clothes, costumes, uniforms, three-dimensional artworks. Fig. 1.1 shows an Italian example of excellence center, where numerous fabrics are conserved and restored: la Venaria Reale, with its royal palace and restauration center. Other than this, there are several conservation centers in Europe and in the world where fabrics are stored, controlled and conserved: Victoria and Albert museum (London, UK), The Royal Danish Academy of Fine Art (Copenhagen, DK), Textile Research Centre (Leiden, NL), KIK-IRPA (Brussels, BE), Centre de Recherche sur la Conservation (Paris, FR), SKR Verband and Abegg-Stiftung (Bern, CH), European Textile Academy (EU), The Conservation Center (Chicago, IL), The Metropolitan Museum of Art (New York), Canadian Conservation Institute (Ottawa, CA), just to name some.

Fig. 1.1. Venaria Reale, close to Torino, Italy. a) external view of the royal residence in Venaria Reale; b) a conservation treatment performed onto fabric at "Centro Conservazione e Restauro dei Beni Culturali" La Venaria Reale; c) ancient costumes conserved at the royal residence; d) original and well conserved furniture details, fabrics are present in painted canvases, curtains, carpets and armchairs.

The study of cellulosic materials, their composition and degradation is of fundamental importance for conservation scientists and restores all over the world, to prevent environmental induced deterioration [1]., [2]. For this reasons, the present chapter is a short review, which aims firstly at describing the cellulose fabrics composition, structure and intrinsic properties. Secondly, the chapter is meant to summarize the main fabrics' weaknesses and possible degradation forms due to environmental factors and/or wrong storing conditions. Finally, the chapter presents the state of the art of conservation treatments and accelerating aging methodologies commonly used by conservation scientists. From this introduction, the needs which are still unsatisfied and the problems which are still unsolved will emerge. Later, in Chapters 2 and Chapters 3, practical solutions to respond to respond to these needs will be proposed.

1.1 Fabric components, structure and properties

Cotton is a vegetal fiber obtained from plants. The cotton mostly used in textiles comes from plant species *Hirsutum, Barbadense, Arboreum* and *Herbaceum* of the *Malvaceae* family. The cotton structure was investigated for nearly one century until its multilayered and hierarchical structure was made clear. Atoms of carbon, hydrogen and oxygen combine to form the glucose units, which make up the long ribbon-like chain of cellulose. The cellulose molecule is composed of about three thousands 1,4-D-glucopyranose structural units. The cellulose chains are build up into sheets, which are held together by hydrogen bonding rising between the chains. The sheets are packed together and thanks to Van der Waals forces, they form microfibrils, which in turn form fibrils, as shown in

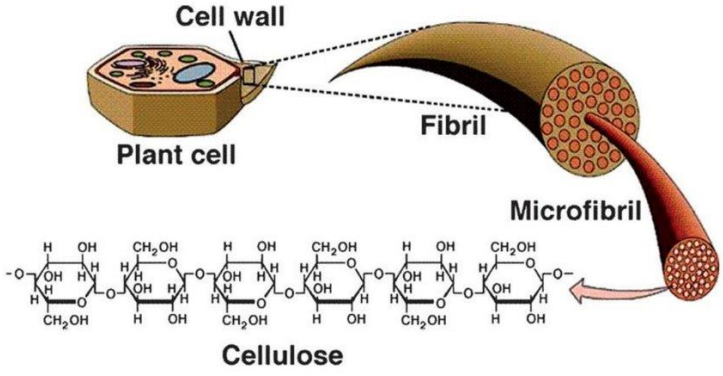

Fig. 1.2.

Fig. 1.2. Cotton cell structure [3].

The fibrillary structure of the cotton fibres further consists of an outer cuticle, a primary wall, a secondary wall and a lumen, as represented in Fig. 1.3. The cuticle is the outside skin providing protection against chemicals and degrading agents. It is usually removed by kier boiling process (treatment with 1% NaOH solution at 100 °C and atmospheric pressure for 24 hours) and bleaching (oxidizing agents like H_2O_2) so that cotton becomes more absorbent and more receptive to dyes. Consequently, it becomes also more susceptible to attack by degradation agents and more vulnerable. Under an optical microscope, a cotton fiber looks like a twisted ribbon, where the twists are called convolutions. There are about 60 convolutions/cm. The typical cross-section view of the fiber exhibit a kidney-bean shape. This shape originates after evaporation of the aqueous proteins, sugars, and minerals, causing a pressure differential and consequent collapse of the hollow lumen canal.

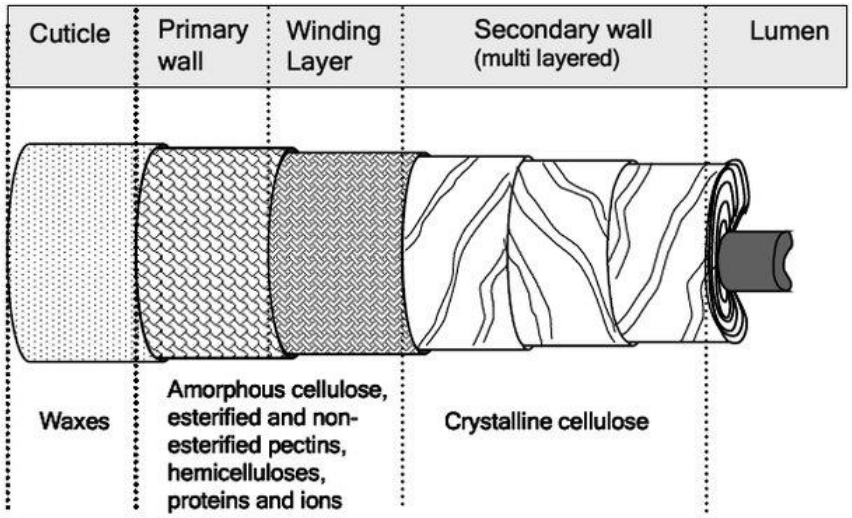

Fig. 1.3. Cotton fiber fibrillar structure [4].

On the molecular level, cellulose, the primary and most stable component of cotton fibers, has properties imposed by its structure, which creates amorphous and crystalline regions in fibrils, as represented in

Fig. 1.4. The amorphous regions are random, flexible and water accessible, while the crystalline regions are ordered, rigid, inert and less permeable to water [5]. The other components of cotton

are hemicelluloses, lignin, some non-cellulose components surrounding the cellulose core and other minor components, which may include bound water, residual protein, waxes and small amounts of inorganic materials [6].

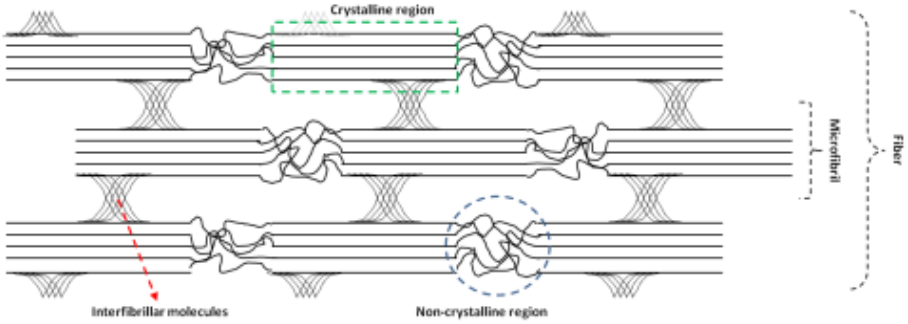

Fig. 1.4. Part of cellulose fiber showing crystalline and non-crystalline regions [7].

The crystallinity index (CI) is commonly investigated in order to study cellulose crystalline composition and to interpret changes in cellulose structure after physicochemical and biological treatments. CI is measured by several techniques, including X-ray Diffraction (XRD), solid-state ^{13}C Nuclear Magnetic Resonance (NMR) spectroscopy, infrared (IR) and Raman spectroscopy. The XRD method is more efficient and consists of separating amorphous and crystalline contributions from the diffraction spectrum. Fig. 1.5 shows the CI calculation via XRD spectra deconvolution. The five crystalline peaks and the amorphous cellulose peak were extracted by a curve-fitting process from the diffraction intensity profiles. The broad peak at approximately 21.5° was the one assigned to the amorphous contribution. The CI can be calculated with the following formula:

Equation 1
$$CI = \frac{Crystalline\ area}{Total\ Area} \times 100$$

In general, a fully mature cotton fiber consists ~73% crystalline and ~27% amorphous regions.

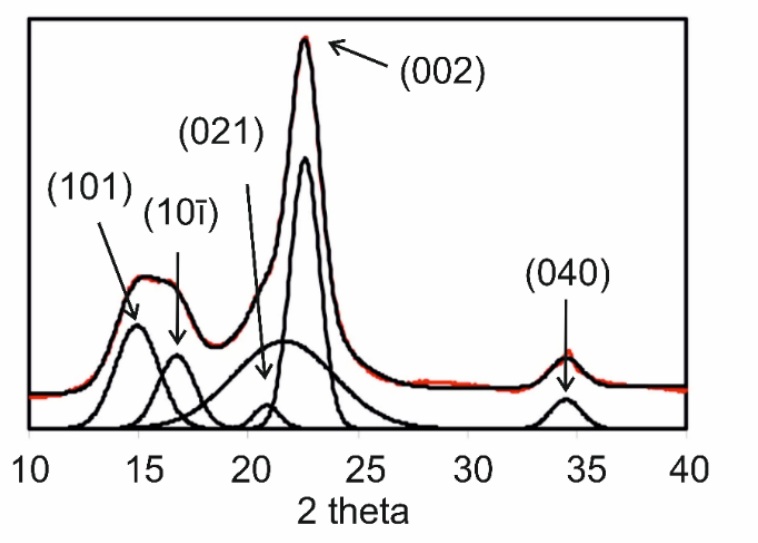

Fig. 1.5. X-ray diffraction spectra of cellulose illustrating the peak deconvolution method commonly used for the calculation of CI [8].

Another important parameter to study cellulose is the degree of polymerization, or DP. It is the number of monomeric units in a polymer. The DP can be calculated as the ratio of the average molecular weight of a polymer (W_p) and molecular weight of the repeating unit (W_m):

Equation 2 $$DP = \frac{W_p}{W_m}$$

Table 1.1. Physical and Mechanical Properties of cotton fibers [6].

Physical and Mechanical Properties	Conditions	Values
Tenacity Grams/denier d/den=(N/tex) x 11.33	Dry	3.5-4.0
	Wet	4.5-5.0
Elongation at break (%)	Standard: 65%RH 21°C	3-7
	Wet	9.5
Moisture regain (%)	Standard: 65%RH 21°C	7-11
Elastic recovery (%)	Recovery from 3% stretch	75
Work of rupture (g-wt/tex)	-	1.52
Initial modulus (g-wt/tex)	-	740

Generally, a higher DP (≥ 10000) is desired for better mechanical properties. In Table 1.1 the typical values for mechanical properties of cotton are reported. Cotton fibers typically exhibit a high modulus with no yield point. Under applied stress, the fibers resist strain linearly up to the breaking point. From Table 1.1, the cotton fibers can be extended from 3 to 7% of their original length before the breaking point. The recovery property after an extension is poor. A release of the stress at any point below the breaking extension leaves the fibers in a state of permanent deformation. The wrinkling of cotton fabrics that result from permanent deformation can be partially alleviated by placing the textile in a humid environment to allow the fibers to relax. The cotton fibers are brittle and a little amount of work is required for their rupture. A careful selection of yarn and fabric characteristics can compensate these limitations. This can be demonstrated by the study of stress-strain curves and the calculation of Elongation at break and Young's modulus [9], whose formula is shown in Fig. 1.6.

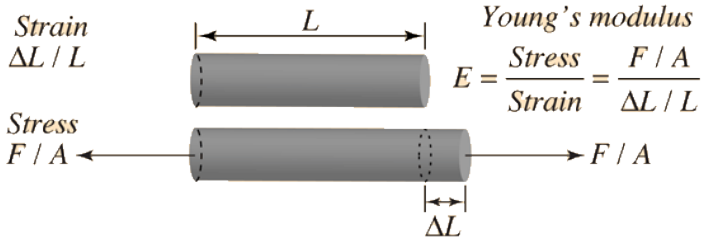

Fig. 1.6. Young's modulus formula and diagram of involved forces [10].

Fabrics are usually composed of knitted or woven yarns that are obtained from fiber spinning. Spinning consists of assembling several parallel fibers and twisting them all together, as shown in Fig. 1.7a. High twisting gives higher resistance to the thread and therefore to the fabric as well. In

this way, fibers undergo torsion and tension, so that it is possible to weave and knit them. More specifically, the threads of a canvas are composed of a various number of yarns. The fabric can be defined as a weaving of warp and weft as it is shown in Fig. 1.7b. The resultant plot is a geometrical distribution, whose resistance is based on the regular distribution of the stress on single yarns. The threads or yarns in the warp have their higher curvature and lower stiffness with respect to those in the weft. Finally, the fabric can be found in different weave patterns and weights (*e.g.*, plain-wave, twill-wave, satin-wave)

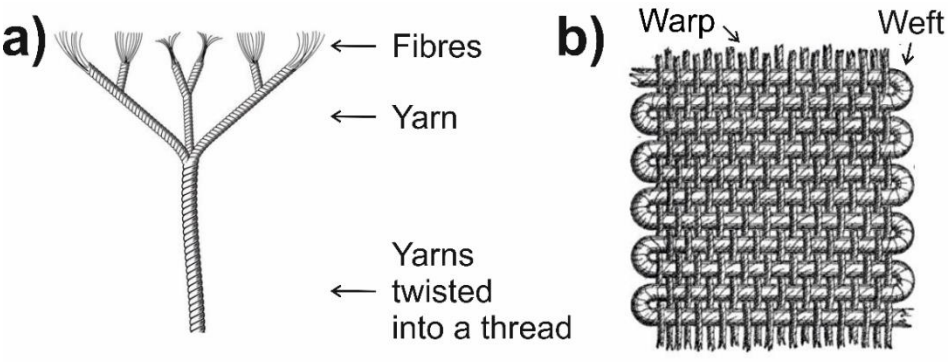

Fig. 1.7. A) shows the structure of a thread made of twisted yarns, made of fibers, b) fabric structure made of warp and weft.

1.2 Degradation of cotton fabrics

Cellulosic fabrics are prone to decay in time due to their chemical composition (see Fig. 1.8) and physical structure and to the environmental conditions, which they are exposed to. Similarly to other organic materials, cotton is likely to lose chemical and structural integrity when exposed to chemical pollutants, microorganisms, relative humidity, ultraviolet radiation and temperature changes. Several intrinsic factors are also relevant such as acidity, presence of fillers, pigments, dyes and impurities [11]. Environmental influences and intrinsic factors can overall cause several degradation processes at the same time: oxidation, hydrolysis, thermal degradation, scission of macromolecular chains and breaking of intramolecular bonds [12].

In many cases, the degradation of the fabric structure becomes evident when the degradation phenomena are already visible, that is when the loss in mechanical structure, embrittlement, pulverization, detachments and color changes are present. In fact, many artifacts undergo natural aging processes for prolonged periods, and when they arrive in the hands of conservation scientists

and restorers, they are already in poor conditions. This makes conservation treatments very difficult to take place. This should also be a motivation for promoting preventive conservation.

The following sections shortly describe the processes involved in cellulose materials deterioration.

1.2.1 Damages due to radiation: photochemical degradation

Cultural heritage fabrics are often exposed to radiation action for the sake of public fruition and visitor amusement. Illumination is connected with degradation because light often provides the activation energy necessary to activate detrimental chemical reactions [13]. The degradation phenomena are proportional to the radiation's intensity and the exposition period, while they are inversely proportional to the wavelength. Specifically, objects directly exposed to solar/lamp radiation risk to undergo damages due to heat and UV radiation or light. The radiation may cause chemical changes in materials (*e.g.*, netting or cleavage of polymer chains) on the one hand, while, on the other hand, it can exhibit thermal effects [14].

Photolysis of macromolecules, such as those of cellulose, will occur only when molecules are exposed to the light of sufficiently high energy content. This radiation will necessarily have to be capable of breaking the intramolecular chemical bonds. In cellulose, the rupture of the chain molecule is fundamentally possible, and it involves single bonds of either C-C or C-O. The energy required for both these changes was calculated to be approximately 80-90 kcal/mol [15].

Moreover, the same ultraviolet radiation was demonstrated to have a more significant effect on the degradation of cotton exposed in the presence of oxygen. Oxygen, present as 21% in air, promotes organic substrates' photooxidation in the formation, reaction and decomposition of peroxides and hydroperoxides. Studies have shown that the term "auto-oxidation" applies whereby oxygen uptake increases with time; and when light is present, the mechanism of degradation is through the initiation, propagation and termination of hydroperoxides [6]. To conclude, particularly dangerous is the UV solar radiation (100-400 nm), which is much more powerful than the radiation of incandescent lamps. On the other hand, incandescent lamps release thermal energy, which consequently causes problems due to environment overheating, as explained in the following section.

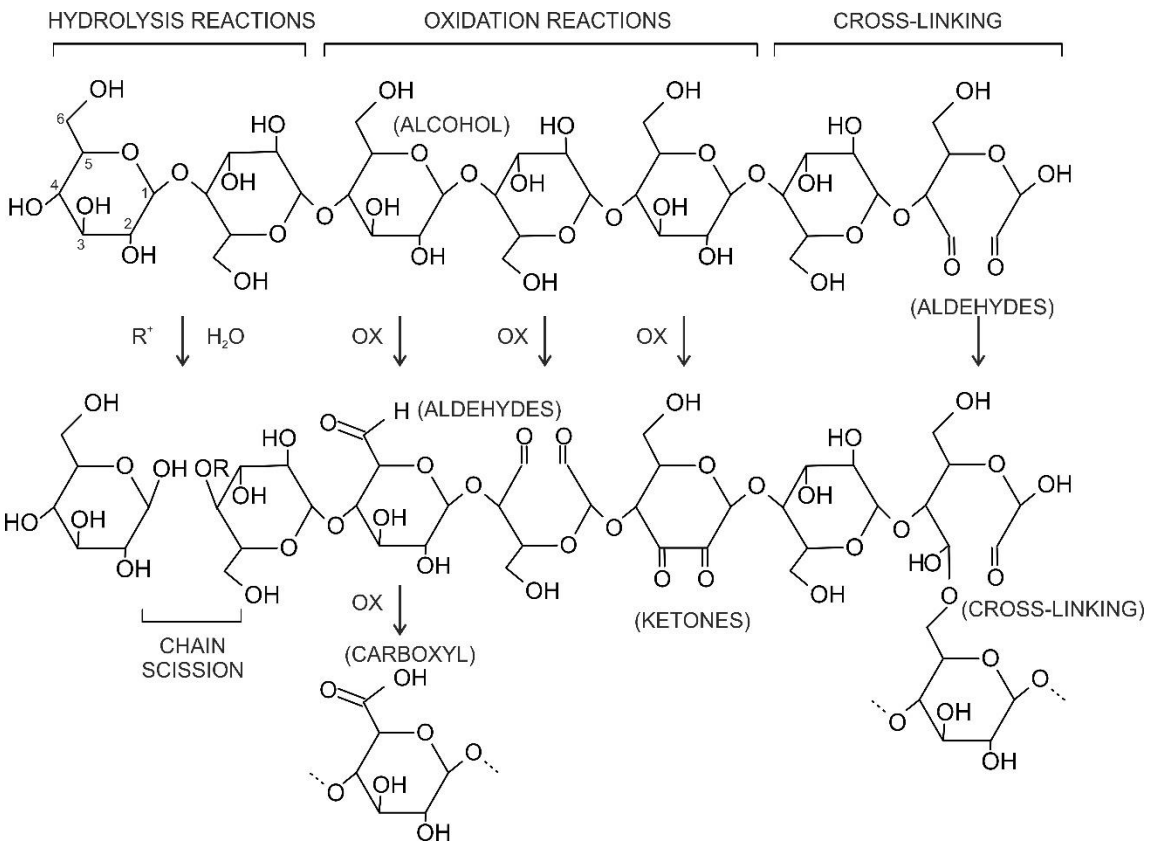

Fig. 1.8 Main degradation reactions of cellulose.

1.2.2 Damages due to temperature

Temperature variations are among the most influential climatic factors with consequences for cultural heritage damage. Several daily/seasonal temperature cycles can occur, depending on the conservation environment (*e.g.*, outdoor, indoor, controlled climate, proximity to heating sources in winter, fans and air conditioning during summer). The reaction time and type of the chemical reaction in cellulose depend on the temperature variations, and their study is mostly associated with humidity exposure time.

Very often, the degradation of cellulose by temperature causes the cleavage of the cellulose chain. The degradation can be quantified through the measurement of the diminishing degree of polymerization (DP). Seves et al. [16] measured losses of DP from 2000 to 875 for canvases thermally aged for 700 hours at 105 °C. This degradation can be somehow representative of the natural aging process. In fact Oriola et al. [17] found the DP of original canvases from old linings to be around 600-700.

1.2.3 Damages due to humidity

Water, in all of its phases, can influence cultural heritage materials and, especially, when acting simultaneously with temperature or other factors, can lead to the deterioration or even completely destroy cellulosic materials [18]. The most dangerous form of water for fabrics is not only the fluid phase, which in museums is mostly due to condensation but mainly the water vapor, which can catalyze reactions, carry or dissolve polluting substances, induce electrochemical reactions that can compromise yarns' mechanical properties and create the ideal conditions for encouraging biological growth.

Cellulose is hydrophilic by nature, and it can easily absorb water molecules, thanks to the presence of OH groups. These OH groups are exposed or accessible to water, especially in the amorphous areas. Instead, the highly crystalline regions of the cellulose are virtually inaccessible to water molecules. Because of hygroscopic nature [19] [20]., water molecules temporarily occupy the space between the microfibrils and this result in cellulose fibers to swell. This phenomenon is known as "temporary microcapillary network" [21].

Especially the fluctuation of humidity, from high level to low level and vice versa, is extremely dangerous for cellulosic and composite materials. In fact, in cellulosic fibers, humidity absorption and humidity loss cause swelling and shrinkage, respectively. These phenomena compromise the dimensional stability and mechanical properties of the fabric.

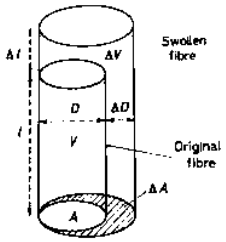

Fig. 1.9 Changes in fiber dimension in swelling [22].

The fibers swelling can be expressed in terms of transversal diameter swelling (S_D)

Equation 3 $$S_D = \frac{\Delta D}{D}$$

where ΔD is fractional increase in diameter and D is initial diameter of the cellulose fiber. Note that moisture-absorbing fibers show a significant transversal swelling but a minimum axial swelling, as shown in Fig. 1.9, so that the swelling anisotropy is high. Moreover, the predominant transversal swelling usually results in a shrinkage of twisted or interlaced structures. This phenomenon depends on the number of torsions of the thread helicoidal structure, as shown in Fig. 1.10c. When the canvas is free from frameworks or any tensioning structure, the swelling results in threads shortening proportional to the rate of twisting. This phenomenon is schematically represented in Fig. 1.10b and c [23].

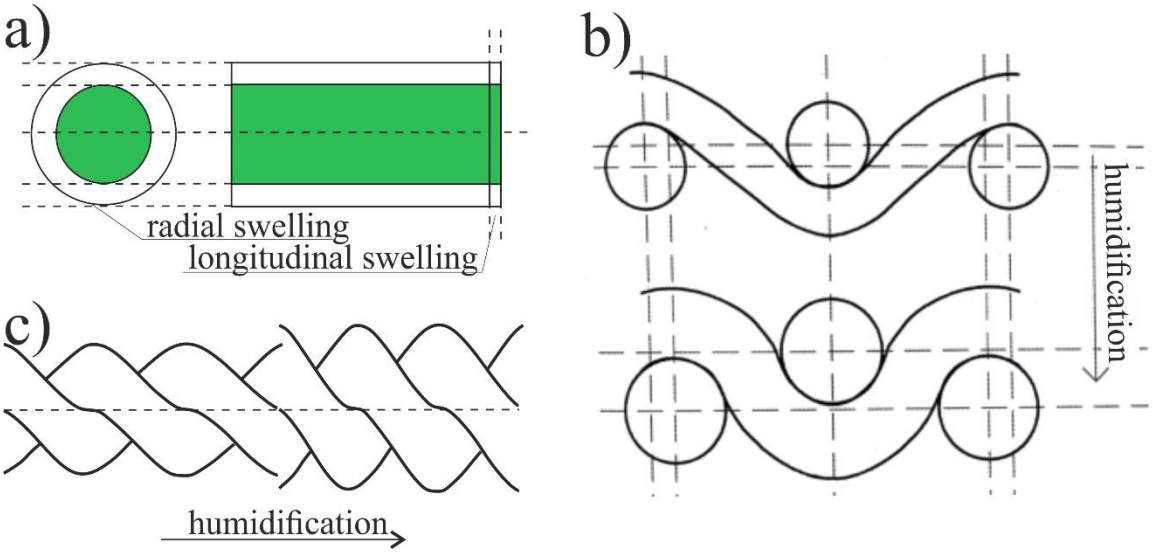

Fig. 1.10.a) Swelling of a cellulosic cylindrical element, b) Shrinkage and thickening of the canvas; reduction of space between threads, c) Radial swelling contribution to the shortening of the thread.

Thus, significant and rapid humidity changes can cause dangerous tensions, especially if the artwork is large, heavy and composed of different kinds of fibers/materials. For example, Mecklenburg [24] demonstrated the behavior of a linen canvas at different humidity. Fig. 1.11a shows the different behaviors of the same canvas in warp direction, at humidity ranging from 17% to 100%.

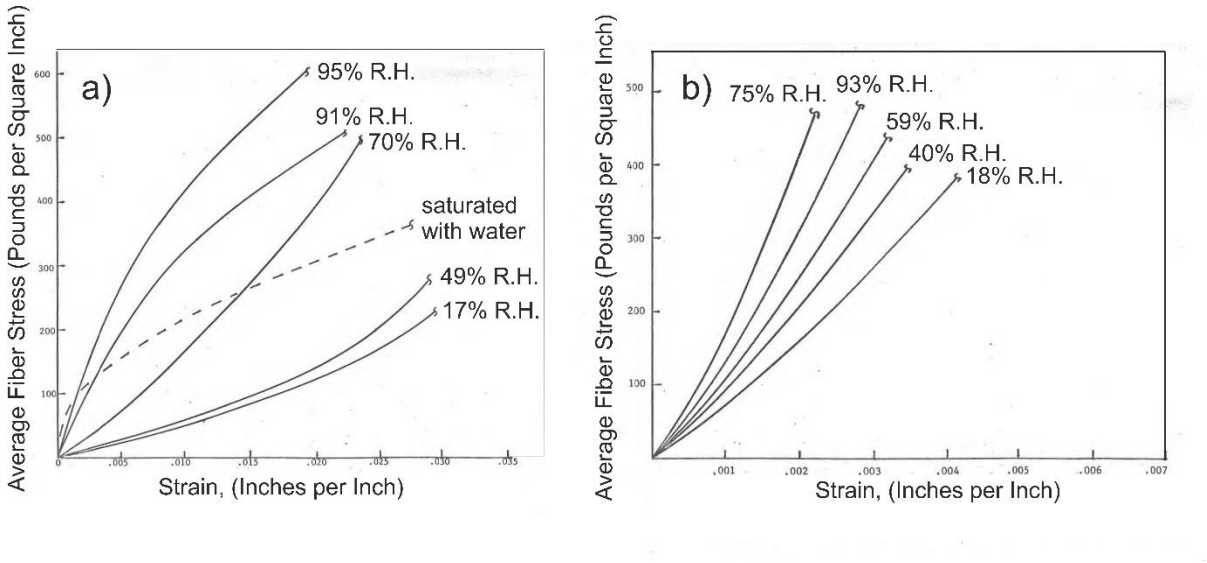

Fig. 1.11. Mecklenburg [24] a) effect of relative humidity on stress-strain properties of linen in warp direction, medium weight, 32 Yarns Per Inch, at 71°F; b) effect of relative humidity on stress-strain properties of linen in weft direction, medium weight, 30 Yarns Per Inch, at 71°F.

At low strain the behavior results from straightening crimped yarns. The first part of the curve is the crimp removal zone. After crimp removal the actual yarn behavior is analyzed. Increased moisture influences the modulus by making the crimp more difficult to be removed and the modulus increased. There is a change in the trend at very high moisture content, when water appears to lubricate the fibers so that slippage occurs, and a lower yarn modulus results *i.e.*, more elongation results from less stress. Fig. 1.11b shows that the same sample analyzed in weft direction had very different behavior. Overall Mecklenburg stated that painting having high modulus undergo small dimensional changes; paintings with generally low modulus undergo fairly large dimensional changes. In a pained canvas, dimensional changes would result in fissures on the painted surface, which are called “craquelure”.

Moreover, there is another factor which plays a fundamental role in the conservation of objects: air flow. It plays an important role by bringing or removing humidity by enhancing or diminishing the chemical action of liquids and gases on objects. The flow generated by ventilation can promote pollutant deposition, biological colonization, drying-wetting cycles and it has the dangerous ability to spread water, dust and gases to the object, but it can also conduct them away in certain conditions.

Concluding, in many cases, relatively high but stable moisture content in the fabric is less harmful than fluctuating lower moisture content. In some cases, drying of permanently humid materials may be very dangerous (*e.g.*, loss of mechanical properties due to a quick loss of freely bound water). For these reasons, wetting-drying cycles should be substantially reduced to the minimum necessary extent during conservation treatments. In Fig. 1.12, the recommended parameters for each material are reported.

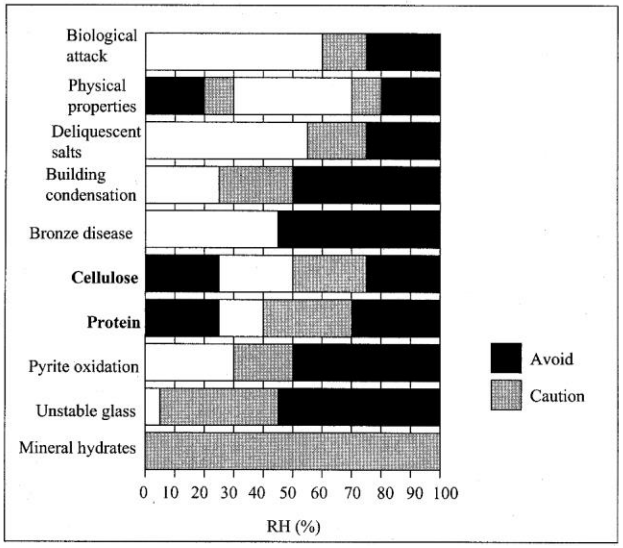

Fig. 1.12. Ranges of relative humidity suggested by consideration of various factors [25]. The ranges of relative humidity are suggested for various materials and situations. According to Erhardt and Mecklenburg [26], "no one RH is ideal, and any value chosen must be a compromise."

Of course, the museum environment should guarantee suitable conditions for each material or find the best compromise to conserve all collection objects. This would be beneficial to avoid the deterioration phenomena described in this paragraphs and illustrated in Fig. 1.8.

1.2.4 Reactions with pollutants

For museum objects, the magnitude of the pollution effect is strictly related to the type and concentration of pollutants to which they are exposed. The exposure is a consequence of the location and characteristics of the emitting sources and the weather conditions surrounding the object. However, control options for natural pollutants emissions are limited, so the scientific community is especially focusing on the identification and control of anthropogenic emissions.

Most of the pollutants present in the atmosphere (SO_2, NOx, and CO_2) can react in presence of solar radiation and water to produce acids [27], [28]. The presence of these acids can catalyze the acidic hydrolysis [29], [30], [31], [32], [33] or the acidic oxidation [34], [35], [36] of the cellulosic textiles.

Ozone is a strong oxidizing agent and it is generated by the action of ultraviolet radiation on oxygen. As an oxidant of organic material, ozone can react with water to form hydrogen peroxide, a powerful oxidizing material

Equation 4 $$O_3 + H_2O + hv \rightarrow HOOH + O_2$$

Hydrogen peroxide can contribute to the oxidation of cellulose, hence to its degradation and embrittlement.

In this paragraph the formation of the pollutants is not described, since it is closely related to the environmental condition of the conservation environment. Rather, the oxidized cellulose, generated by the interaction of cotton and the above-mentioned pollutants, is reported in the next section.

In fact, pollutants can activate the oxidation by reacting with the large number of hydroxyl groups present in the highly crystalline cellulose of cotton, and resulting in the formation of carbonyl, ketone, and carboxylic acid products and possible chain degradation [37], as shown in Fig. 1.8.. The rise of carbonyl groups in aged samples can be verified through Fourier-transform infrared (FTIR) spectroscopy, by comparing those spectra with spectra of pristine cotton or unaged cellulose [38]. As shown in Fig. 1.13, the formation of oxidized cellulose is proven in literature by FTIR spectra from ancient samples. These spectra show the appearance of peaks associated with the carbonyl area (1600-1750 cm^{-1}).

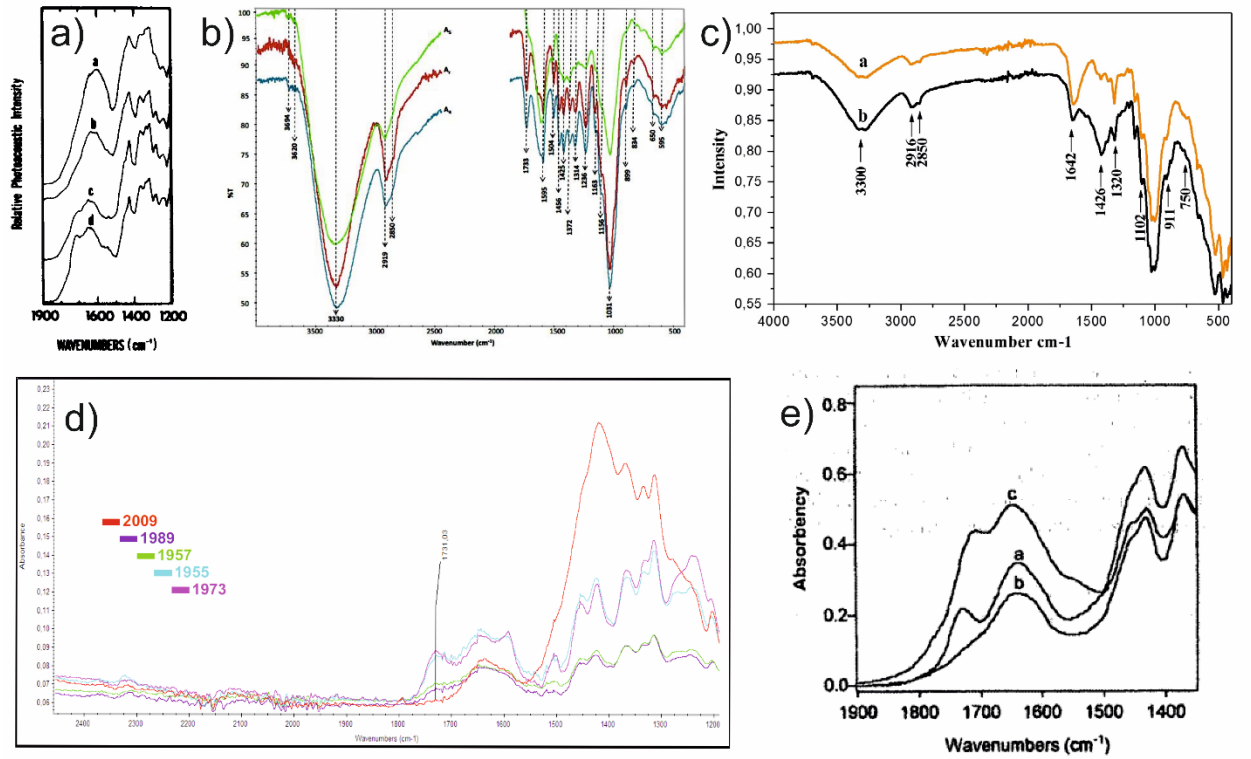

Fig. 1.13. FTIR spectra of oxidized cellulose from literature. a) Cardamone et al. [37], b) Boukir et al. [39], c) Hajji et al. [11], d) Librando et al. [40], e) Ferrero et al. [14]

Fig. 1.13a shows textile cotton fibers analyzed by Cardamone et al. [37] and dated (a) A.D. 1325-1400, (b) A.D. 900-1100, (c) A.D. 1250-1300, (d) A.D.1125-1300. All samples were naturally aged cotton fibers from archeological sites in the southwest United States. They exhibited pronounced absorption bands in the C=O stretch region of the infrared spectrum as proof of aging. Fig. 1.13b reports the spectra of (Ar) recent, (A4) 16thcentur and (A5) 15th century cotton fibers (Boukir et al.). Especially in the sample dated 15th century, the C=O peak is more evident. Spectra represented in Fig. 1.13c were taken by Hajji et al. [11] from a 150-year-old manuscript (a) before and (b) after restoration. The carbonyl peak is visible before restoration and decreased in intensity after restoration. Fig. 1.13d shows cellulose paper dated A.D. 2009, 1989, 1957, 1955, and 1973. Librando et al. [40] noted a correlation between the age of the samples and the intensity of the peaks of the carbonyl groups. Finally, in Fig. 1.13e, Ferrero et al. [14] reported the spectra of (a) modern bleached linen fabric, (b) linen sample dated 1200 B.C. and (c) linen sample dated 2500 BC. The authors attribute the peak at 1648 cm^{-1} to the carboxyl group.

Cardamone [6] compared several articles analyzing ancient cotton samples and concluded that long-time natural aging not only shortened cellulose chains, but also created IR absorptions representing oxidative transformations of the native reducing end aldehyde groups to acid carboxyl groups.

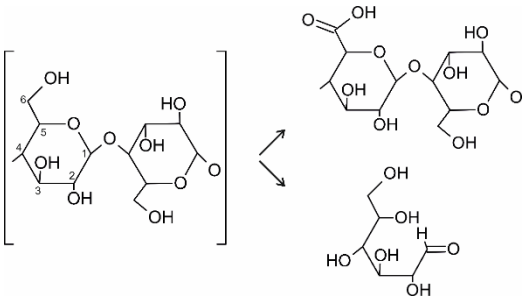

Fig. 1.14. The hypothesis of degradation forms of cellulose due to oxidation processes.

In summary, the oxidation of the OH groups of cellulose causes the formation of ketones, aldehydes and carboxylic groups, which is verified by the presence of C=O bands in the aged cellulose spectra [38]. A hypothesis of cellulosic degradation forms is reported in Fig. 1.14. Oxidation is more likely to happen on C_6, where a carboxyl acid group appears, or on C_1, when there is the breakage of the cellulose chain, with a consequent loss of polymerization degree and mechanical properties of the fabric. In fact, oxidative degradation of the cellulose polymer is often associated with the loss of fiber tensile strength. In conclusion, protecting cellulosic fibers from oxidative conditions [41] is a key factor to preserve fabric crystallinity, hence its mechanical properties and stability.

1.2.5 Biodeterioration by pests and fungi

The main pests affecting textiles included carpet beetle (Anthrenus verbasci), two spot carpet beetle (Attagenus Pellio), case-bearing clothes moth (Tinea pellionella) as well as other varieties of moth, *e.g.* white shouldered house moth (Endrosis sarcitrella) [42]. One of the main difficulties, especially in large collections, is the impossibility to define with certainty which object are infested and which are not. Therefore, conservators developed disinfection methods, which can be applied in large scale collections and in situ. The insects' attacks can be defeated, without using chemicals, mainly by freezing [42] or anoxic treatment of the fabric [43].

The first method consists in drying and ideally stabilizing the fabric at 50-60% relative humidity (RH), wrapping it in plastic, placing it at -29/-30°C for sixty hours, letting it unfreeze and unwrapping it. Freezing can also be performed by freezing twice to -18/-20°C. Most textiles can withstand freezing safely, except for objects containing textiles in combination with other materials, objects that are desiccated or seriously degraded, some painted textiles or certain mixed media objects containing adhesives.

The second method [43][44] consists in removing the O_2 from the atmosphere surrounding the objects, in order to interrupt the life cycle of the aerobic organisms. First, the object is treated with an oxygen scavenger (*e.g.* Ageless®) in heat-sealed bags. The bag is then filled with nitrogen to minimize the amount of oxygen to be scavenged, thus reducing the heat given off by the sachets, which could affect the results. The bag is then double sealed and enclosed in a second polyethene heat-sealed bag for security reasons. The RH in the bag is kept constant by silica gel granules conditioned at around 50%. The oxygen concentration is monitored (*e.g.*, with Ageless Eye® indicator tablets), and the RH is monitored with humidity indicator strips. The fabric is treated for three weeks and possibly stored in dark conditions to avoid effects from light.

Moreover, cellulosic fabrics are very sensitive to fungal growth[12], since they are very hygroscopic. The proliferation of fungi is also promoted by the presence of light and oxygen. The presence of UV radiation causes oxidation and breaking of the intermolecular bonds in the amorphous regions of the fibers and enables the penetration of fungi into the lumen where they can proliferate. The spreading of fungi is more prominent at the cracks and the cut-off cotton fibers. Spores reach a fiber lumen via fissures in the wall and then germinating hyphae grow into and form mycelium within the lumen. The mycelium grows from the inside towards the fiber wall, secretes cellulolytic enzymes that cause its destruction, and then begins to sporulate on the outer surface of the fiber [45].

Among the fungi that attack historical fabrics are cellulolytic, proteolytic and lipolytic fungi [46]. Zotti et al. performed mycological and FTIR analysis of biotic foxing on paper substrates [47]. Kavkler et al. [48] analyzed the deterioration of cotton fibers caused by selected strains of fungal species from historical cotton textiles. They state that not all of those fungal species were dangerous to cotton fibers but they all caused visible changes that could lead to disintegration of

the objects. Since fungi attack mainly pre-degraded fibers, the conservation environment (*e.g.*, humidity, temperature UV, aeration system) is of crucial importance.

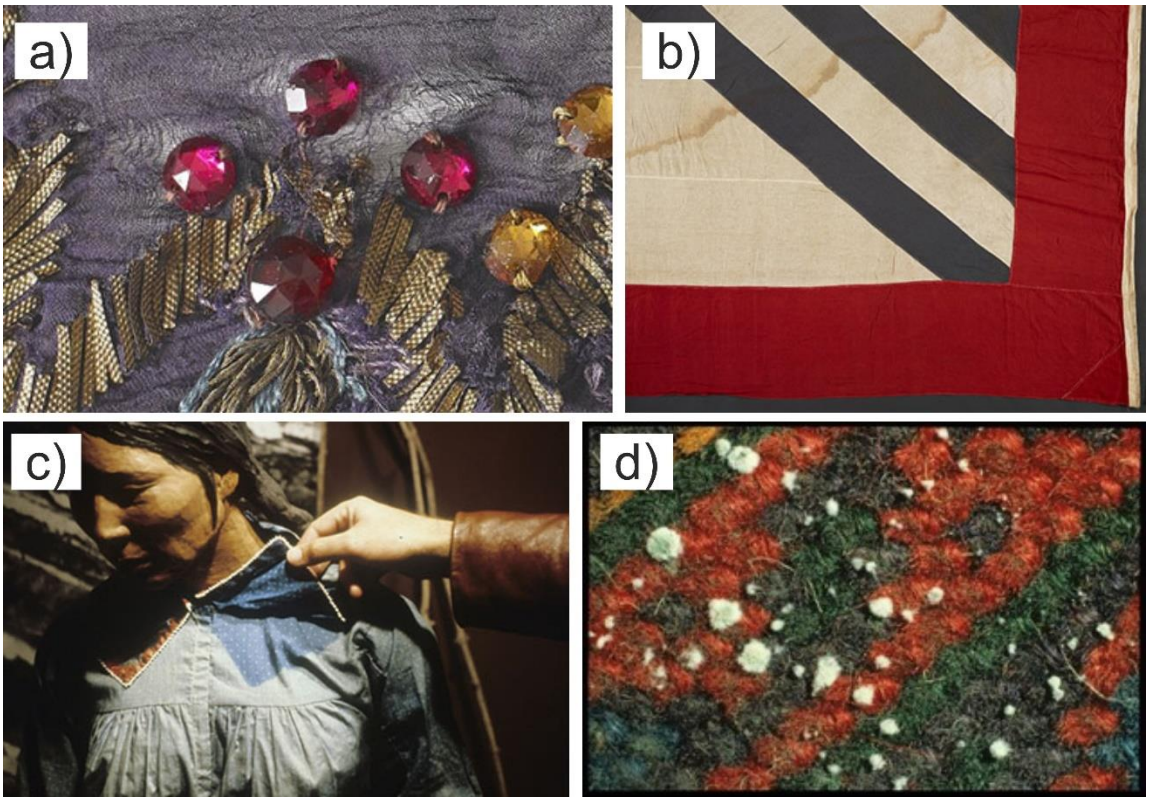

Fig. 1.15. Pictures of © Government of Canada, Canadian Conservation Institute [49]. A) Mechanical-, b) humidity-, c) light- d) mold-linked degradation forms are shown.

Emblematic are the degradation cases reported by Canadian Conservation Institute in Fig. 1.15, where conservation acts were required. Fig. 1.15a) shows a delicate crepe fabric which became distorted and torn around red glass faux jewels due to the weight of the ornamentation. Fig. 1.15b) shows how tide lines have formed on a textile, after drying form accidental wetting. Fig. 1.15c) shows the fading of a blue-dyed fabric due to exposure to light while on display. Fig. 1.15d) is a case of velvety growth of mold on a textile. Conservation acts need to be performed in order to guarantee a long life to these objects.

1.3 Conservation of cotton fabrics: state of the art

The previous section described the intrinsic properties of fabrics, their behavior in presence of different conservation conditions, pollutants and aging factors. The present section deals with conservation actions, which can be taken by restorers in order to guarantee to the piece of art the longest possible conservation. Usually, the first essential conservation action is cleaning, and lot of literature can be found about wet cleaning [50], [51], dry cleaning [52], [53] and laser cleaning [54], [55], [56].

Rather, this section illustrates protection and consolidation treatments, which normally take place after the preliminary cleaning of the object [49].

1.3.1 Protectives polymers for cotton fabrics

Several natural and synthetic products were used by conservation scientists and restorers onto cotton textiles in an attempt to prolong the life of valuable historical fabrics and to hand them down to the next generations.

Consolidation, adhesion, hydrophobicity and UV protection are among the most desired properties to achieve for protection of the fabric. Not only the treatments should confer the desired properties to the fabrics, but they should also fit with the Cultural Heritage conservation requirements. This means that, when applied on the object, the polymers should not cause any visible color variation and should be chemically stable in time, so to maintain its original appearance and to prolong the lifetime of the object.

There are several possible treatments which can be performed on cotton textiles. These treatments are chosen by conservators according to the needs of the artwork, the availability of the products, the cost of the treatment and health issues. Especially in the past, commercial products coming from other research fields were applied to the artworks. If the artwork could benefit from the treatment, the restorers would spread the voice and the product would become of common use. Customization of the commercial product is performed by restorers, according to their experience. For these reasons, a lot of information about conservation treatments is not easily reachable in academic journals and papers as they are rather owned by expert artisans and headmasters.

In Table 1.2, the information available in the literature about conservation treatments on cellulosic substrates and/or fashion clothes are reported. The table is structured so that products are gathered according to their chemical composition, from which it appears that the main categories of products are acrylates, acetates, fluoropolymers, silicones and some nano-compounds. The tests performed to evaluate the conferred properties depend on the starting conservation state of the object and on its needs.

Acrylates demonstrated features such as good ability to create films, good adhesive properties and moderate water repellence. Therefore, they are considered suitable both for consolidation and protection purposes. Acetates are mainly used for their adhesive property, to attach a reinforcement textile to the old deteriorated canvas. Acetate polymers display a varying degree of flexibility. There is an inverse relationship between flexibility and film strength. So, according to the materials, the conservator can choose the polymer with the most suitable characteristics. Generally, for the conservation of ancient textiles, high flexibility is preferable [57].

Fluorinated polymers, specifically with long fluorinated chains ($C \geq 8$ known as C8 chemistry), have excellent hydrophobic and oleo phobic properties and for these reasons, they were extensively applied onto textiles in the last decades. Despite their good water-repelling properties, C8 fluorinated polymers are recognized as a source of toxic chemicals in the environment. As such, when C8 fluorinated polymers degrade, they produce perfluorooctanoic acid (PFOA) and perfluorooctane sulfonate (PFOS). PFOA and PFOS have very low bio-elimination rate, are persistent in nature and likely to be carcinogenic. Therefore, the environmental protection agency (EPA) banned their excessive usage and invited major manufacturers to replace them with environmental friendly polymers. Consequently, new C6 fluorinated polymers with ≤ 6 fluorinated carbon atoms were developed [58].

Silicones are also considered to be a good alternative set of products. But they often need to be added with nanoparticles to reach comparable hydrophobic performances. The use of nano compounds originally intensified in the attempt to imitate naturally occurring hydrophobic plants. For example lotus leaf demonstrated excellent water-repelling and self-cleaning properties thanks to the presence of several papillae on the surface having hierarchical structures and specific waxes. The main drawbacks of nanoparticles are the variation of the original color and possible health issues.

Table 1.2. Description of treatments used onto ancient fabrics or fashion clothes. Treatments are grouped by chemical composition. Commercial names, the purpose of the treatment and the checked properties are also reported.

Category	Polymer, filler	Use	Main evaluated characteristics	Ref.	Year
Acrylate	Polyethylacrylate (Acrilem RP6005)	Fabric finishing, Binder in nonwoven textiles, consolidating treatments	No color variation	[59], [60]	2006
	Ethylacrylate-co-methylmethacrylate (Acrilem 674)	Coating for stiff curtains, Consolidating treatments	No color variation	[59], [60]	2006
	Ethyl acrylate/methyl methylacrylate (Plextol B-500)	Adhesive	Visible color change both after application and after aging	[61]	2005
	Butyl acrylate/methyl methylacrylate (Lascaux 360 HV)	Pressure sensitive adhesive	Visible color change both after application and after aging	[61]	2005
	Ethyl acrylate/methyl methacrylate (Paraloid B72)	Consolidation of textiles	Problems due to fungal deterioration	[62]	2008
	Ethyl acrylate/methyl methacrylate (Paraloid B72)	Consolidation of a roman Egyptian painted Linen fragment	Good qualitative compromise between strength and appearance	[63]	1992
	Ethyl acrylate-co-methyl-methacrylate (Primal AC33)	Consolidating treatments	No color variation	[60]	2004
	Carboxymethyl cellulose Si / polyacrylate	Protective coating material for paper relics	Hydrophilic	[64]	2016
	Aqueous acrylic emulsion (Rhoplex N-580)	Adhesive for fabrics and leather	Problem: Out of production	[65]	2011
	Methyl methacrylate, ethylacrylate EA/MMA 75/25 wt %	Consolidation and the restoration of naturally oxidized cellulose-based textiles	Tg (10°C) appropriate for application and resistant to biological attack	[66]	2005
Acetate	Vinylacetate-co-vinylversatate (acrilem 30wa)	Binder for non-woven textiles, used for glueing, consolidating treatments	Water resistance, No color variation	[59], [60]	2006

	Ethylenevinylacetate (BEVA 371)	Consolidant and adhesive	No color variation after application and after light aging. Color variation after heat ageing	[61]	2005
	Vinyl acetate/acrylic ester copolymer (Mowilith SDM5)	Consolidating treatments	No color variation	[61], [60]	2005
	Vinyl acetate-co-di-n-butylemaleate copolymer (Mowilith DMC2)	Consolidating treatments	No color variation	[61], [60]	2005
	Polyvinyl acetate/ethylene copolymer (Vinamul 3252)	Reinforcement for the conservation of an ancient Egyptian mummy, cartonnage cover and mask	Good adhesion	[67]	1985
Fluoropolymers	C-6 perfluorinated acrylic copolymer and PDMS, silica nanoparticles	Fabric protection	Hydrophobic	[68]	2017
	C-6 perfluorinated acrylic copolymer and PDMS, silica nanoparticles	Fabric protection	Hydrophobic	[19]	2017
	Fluoroalkyl Silane, functionalized silica nanoparticles	Fabric protection	Super-hydrophobic, Excellent durability	[69]	2012
	1H,1H,2H,2H-perfluorodecyltriethoxysilane ($C_{16}H_{19}F_{17}O_3Si$) and poly(vinylidene fluoride-co-hexafluoropropylene), modified Silica Nanoparticles	Fabric protection	Super-hydrophobic, Self-healing ability, Durability to washing cycles and cycles of Martindale abrasion.	[70]	2013
	Methyl methacrylate, ethylacrylate, and 2,2,2-trifluoroethyl methacrylate EA/MMA/TFEMA 73/24.5/2.5 wt%.	Consolidation and the restoration of naturally oxidized cellulose-based textiles	Resistant to biological Attack, improvement of mechanical resistance and flexibility	[66]	2005

Silicone	Poly-hydroxy-amino methyl silicone, nanoparticles of zinc oxide	Uv protection and antimicrobial finish on cotton	UV protection, 96.8-99.9% bacterial reduction, stability to washing cycles.	[71]	2019
	Aminosilicone	Fabric protection	Hydrophobic	[72]	2019
Others	Maleated Castor oil and styrene resin (macops)	Reinforcement for fabrics	Flexible but tough matrix. It loosed hydrophobicity with aging	[73]	2019
	Methyl hydroxy ethyl cellulose (Tylose MH300)	Adhesive	No color variation after application and after light aging. Color variation after heat ageing	[61]	2005
	Nanocellulose	Consolidation	Good mechanical reinforcement, no alteration of canvas color	[74]	2018
	Nanocellulose and nanosilica	Consolidation	Tensile testing	[75]	2018
	Polyamidoamine−epichlorohydrin (PAAE), nanocellulose	Consolidation	Strong mechanical properties and the high adhesion	[76]	2018
	Hydroxyethyl methyl cellulose (Tylose® MH), hydroxyethyl cellulose (Tylose® H) and methylcellulose (Metolose®), $CaCO_3$ and MgO	Consolidation and deacidification	Good consolidation, slightly yellowing	[77]	2020
	UV FAST®, sodium sulfite (Na_2SO_3), citric acid, sodium citrate, and glucose	UV adsorbers and reducings agents	Not efficient in inhibiting the photo-fading rate of the dyed fabrics	[78]	2020
	Hindered phenols, Aromatic amines, Sulfur compound, Metal chelates, Ultraviolet absorbers, Hindered amine light stabilize	Stabilizing additives efficiency	Protection against thermal degradation as well as against photochemical degradatio	[79]	1988

1.3.2 Evaluation of the durability of treatments

The behavior of the treated fabric over time by accelerated aging is essential to evaluate the effectiveness of the treatments and their stability. Through ageing it is possible to predict the change of properties such as mechanical, chemical and color. Hence, it is worth investing some pages of this thesis for collecting information about ageing methods used in the literature. All accelerated aging methods reported in Table 1.3 were applied onto cotton substrates to imitate natural ageing or to test conservation procedures. Table 1.3 contains the objects of the study, the parameters of the aging, the tested properties and the reference. It is important to note that the ageing parameters are very diverse from one case to the other (temperature, humidity, radiation, chemicals, and duration).

Table 1.3. Ageing procedures

Object	Parameters	Tests performed	Ref.	Year
Natural cellulosic fibers inoculated with fungi	80 °C, 65% RH, 13 + 12 days	FTIR, Raman Spectroscopy	[12]	2012
New linen canvas, washed and loomed	60-65% RH, and at 35% RH. Exposed to daylight, inclined at an angle of 45° facing south. Samples received a total of 34.8 x 106 Lux hours (roughly 70 years at 150 Lux assuming reciprocity). Filters used in museums, such as the various types of Perspex (Le. VE, VA and plain)	Mechanical tests	[80]	1982
Single cotton fibers and yarns	Temperatures ranging from 110 °C to 162 °C, various moisture conditions from 3% RH up to saturation. Periods of heating from 2 to 128 hours	Strength and elongation measurements	[81]	1954
Cotton canvas	• Moderate degradation (md): 200 mL of H_2O_2 (35 wt%) and 1 mL of H_2SO_4 (95wt%) • High degradation (hd) 200 mL of H_2O_2 (35 wt%) and 10 mL of H_2SO_4 (95wt%) Mild magnetic stirring for 72 hours at 40 °C	Degree of polymerization (DP), tensile testing, SEM	[82]	2017
Pristine cotton canvas	200 mL hydrogen peroxide solution (35 wt%) and 10 mL sulfuric acid During 72 hours at 40 °C	Degree of polymerization (DP), Breaking force	[74]	2018
Cotton canvas	H_2O_2/H_2SO_4	Breaking force (kN/m), elongation at Break (%)	[75]	2018
Cotton canvas	RH cycles 20−60−20% RH at 25 °C	Macro-peeling tests, stiffness	[76]	2018

Linen, jute and cotton canvas	• 90 °C and 65% RH in a climate chamber for 18 days • Hydrogen peroxide and sulfuric acid • 2 weeks at 80 °C and 65% RH	pH measurements, mechanical testing, color change, adhesion test, ATR-FTIR	[77]	2020
Cotton cellulose	100 °C and RH 100% for 17 days	Degree of polymerization (DP)	[83]	2003
Cotton cellulose	150 days at 80 °C	Degree of polymerization (DP), pH and color change, mechanical properties	[84]	2005
Cellulose fabric supports	• Aqueous acid ageing (H_2O_2/ H_2SO_4) • Vapor acid ageing (Sulphur dioxide and nitrogen dioxide) • Thermal ageing at 60 °C and 55% RH • Light ageing	Ultimate tensile strength	[85]	2020
Cotton canvas	• Hot aging (105 °C) for 144 hours • Wet aging (80 °C, 65% RH) for 144 hours	Microbiological test	[86]	2017
Bleached cotton cloth	From 1 to 14 weeks, 80 °C< T <95 °C, 40%< RH <80%, either exposed to light (UV-light with maximum in 340 nm, 1 Wm^{-2}) or aged in darkness	Degree of polymerization (DP) of cellulose, Tensile strength, Infrared spectroscopy	[87]	2012
Cotton cloth compared to naturally aged cotton	• > 160 °C in air • 190 °C in a nitrogen atmosphere	FTIR to study the carbonyl peaks	[37]	1987
Linen	• 150 °C for about 4 hours	Color change	[6]	2000
Contemporary cotton fabric	• Irradiated with 100-Mrad exposure for 90 to 120 hours • Hydrolysis by 40% sulfuric acid for 38 hours	Study of acidity, degree of polymerization.	[6]	2000
Modern cotton fabrics	• At 100, 130, 160 and 190 °C in the presence of 50 Lux tungsten illumination, in the dark, in air and in nitrogen	Study of Arrhenius relationship, study of carboxyl peak at 1730 cm^{-1} with FTIR	[6]	2000
Cotton and flax fabrics	• 105 °C in air and in dark for time intervals up to 65 days, plus application of *Aspergillus Niger*	Degree of polymerization (DP)	[6]	2000
Cotton and linen	• Samples exposed south at an angle of 90° from horizontal, 6 months (March to September) characterized by sun, no rain, high temperature and high humidity • Pollution from local traffic • Oxidative reaction: [$NaIO_4$] 0.1M for 4 hours	Tensile testing, water repellence	[66]	2007

Linen textile	• 140 °C in precision forced convection oven for 72 hours • Light irradiation for 200 hours using Tera Light Fastness Tester • Buried in soil for 10 days.	Color change, Tensile properties, XRD analysis, study of infrared absorptions at 1750-1600 cm^{-1} with FTIR Spectroscopy	[61]	2005

1.3.3 Scope of the research: development of innovative conservative technology

Table 1.2 showed several conservative treatments, which are present on the market and currently used. Looking at those past and present treatments it is clear that there is lot of space for improvement of conservation treatments. For instance, there is a lot of knowledge, which can be learnt from commercial products and implemented and adjusted to cultural heritage field to avoid deterioration phenomena, by paying particular attention to conservation issues, such as esthetical problems, brittleness and color changes.

The literature search reported in the previous section demonstrated that products with good properties are available on the market, but they often have drawbacks. *E.g.* fluoropolymers demonstrated excellent hydrophobicity, but there are lot of concerns about health issues; nanoparticles improve the surface roughness increasing water repellency, but also impacting aesthetical properties; other polymers demonstrated to be prone to biological deterioration; in some other cases the protective/consolidative treatment is efficient, but the aging performances or the color variation were not tested.

Concluding, the aim of this study is to propose and develop innovative pathways toward the production of conservative technology suitable for fabrics of inestimable historical and cultural value. Hence, the treated objects should not undergo any substantial change, they should maintain chemical, physical, aesthetical properties, both after the protective treatment and even after the aging of the fabric together with the treatment. Taking into consideration all these factors, it is possible to valorize, preserve and transmit Cultural Heritage objects to future generations.

Hence, the milestones to reach the ideal treatment for fabrics conservation are:

- The study of multifunctional bulk fabric protection able to penetrate in the substrate to fully prevent from several of the above-mentioned deterioration forms;
- The preservation of the original and fundamental fabric characteristics after conservation treatment;
- The long term chemical stability of the protective treatment, tested with accelerated aging;
- Particular attention to the aesthetical impact of the treatment on the fabric and to the aging process, considering the cultural-historical value of samples;

- The use of environmentally friendly polymers, solvents and processes;
- The implementation of zero-waste, convenient and scalable procedures, beneficial for conservators.

2. Hydrophobic treatment with polyurethane modified aminosiloxane emulsions

The research project illustrated in Chapter 2 was born to respond to the need of fabric protection in the field of Cultural Heritage. As it was explained in the previous chapter, most of the deterioration phenomena are linked to the presence of water: swelling and shrinking, mold proliferation, moth attack, solubilization of polluting agents.

In the past, several fluorinated chemicals were used in force of their extremely low surface free energy [88], [89], [90], [91], [92], with potential risks for human health and environment. In alternative, chemically modified nanoparticles were widely used onto fabrics [89] [93] [94] [95], but they often lack in transparency, which is a fundamental issue in conservation science. Silicones are highly popular hydrophobic compounds that are also biocompatible [96], [97].

Hence, this chapter focuses on the development of a new hydrophobic, transparent and resistant cotton fabric treatments, based on the synergic action of siloxane and polyurethane polymers. The amino-siloxane polymer was chosen for the hydrophobic properties and for conferring softness and potentially good mechanical properties. Polycarbonate polyurethane was chosen due to its good hydrolytic stability, low water absorption levels, good breathability and excellent adhesion to surface. Sustainability is desirable and crucial in Cultural Heritage conservation[98] [99] [100], hence it was one of the main goals of this study. For this reason environmentally friendly solvents and polymers were selected, low wastage applications methods were tested and long-lasting aesthetical properties were monitored over time.

The so obtained formulation is tested as coating of historical textiles conserved in museums or indoor environments.

2.2 Materials and Methods

2.2.1 Materials

The used fabric was a plain woven and bleached 100% cotton. The mass density of the fabric was 180 ± 5 g/m^2 with 24 threads/cm density in each direction.

ESACOTE PU 77 (hereafter, PCU) was purchased by Lamberti S.p.A. (Italy). It is a solvent-free, waterborne dispersion of an aliphatic polyurethane based on polycarbonate diols [101], [102].

The amine modified silicone fluid was purchased from WACKER® (Germany) with the commercial name FINISH WR 1300. It was specifically developed for impregnation of fibers and textiles. According to the supplier, the fluid contains more than 85 wt.% aminofunctional polysiloxane resin, and the rest 15 wt.% is made up of octamethyl cyclotetrasiloxane and trace amounts of ethanol. The appearance is slightly turbid and fluid. The amine number is approximately 0.3 mL 1N HCl/g. Fig. 2.1 a) and b) show the starting hypothetical formula of the chemical components.

2.2.2 Preparation and characterization of polymer dispersions

A sample was taken from the as-received waterborne PCU dispersion; it was placed on a glass slide and let dry in order to calculate the solid content, which resulted to be 36wt. %. The same procedure was repeated for the silicone fluid, which resulted to be 98 wt.%. Both the PCU and the aminosiloxane were diluted to obtain 2wt.% solutions, with distilled water and isopropyl alcohol (IPA), respectively. Then, 40 mL of 2wt.% PCU ethanol dispersion was emulsified together with 40 mL of aminosiloxane at 2wt.% in IPA through gentle mechanical mixing. It was fundamental to perform this step slowly, to avoid the formation of clumps. Once the emulsion was accomplished, it was stable for several months. Fig. 2.1 c) shows the appearance of the diluted chemical components and the milky emulsions resulting from the mix of the two. It was easy to find a relationship between the color of the dispersions and the relative data from Dynamic Light Scattering (DLS). This technique was in fact used to determine the size distribution profile of the particles in the solutions and dispersions. DLS measurements were acquired using a Zetasizer Nanoseries from a Malvern Instruments (Worcestershire, UK) technique. The temperature was set at 25°C. Five measurements were used with an automatic duration of a minimum of 10 and a

maximum of 100 runs. PCU dispersion, aminosiloxane solution and the emulsion of the two were analyzed to get info about their droplet size distribution. The transparent solution corresponded to particle of aminosiloxane with 5 nm diameters, the hazy white PCU emulsion correspond to particles with 30 nm diameter. The milky white emulsion correspond to the mix of the two, where the DLS peaks corresponding to the single components disappeared, while a peak corresponding to 1,1 μm appears. Hence, the DLS analysis confirmed that all PCU and aminosiloxane got completely emulsified together.

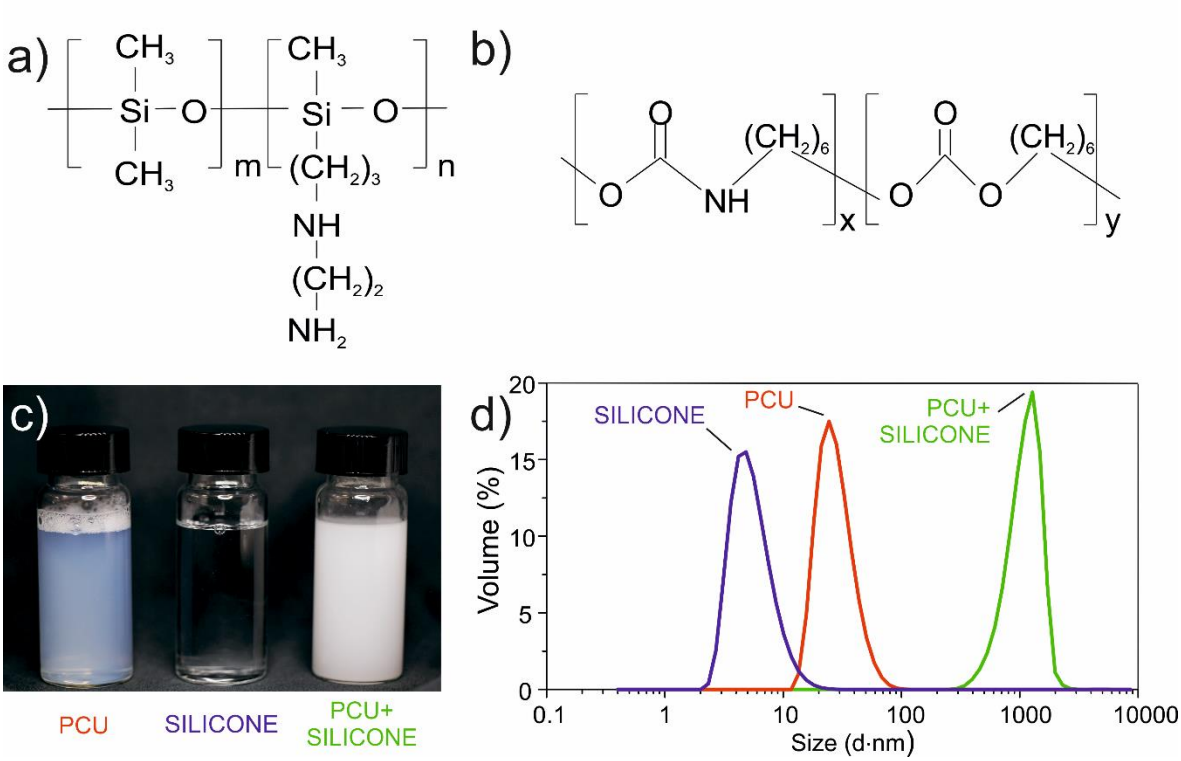

Fig. 2.1. a) hypothetical chemical structure of aminosiloxane, b) hypothetical chemical structure of PCU, c) photograph of diluted PCU (hazy white) and the silicone softener (transparent) dispersions and the emulsion of the two (white), (b) DLS analysis indicate droplet size distribution of the dispersions and the emulsion.

In order to characterize the both PCU and aminosiloxane, 1H NMR analyses were performed by dissolving the solid polymers in deuterated chloroform (CDCl3) from Sigma-Aldrich. The analyses were carried out at room temperature using 5 mm tubes on the Bruker Avance III 400 MHz spectrometer equipped with a road Band Inverse probe (BBI). Chemical shifts are reported in ppm and were determined by the reference to tetramethylsilane (TMS).

2.2.3 Fabric treatment and sample preparation

First of all the cotton fabric was washed with water and laundry soap, followed by thorough rinsing. Then it was dried at room temperature, to ensure there was no dirt or contamination of the cotton fabric. Then, cotton samples were cut into pieces of 10 × 15 cm^2. This dimension was chosen so that it would be possible to perform several tests on each samples, including mechanical tests which require a specific surface area. Control samples with silicone only and PCU only were performed. Double layer treatments were performed by applying PCU polymers first, letting the sample dry at 60 °C for 24 hours, then applying siloxane solution and again letting it cure at 60 °C for 24 hours. Single layer treatments were performed by applying the micro-emulsion (PCU+aminosiloxane) directly on the fabric surface and letting it dry at 60 °C for 24 hours.

Double layer application and micro-emulsion application were performed both by dip- (Fig. 2.2) and spray- (Fig. 2.3) coating to compare the methods and find the optimum one.

Dip coating consisted in dipping the fabric in the specific polymeric solution for 15 seconds. Spray coating was performed with an airbrush (Paasche Airbrush VL with 73 mm head and 1.06 mm tip). A total amount of 40 mL of the polymeric solutions were applied on both sides of the fabrics. Spraying distance between fabric and airbrush was optimized with the respect to the solvent volatility: 20 cm for siloxane in IPA, 30 cm for the PCU/Siloxane polymer dispersion in ethanol/IPA and 40 cm for PCU dispersion in water. After the treatment, the samples were stored at room temperature and then characterized.

Table 2.1. Description of samples name, composition and application methods.

Sample name	Treatment			Application method	
	untreated	double-layer	micro-emulsion	dip	spray
S1	✓				
S2		✓		✓	
S3			✓	✓	
S4		✓			✓
S5			✓		✓

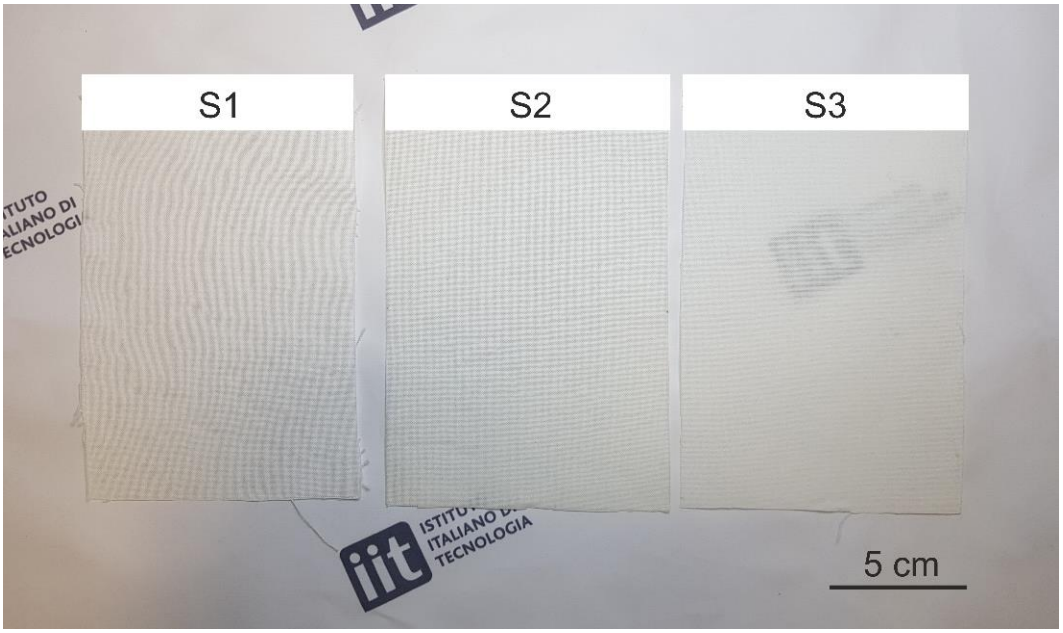

Fig. 2.2. Pictures of untreated cotton (S1), cotton treated with PCU and aminosiloxane by dip-coating (S2) and cotton treated with micro-emulsion of PCU and aminosiloxane by dip-coating (S3).

Fig. 2.3. Pictures of untreated cotton (S1), cotton treated with PCU and aminosiloxane by pray-coating (S2) and cotton treated with micro-emulsion of PCU and aminosiloxane by spray-coating (S3).

2.2.4 Morphological characterization of the treated samples

Scanning electron microscopy (SEM) JEOL JSM-6490LA (Japan) was used to investigate the morphology of the untreated and treated fabrics' surfaces: S1, S2, S3, S4 and S5. First, the fabrics' surfaces were sputtered with a 10 nm thick film of gold (Cressington 208HR sputter coater, UK), then SEM images were collected operating at 10 kV acceleration voltage, at different magnifications such as 25×, 50×, 1000×. Moreover, elemental analysis and mapping by energy-dispersive x-ray spectroscopy (EDX) were performed both on surfaces and on cross-sections to confirm the homogeneity and penetration of the polymeric treatments.

Atomic force microscopy (AFM) was also performed to analyze the micro-morphology and roughness of the S1 and S5 fibers' surfaces. AFM measurements were performed though XE-100 instrument (Park Systems, Korea) stabilized on an anti-vibration platform TS-150 (Table Stable, Switzerland). The cantilever probes used were Non-Contact Cantilever (Park, Korea) with nominal resonance frequency of 330 kHz. The scan rate was 0.1 Hz and the scan area selected was 2x2 μm^2. WSxM 5.0 software and Gwyddion software have been used to process the images and calculate the surfaces' roughness, respectively. Root mean square roughness (Sq) and average roughness (Sa) were the two obtained parameters. Averages and standard deviation of 4 to 6 analyses are reported [103], [104].

2.2.5 Chemical characterization of the samples before and after treatment

The chemical characterizations were performed with a Fourier Transform Infrared (FTIR) spectrometer (VERTEX 70v, FT-IR, Bruker) equipped with a single-reflection attenuated total reflection (ATR) accessory (MIRacle ATR, PIKE Technologies). Aminosiloxane, PCU, S1, S2, S3, S4 and S5 were analyzed. The samples were placed on top of the diamond crystal and underwent pressure to ensure maximum contact between the fabric and the diamond. All spectra were recorded in the range from 3800 to 600 cm^{-1} with a resolution of 4 cm^{-1}, accumulating 128 scans. Three repetitions were performed for each analysis to ensure the reproducibility of obtained spectra.

2.2.6 Wettability and surface energy estimation on treated samples

Water contact angle (WCA) and water roll-off angle of S1, S2, S3, S4 and S5 samples were measured with a contact angle instrument (OCAH-200 DataPhysics, Germany). The static angle between a liquid drop and a solid surface is named Young's contact angle, and it is related to the surface tensions of the three interfaces according to the relationship:

Equation 5 $$cos\theta_Y = \frac{\gamma_{solid-vapor} - \gamma_{solid-liquid}}{\gamma_{liquid-vapor}}$$

Where γ is the critical surface tension. In the cases where the liquid-vapor surface tension is smaller than the solid-vapor surface tension ($\gamma_{LV} < \gamma_{SV}$), the liquid-solid interface increases to minimize energy. As the water droplets wets the surface, the contact angle approaches zero.

Gastight 500 µL Hamilton precision syringe with blunt needle of 0.52 mm internal diameter was used to deposit 5 µL droplets onto surfaces. The WCA was measured after 30 s. From each sample, a strip of 1×5 cm^2 was cut and attached to contact angle table with double sided adhesive tape to get a wrinkle free surface for WCA measurements. Static WCAs at 10 different positions on each sample were measured and reported as mean values with standard deviations.

For roll-off angle measurements, different droplet volumes corresponding to 17.5µL, 20 µL, 25 µL, 30 µL and 35 µL were deposited and the substrate holder was tilted with an angular speed of 1.42°/sec. Side view videos of the rolling drops were captured and from the video the roll-off angle was extrapolated. Measurements were repeated 5 times [105].

Moreover, the ability of water to spread in the fabric was tested by using 1 mL of colored water droplet. Other than the penetration of water, this test was used to quantify the long term wetting stability. The colored water was created by mixing water and 0.1 wt.% of food colorant (Color Dolci F.lli Rebecchi Valtrebbia S.p.A). The colored droplet was examined hour after hour, until it was completely absorbed or evaporated depending on the hydrophobicity of the fabric. Residual color stains allowed assessment of fabric performance against liquid water. The last property related with wettability which was tested is critical surface tension (γ) of solidified micro-emulsion on a glass slide. It was measured with the of Zisman's method [106], which is based on the experimental finding that the surface tension of a liquid spreading away from a surface is lower than the surface tension of the surface upon which it is spreading. Zismann called this value: γc

(critical surface tension) [106]. To obtain the γc value, a series of contact angles was measured using the following liquids: water, glycerol, dimethylformamide, toluene, isopropyl alcohol and n-hexane. Then a graph was plotted of surface tensions against the cosine value of the corresponding static contact angles. The best fit of the points was extrapolated from the graph and, from this fit, at the intersection with the value of cosine = 1, on horizontal axis the value of γ was obtained.

2.2.7 Water vapor permeability

Water vapor permeability (WVP) of the pristine cotton (S1) and treated cotton fabrics (S2, S3, S4 and S5) was calculated at 25°C and 100% RH (%) according to the ASTM E96 standard method. 100%RH was reached by placing 400 µL of deionized water in the permeation chambers of 7 mm inner diameter and 10 mm height. Samples were cut in circular shape and placed on the top of the permeation chamber, which was then close with sealing rings, lid and screws. The chambers were then placed in a desiccator, maintained at 0% RH by silica gel. The chambers were weighted every hour for a total of 8 consecutives hours in order to register every weight change and to monitor the permeation of water vapor from the chamber, trough the porosity of the fabric, to the silica gel.
An electronic balance (with 0.0001 g accuracy) was used to weight the chambers containing water and fabric samples. The water mass loss versus time was plotted and the slope of the line was calculated by linear regression. Then, the water vapor transmission rate (WVTR) was determined as below:

Equation 6 $$WVTR(g(m^2d)^{-1}) = \frac{slope}{area\ of\ the\ sample}$$

The water vapor permeability (WVP) of the samples was calculated as follows:

Equation 7 $$WVP(g(mdPa)^{-1}) = \frac{WVTR \cdot L \cdot 100}{p_S \cdot \Delta RH}$$

where L(m) is the thickness of the sample, measured with a 0.001mm accuracy micrometer, ΔRH (%) is the percentage relative humidity gradient, and ps (Pa) is the saturation water vapor pressure at 25°C [107], [108], [109]. Every measurement was repeated 3 times.

2.2.8 Stress-strain measurements

The mechanical properties of S1, S2, S3, S4 and S5 fabrics were tested with 3365 Instron (USA) tensile tester. First of all, the samples were conditioned at room temperature. Specimens were cut in a dog-bone shaped, having the standard dimension of 25 mm length along the axis of warp threads and 3.98 mm width. Samples were placed in between pneumatic clamps. The extension speed was maintained constant at 5 mm/min. in this study, the elastic modulus (MPa) was calculated using the initial slope of the curve, between the starting point 0 and 0.1 mm/mm. Elongation at maximum load was also calculated. The analyses were repeated 5 times for each specimen in order to calculate the averages and standard deviations of elastic moduli and elongation values [110], [111].

2.2.9 Flexural rigidity

The variation of tactile properties of fabrics after a hydrophobic treatment are very likely to happen. This variation can be quantified by measuring various structural, mechanical, and surface parameters [110], [112], [113]. The bending properties and the drapability (degree to which a fabric can be draped) cannot be determined from in-plane properties such as Young modulus test; hence a different test is required. Hence, the flexural rigidity of S1, S2, S3, S4 and S5 was determined with the Peirce cantilever test [114] (ASTM D1388), to provide a more complete assessment of the anisotropic mechano-physical properties of the cotton textiles [113].

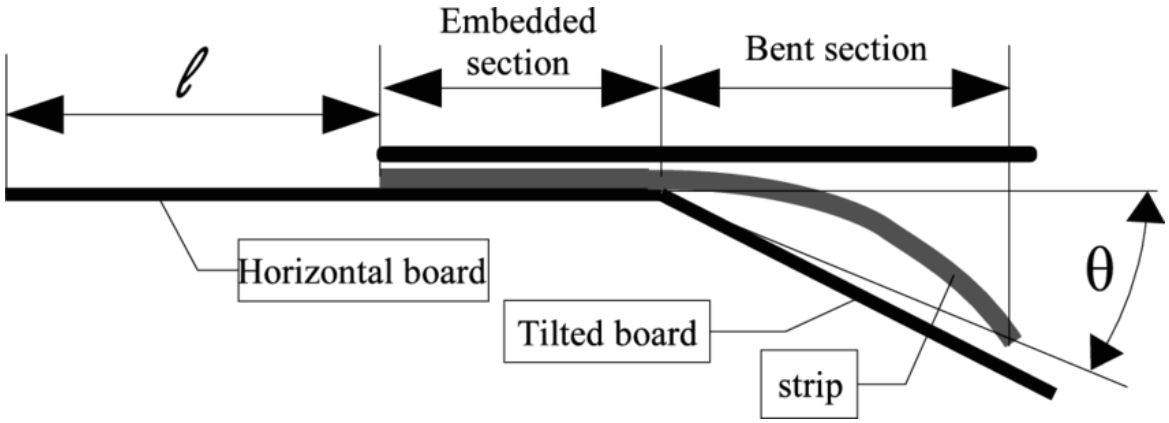

Fig. 2.4. Cantilever bending test equipment.

Fig. 2.4 shown the standard cantilever bending test equipment. The samples were cut in dimensions of 200mm × 25mm, they were placed on the horizontal board with a metal plate on them. The metal plate gradually slid, until the leading strip of the fabric made contact with the bending angle (Θ=41.5°) indicator. The flexural rigidity G_{Pierce} (Nm) was calculated according to the formula [114]:

Equation 8 $$G_{Pierce} = 9.81 \cdot 10^{-12} \cdot w \cdot l^3$$

where w (g/m^2) is the weight of the analyzed fabric and l (mm) is the bending length measured when the strip touched the Θ angle. Therefore, there is a proportion between the stiffness and the bending length of the fabric. A higher value of the bending length indicates higher fabric stiffness [104]. For each fabric, the front and rear side of both extremities were tested, leading to a total of four measurements per sample [114].

2.2.10 Determination of color variations

Especially in the conservation field, the evaluation of colorimetric parameter is of primary concern. The proposed treatment should guarantee the preservation of the original color and aesthetic properties of the object [112].

A portable spectrophotometer and colorimeter Konica Minolta CM 2600d was used to measure the color of fabrics before and after treatments. The surface area analysis was the small area view (SAV) of 3 mm, used with the 10° detector and the D65 primary source.

Reflectance measurements were analyzed according to the CIEL*a*b color parameters, which gave the Cartesian (L*a*b*) coordinates to identify any colorimetric variation produced by the polymers on the fabric. The color space in which the coordinates are placed is represented in Fig. 2.5.

The overall color variation, ΔE, represents the deviation from the original value due to the coating, and it is calculated from all the variations of L*, a* and b* parameters:

$$\Delta E^*_{ab} = \sqrt{(\Delta L^*)^2 + (\Delta a^*)^2 + (\Delta b^*)^2}$$

where L* stands for the brightness vector on a gray scale from 0 to 100, from black to white, respectively; a* stands for the red/green color vector with positive values and negative values corresponding to red and green respectively; b* stands for positive values and negative values corresponding to yellow and blue respectively.

Colorimetric measures were performed onto cotton before any treatment (S1), and after the proposed treatments (S2, S3, S4 and S5). Moreover, colorimetric analyses were performed after accelerated aging of the samples in the climatic chamber, as explained in the next session.

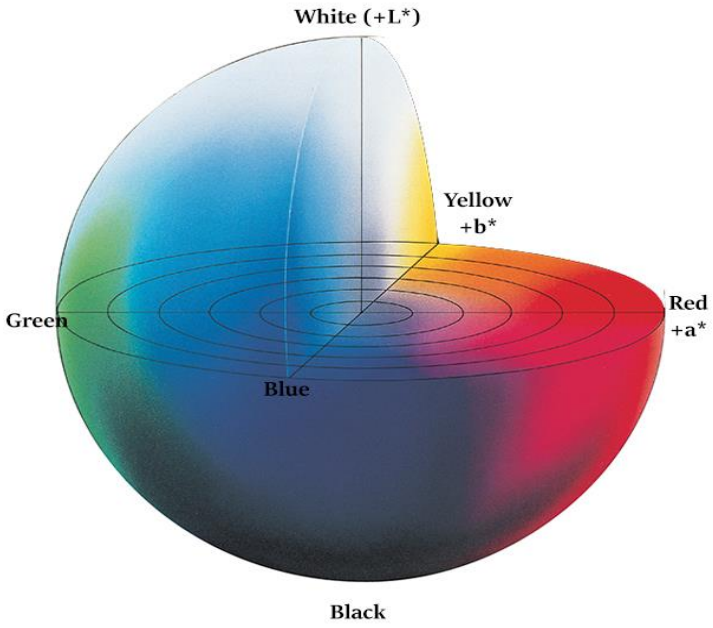

Fig. 2.5. CIE 1976 Lab Color space

2.2.11 Aging in climatic chamber

Accelerated aging was performed in order to test the long term stability of the treatments onto fabrics. Performing accelerated test is very common in conservation science, as reported in Table 1.3 in the previous chapter. In order to simulate the action of aging factors present in museum environment, untreated and treated samples were placed in a Memmert Climate chamber with three cold light fluorescent lamps (D65, 6500K) and two UV lamps (320-400 nm), at 20°C and 40% R.H. Samples were exposed to accelerated aging for a total amount of 1.5 Mlxh (million lux hours). This amount of lux is comparable to five times the average annual exposure present in museum illuminated environment [115]. After the aging, colorimetric tests were performed again, to evaluate the impact in time of the coatings on the aesthetical properties of the fabrics [116].

2.3 Results and discussion

The samples were measured after being treated and the overall changes are reported in Table 2.2. Minor variations were due to the dip-coating applications, which caused thickness increase of 2.7% and 1.0% and mass density increase of 4.2% and 2.1%. Higher variations were due to spray-coating application, which caused variations of 4.0% and 3.0% in thickness and 6.9% and 5.8% in mass density.

Table 2.2 Names, thickness and weight/area of samples

Sample name	Description	Thickness (μm)	Percent increase in thickness (Δμm%)	GSM (Grams per Square meter)	Percent increase in GSM (Δg/m²%)
S1	untreated	297 ± 2	-	189 ± 1	-
S2	dip-coating, double-layer	305 ± 2	2.7%	197 ± 3	4.2%
S3	dip-coating, micro-emulsion	300 ± 3	1.0%	193 ± 3	2.1%
S4	spray-coating, double-layer	309 ± 3	4.0%	202 ± 2	6.9%
S5	spray-coating, micro-emulsion	306 ± 2	3.0%	200 ± 3	5.8%

2.3.1 Morphological characterization of the treated samples

Untreated and treated fabrics were analyzed with SEM microscopy in order to investigate possible changes in the surface morphology. Fig. 2.6 a) shows the mesh created by the warp and the weft of the original untreated fabric, S1. The boundaries between warp and weft are clearly visible, that is the porosity of the fabric. In Fig. 2.6 b) the single cotton fibers present in a thread are visible. They are characterized by the typical ribbon-like shape with periodic convolutions along the length of the fiber. Even at this higher magnification, the porosity of the thread is visible, *i.e.* the fibers are well distinct one from the other. Similarly, Fig. 2.6 c) d) and e) f) show the morphology of dip-coated S2 and S3 respectively, in which the porosities between threads and fibers are unchanged with respect to S1. Hence, dip-coating seems to be an optimum method to coat each and every fiber by promoting the penetration of the solutions through the fibers. Fig. 2.6 g) and h) represent sample S4, on which the polymeric solutions were sprayed. In the 50 × picture the porosity between warp and weft seemed to be partially occluded and, in fact, in 1000× magnification some agglomerates are visible. They were probably generated by the evaporation of the solvents during the path from the airbrush to the fabric surface. Fig. 2.6 i) and j) represent S5 samples, where the polymeric micro-emulsion was sprayed. Some micrometric agglomerates are visible, but they do not seem to occlude any porosity. Hence, spray coating is a suitable application method, especially for the application of the PCU and siloxane micro-emulsion.

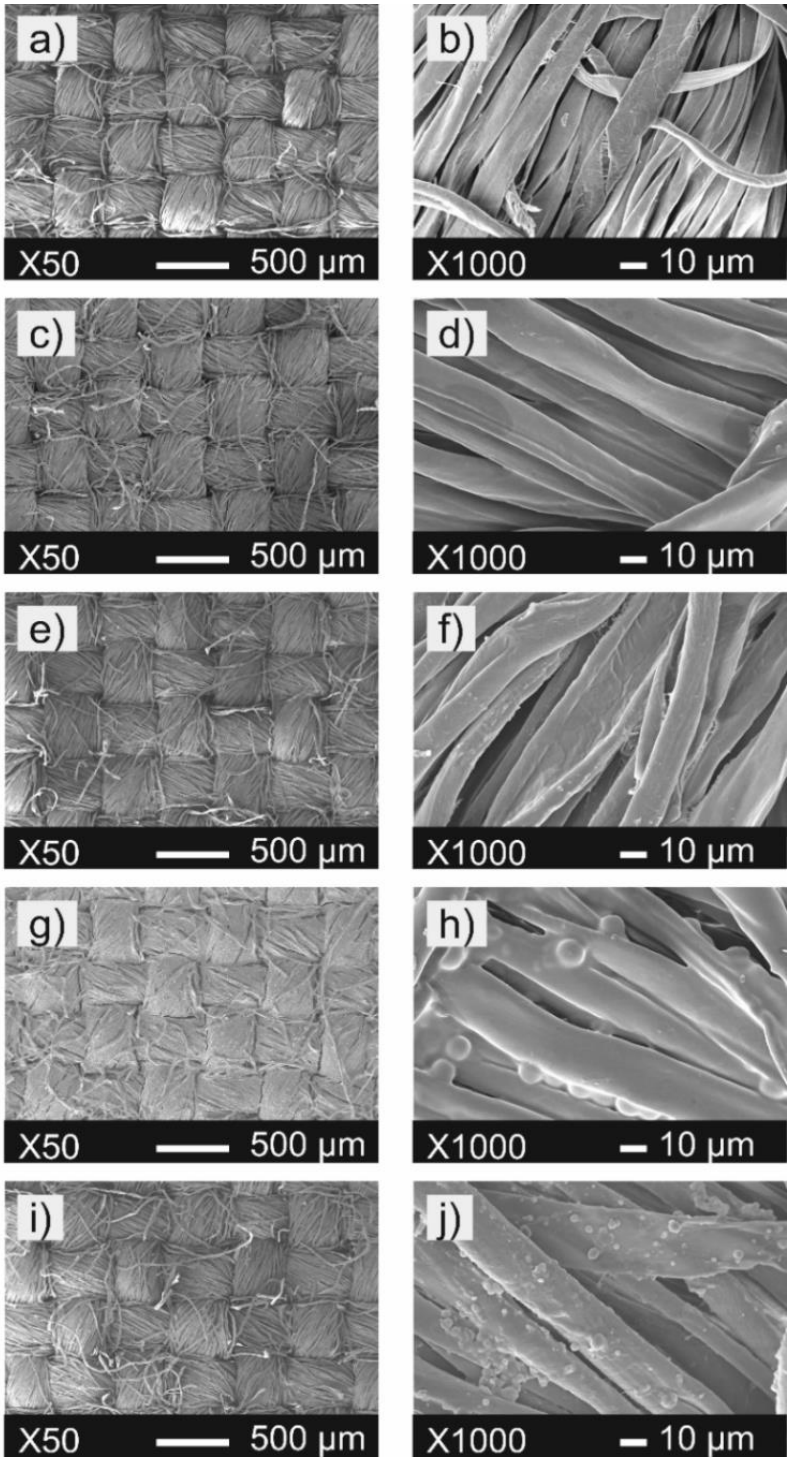

Fig. 2.6. SEM images at 50× and 1000× of a) untreated cotton S1 at 50×, b) untreated cotton S1 at 1000×, c) double-layer dip-coated S2 at 50×, d) double-layer dip-coated S2 at 1000×, e) micro-emulsion dip-coated S3at 50×, f) micro-emulsion dip-coated S3 at 1000×, g) double-layer spray-coated S4 at 50×, h) double-layer spray-coated S4 at 1000× and i) micro-emulsion spray-coated S5 at 50×, j) micro-emulsion spray-coated S5 at 1000×.

SEM-EDX analyses were performed on the fabric surfaces to verify the distribution homogeneity of the hydrophobic coating. EDX probe detected the presence of the characteristic components of natural and synthetic polymers: carbon (C), oxygen (O), Silicon (Si) and gold (Au) atoms. C and O are associated both to PCU, siloxane and cotton; Si is associated to the presence of the siloxane polymer; Au is due to the pre-analysis sputtering for sample preparation. Fig. 2.8 a), d), g) and j) show the homogeneous distribution of the siloxane polymer on the surfaces. Thanks to these top view, we can state that both spray and dip-coating were efficient to perform a uniform surface treatment. Fig. 2.8 b), e), h) and k) are images of threads cross-sections. In all cases, fibers are clearly distinguishable and well defined. Polymer clumps are not present. Fig. 2.8 c), f), i) and l) are the results of elemental search performed in the core of the treads. Regardless application methods or layer-by-layer/emulsion application, Silicon was found in every sample. Hence the aminosiloxane was able to penetrate through the outer fibres and reach the core of the thread, as shown in in the scheme of the micro-emulsion behavior.

Therefore, this hydrophobic treatment is not only a surface treatment, but it is conferring hydrophobicity to the full fabric bulk.

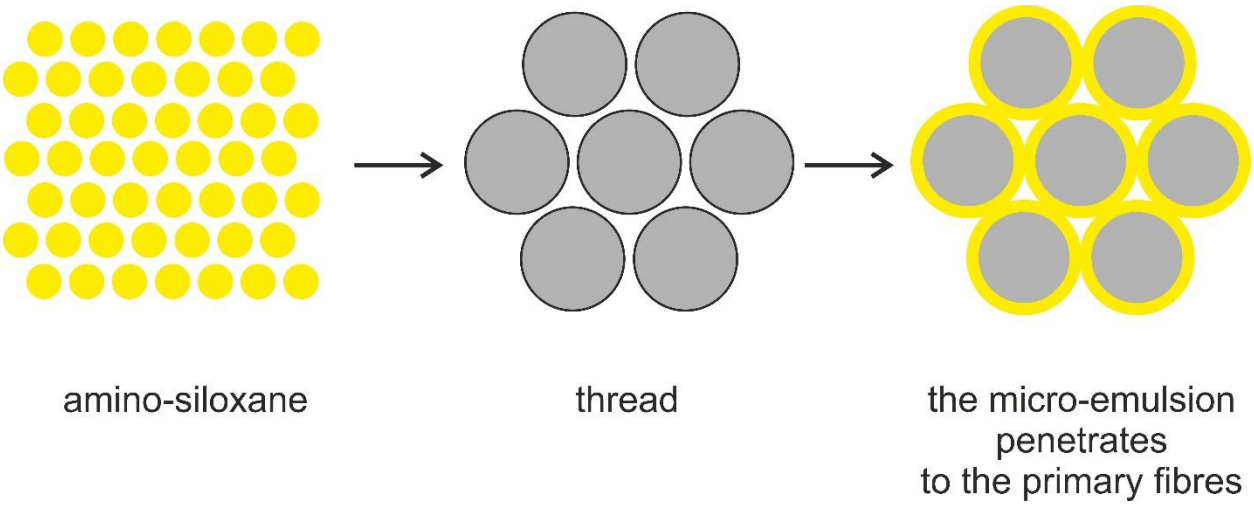

Fig. 2.7. Schematic micro-emulsion behaviour on threads.

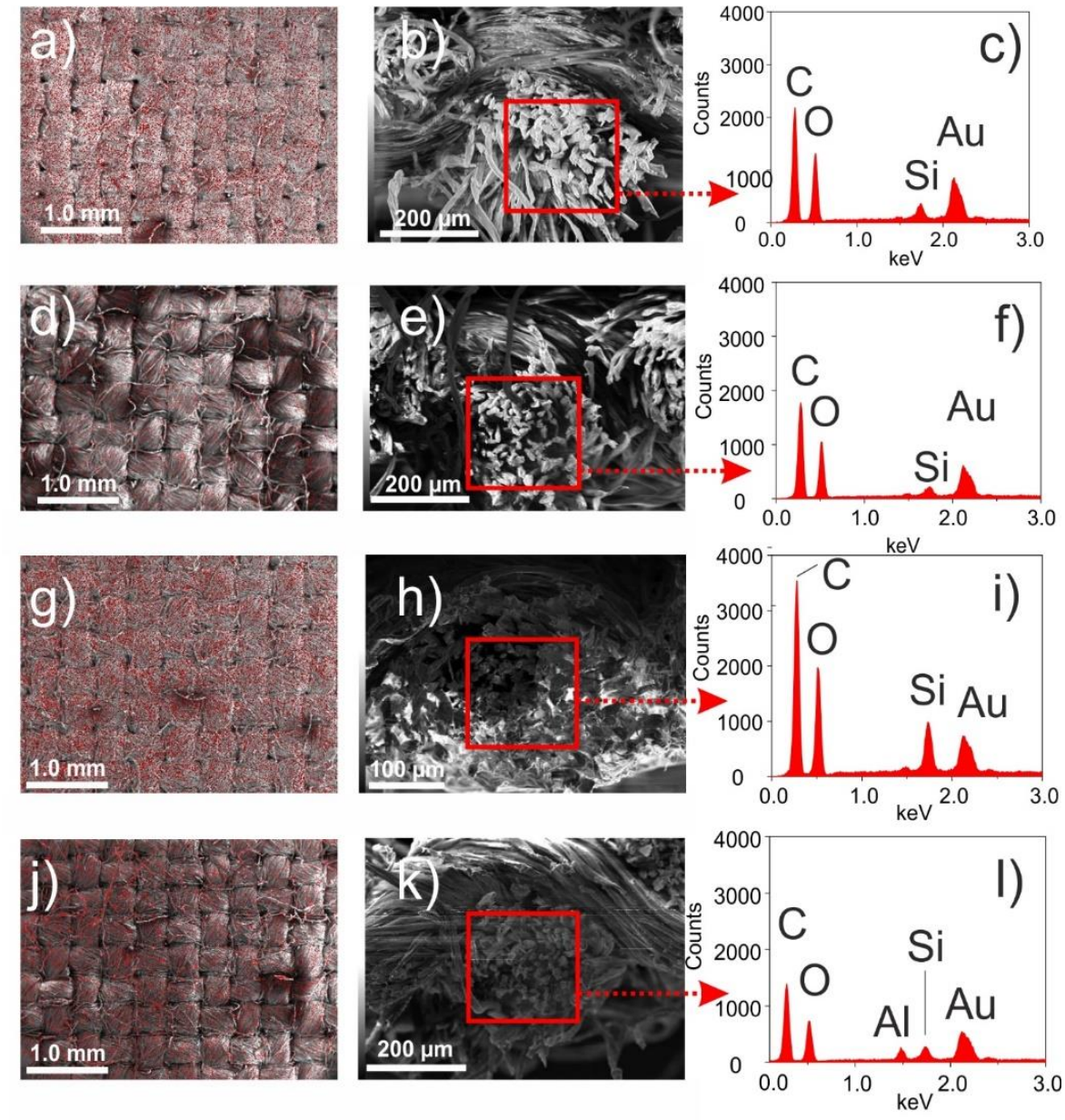

Fig. 2.8 SEM images of a) S2 top view, b) S2 cross section, c) S2 cross section EDX, d) S3 top view, e) S3 cross section, f) S3 cross section EDX, g) S4 top view, h) S4 cross section, i) S4 cross section EDX, j) S5 top view, k) S5 cross section, l) S5 cross section EDX. The element mapped in red on the top-view is Silicon.

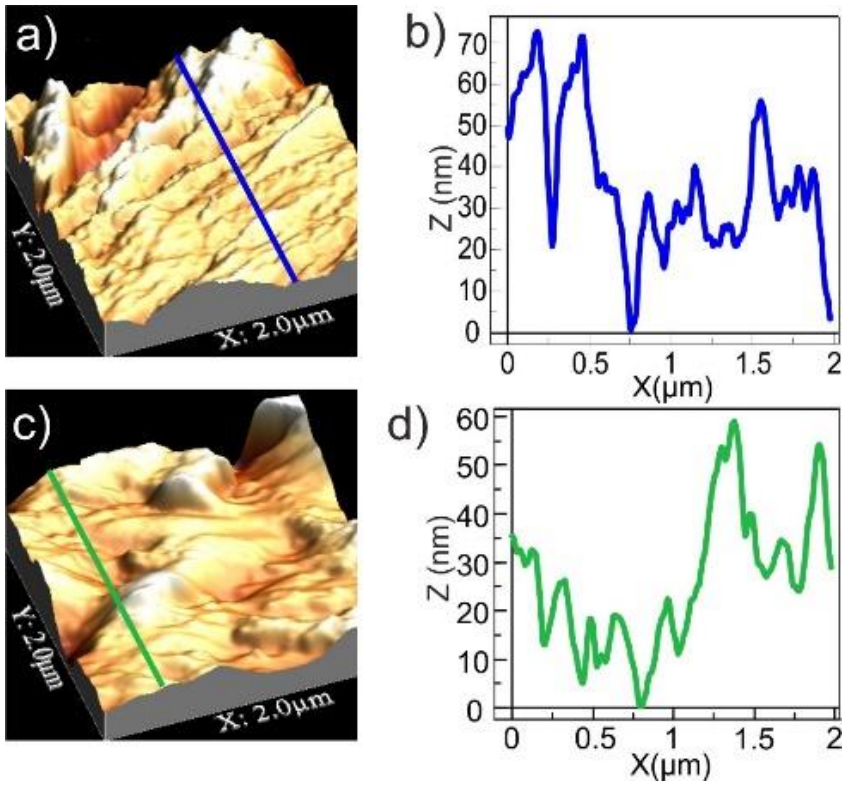

Fig. 2.9. AFM surface analyses. a) 3D topographic reconstruction and b) roughness profile of untreated cotton fabric; c) 3D topographic reconstruction and d) roughness profile of S5 cotton sprayed with micro-emulsion of PCU and aminosiloxane.

The AFM analyses revealed the micro-surface topography of both the untreated cotton (S1) and the one treated with the mix of PCU and siloxane by spray (S5). 3D representations or surface roughness and representative profiles are shown in Fig. 2.9. Both root mean square roughness (Sq) and average roughness (Sa) were calculated. The average Sq roughness of untreated cotton fiber is 56.3 ± 19.4 nm, Sq of S5 treated cotton is 64.3 ± 9.7 nm. The corresponding average Sa of untreated is 45.7 ± 14.4 nm, Sa of treated is 47.2± 11.5 nm.

By comparing these roughness data, it was found that the polymeric coating did not significantly alter the initial intrinsic roughness of untreated cotton fibers. Despite the process of atomization of the micro-emulsion during spray application, the overall roughness has not increased. This is probably due to the self-leveling property of silicone [117] and smoothening property of PCU [118]. Hence, due to these opposed contributions, submicro-scale roughness was maintained similar after the treatment. Nevertheless, the intrinsic micro-roughness of the original untreated fibers evidently contributed to obtain the final high hydrophobicity. In fact, water CA on smooth surfaces cannot generally exceed 120° through tailoring surface chemistry [89], but all rough

surfaces coated with PCU and siloxane gave CAs of ~ 145° and high droplet mobility, as shown in Fig. 2.13.

2.3.2 Attenuated Total reflection-Fourier transform infrared (ATR-FTIR) Spectroscopy

Chemical characterization of starting materials was performed through ATR-FTIR spectroscopy. Table 2.3 shows the wavenumbers of the peaks present in each spectrum and the attributed vibration. Pristine cotton peaks corresponded to the characteristic peaks of cellulose, without any contamination. Amino-siloxane spectrum contained peaks associated to methyl and siloxane groups. PCU spectrum was composed of urethane, carbonate and aliphatic groups.

Table 2.3. ATR-FTIR peak interpretation of Cotton, amino-siloxane and PCU.

Cotton [38], [119], [120]		Amino-siloxane [121]	
Wave number (cm^{-1})	Functional group	Wave number (cm^{-1})	Functional group
3279	OH stretching	2963	Asymmetric CH_3 stretching
2897- 2883	Asym. and sym. CH_2 stretch.	2905	Symmetric CH_3 stretching
1642	O-H bending. Adsorbed H_2O	1258	CH_3 symmetric bending
1430	CH_2 scissoring	1074	Si-O-Si symmetric
1372	CH bending	1007	Si-O-Si asymmetric
1336	OH in-plane bending	783	CH_3 rocking
1320	CH_2 rocking	PCU [122]	
1282	CH deformation stretch	3335	N-H stretching
1201	C-O stretching	2922	Asymmetric CH_2 stretching
1159	Asym. bridge C-O-C stretch.	2855	Symmetric CH_2 stretching
1105	Asym in-plane C-O-C stretch	1740	C=O stretching
1053	Asym. C-O stretching	1707	H-bonded C=O stretching
1028	Sym. C-O stretching	1526	N-H bending and C-N stretch
986	ring stretching modes	1242	O-C-O stretching
898	Asym. out-of-phase ring stretch: C_1–O–C_4; b glucosidic bond	1088	C-O-C stretching

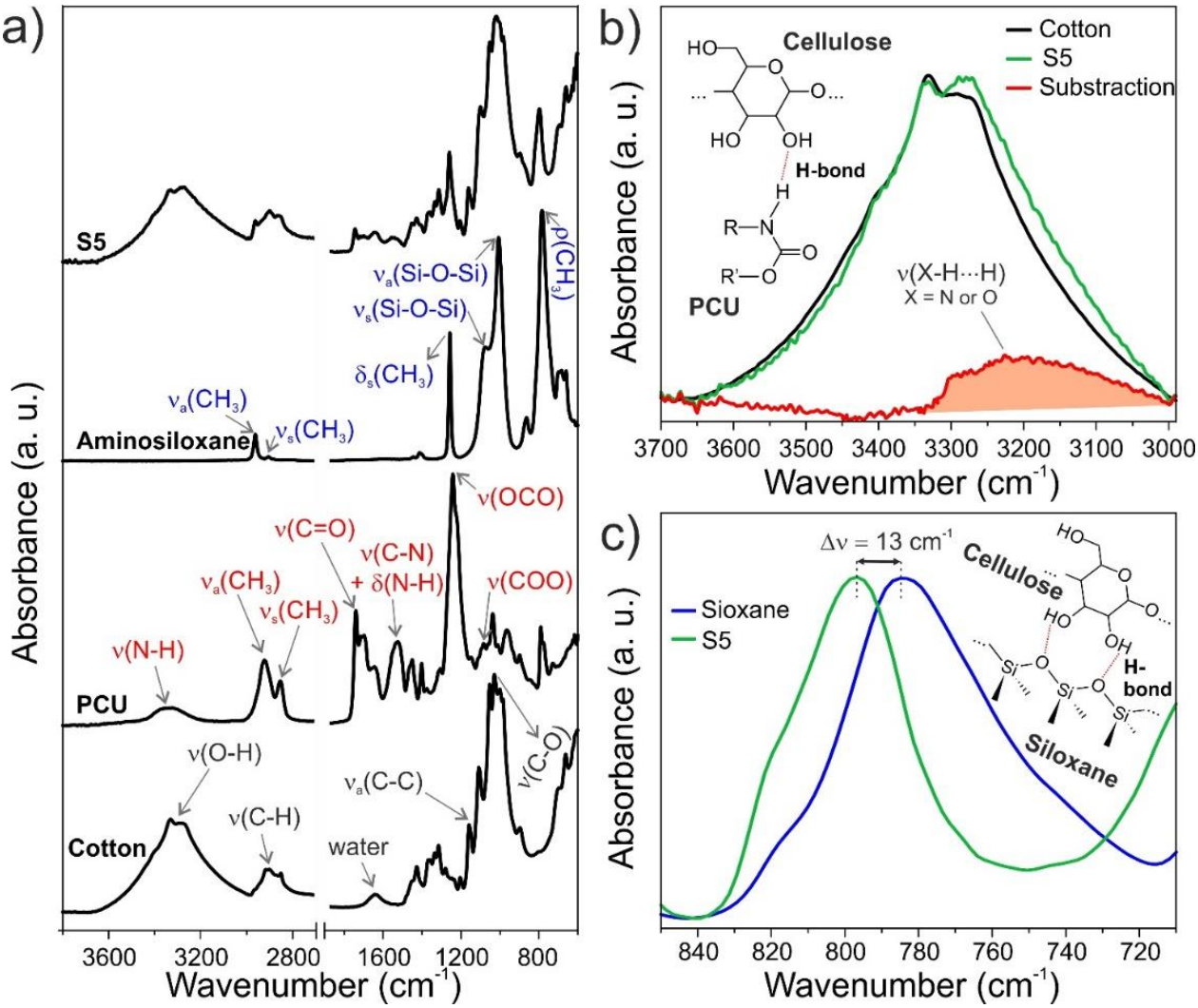

Fig. 2.10. a) ATR-FTIR spectra of cotton, PCU, amino-siloxane, and S5 samples. The main assignments for cotton (black), PCU (red), and amino-siloxane (blue) are included. b) OH stretching band of cotton and sample S5, which is cotton coated with the PCU-siloxane micro-emulsion. The intensity difference is shown by the subtraction of the two spectra. The possible interaction sketch between cellulose and PCU by H-bonds is included. c) CH_3 rocking band of siloxane and cotton coated with the PCU-siloxane micro-emulsion. The shift of the peaks maxima and the interaction sketch between cellulose and siloxane by H-bonds are included.

Fig. 2.10a) shows the single spectra of cotton, PCU and siloxane, described in details in Table 2.3. Moreover, in Fig. 2.10a), the spectrum of cotton treated by spray with the PCU-siloxane micro-emulsion. S5 shows all the characteristic peaks of cellulose, plus contributions coming from both PCU and siloxane. Fig. 2.10b) shows in detail the 3700-3000 cm^{-1}, which corresponds to O-H and N-H bonds. After the protective treatment application there is an increase in O-H/N-H stretching

region. The calculation of the spectra difference highlighted the presence of a band at ~3225 cm^{1}. Hence, it is assumed that urethane groups of PCU and hydroxyl groups of cotton strongly interact with each other by H-bonds [123]. Moreover, Fig. 2.10c) shows the detail of the 840-720 cm^{-1} region, where a ~13 cm^{-1} shift is observed in S5 with respect to pure aminosiloxane. This interaction has already been described in literature [68], [121], [124], [125], [126] in presence of cured PDMS and polysaccharide-rich materials, such as starch, cellulose, and ethyl cellulose. This shift was attributed to the presence of H-bonds between the O-H groups of the polysaccharide and the oxygen of the siloxane groups.

Hence, cellulose molecules of cotton interacted through OH bonds with both components of the micro-emulsions. In particular, we assume that the siloxane bond with cellulose promoted the exposure of the methyl groups to the outer surface and contributed to the enhancement of the hydrophobicity.

2.3.3 Nuclear magnetic resonance NMR

Polymers where studied though nuclear magnetic resonance to further investigate their chemical structure. Fig. 2.11 shows the structure and the NMR spectrum of PCU, which is an aliphatic polyurethane based on a polycarbonate diol. The mol ratio between the isocyanate and polycarbonate monomer was calculated from the ratio between the peaks integration. The blue (2.0) area divided by the red (10.0) area corresponds to 1:5 ratio. Hence, the isocyanate and polycarbonate monomer are present in the polymers with a ration of 1:5, as reported in the chemical formula.

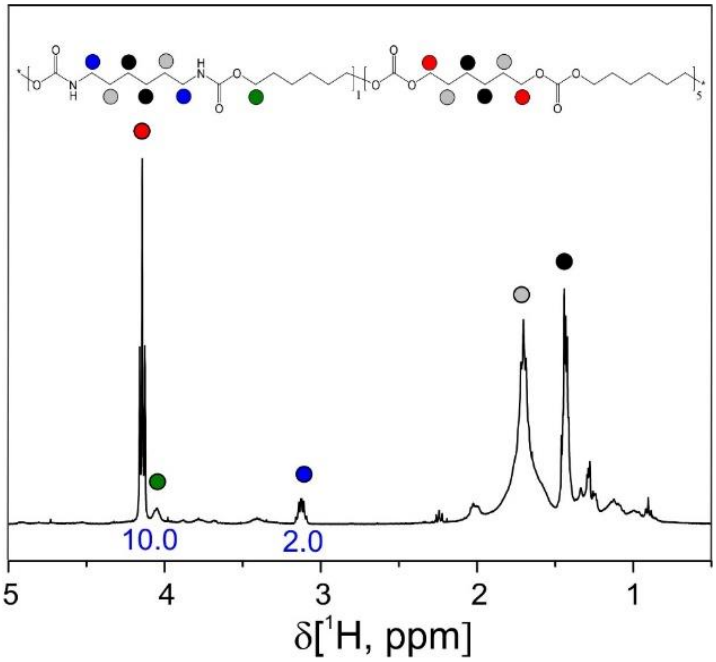

Fig. 2.11. NMR spectrum of PCU.

Fig. 2.12 shows the NMR spectrum of Wacker finish WR 1300, the amino-siloxane. In this paragraph, two methods are used to calculate the monomers ratio in the amino-siloxane polymer.

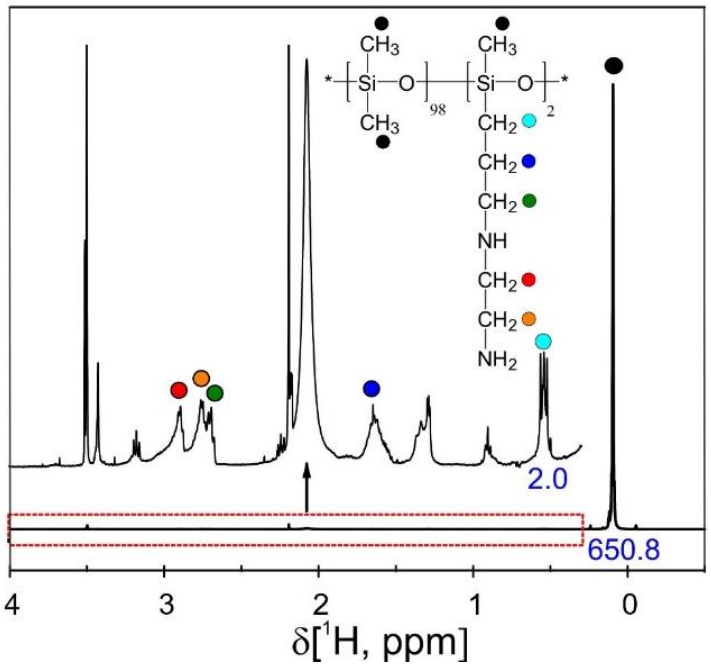

Fig. 2.12. NMR spectrum of amino-siloxane.

The first method is the titration method. It is based on the information on the technical data sheet of the product, which stated that the amine number of the aminoethyl-aminopropyl siloxane is 0.3 mL 1 N HCI/g. So the number of mol cointained in 0.3mL of HCl 1N is:

$$n_{HCl} = \frac{0.3\ mL\ \cdot 1mol}{1000mL}$$

$$n_{HCl} = 3 \cdot 10^{-4}$$

which is the number of mol (n) of HCl used to titrate the 1 g of aminosilicone.

According to NMR analysis, every aminosiloxane-monomer contains two amino-units. So the number of mol of aminosiloxane-monomers in 1 g corresponds to:

$$n_{am.sil.} = \frac{3 \cdot 10^{-4}}{2} = 1.5 \cdot 10^{-4}$$

The structures of the dimethylsiloxane and of the aminosiloxane were identified from the NMR.

The deduced molecular weights (MW) are:

- 74.15 g/mol for the dimethylsiloxane monomer
- 176.29 g/mol for the aminosiloxane monomer

The mass (m) of aminosiloxane monomers in 1 g is:

$$m_{am.sil.} = n \cdot MW$$

$$m_{am.sil.} = 1.5 \cdot 10^{-4} \cdot 176.29 = 0.0264435\ g$$

So the remaining mass is the dimethylsiloxane monomer:

$$1g - 0.02644g = 0.97356g$$

The number of mol (n) of aminosiloxane in 1g is equal to:

$$n_{SiOCH_3} = \frac{0.973556}{74.15} = 0.01313$$

So the percentage fraction of aminosiloxane is:

$$n_{am.sil.}\% = \frac{n_{am.sil.}}{n_{am.sil} + n_{SiOCH3}} \cdot 100$$

$$\frac{0.00015}{0.01313 + 0.00015} \cdot 100 = 1.13\%$$

And the percentage fraction of the dimethylsiloxane monomer is:

$$n_{SiOCH_3}\% = \frac{n_{SiOCH3}}{n_{am.sil} + n_{SiOCH3}} \cdot 100$$

$$\frac{0.01313}{0.01313 + 0.00015} \cdot 100 = 98.87\%$$

Hence, according to the titration method, the two monomers are present with ratio 99:1.

The second method is the peaks integration method. The ratio between the monomers can be calculated from the peaks integration ratio. In Fig. 2.12 a peak is labeled with a light blue dot. It corresponds to the CH_2 group of the aminosiloxane and it has an integration area equal to 2.0. This integration corresponds to 2 protons of CH_2 groups, so to 1 mol of aminosiloxane monomer. Moreover, the most intense peak is labeled with a black dot. It corresponds to the CH_3 groups and its integration area is equal to 650.8. Dividing this value by the 3 protons of the CH_3 group, the resulting number of mol is 217. It is already known that there is 1 mol of aminosiloxane, which also has 1 methyl group. So, the remaining mols of methyl groups coming from dimethylsiloxane are 216. Considering that each mol has two methyl groups, 216 is divided by 2 and the resulting mol number of dimethylsiloxane is 108. The total number of mol is 109, coming from aminosiloxane (1) and dimethylsiloxane (108). Percentage of aminosiloxane monomers is equal to $1/109 \approx 1\%$. The maining 99% corresponds to dimethylsiloxane. So, the final ration is confirmed to be 1:99.

The results obtained from the peaks integration method correspond to the titration method results.

2.3.4 Wettability measurements and surface energy estimation

The surface wettability was measured though water contact angle (WCA) analyses. Pristine cotton is a highly hydrophilic material and its high affinity to water causes several degradation forms, as described in Chapter 1. For this reason, the decrease of the original wettability is a key factor in the efficiency evaluation of applied protective polymers.

The hydrophobicity of treated samples was measured by placing 10 droplets of 5µL each and observing the angle formed by water in contact with the surface. The averages values are reported in Fig. 2.13a. The WCA was not measurable on untreated cotton, since water was immediately adsorbed. All treated samples demonstrated contact angles between 143° and 147°, hence, very high hydrophobicity.

Moreover, the impact of heavier quantity of water was qualitatively evaluated by placing 1 mL of colored water on uncoated and coated fabric. Fig. 2.13b shows the behavior of water, which was immediately adsorbed by S1 untreated cotton. All the other samples, on the contrary, had very low affinity with liquid water. The droplets never penetrated in the cotton threads, it rather evaporated in approximately 10 hours, leaving the colorant on the surface of cotton, as shown in Fig. 2.13d. Here, the shape of the colorant on the surface is exactly the same of the droplet of water, which evaporated and never penetrated. This is also proved by the picture of the rear side of the cotton, reported in Fig. 2.13e.

Dynamic contact angle measurements (roll-off) have also been analyzed to better characterize the hydrophobicity of samples having all similar WCA ranging from 143° to 147°. For this purposed, the concept of droplet mobility has been used: the higher the mobility, the better the hydrophobicity [127]. This study is based on the competition between gravitational and surface tension forces [105] of water droplets on tilted surfaces.

Thus, roll-off or sliding angles of water droplets with volumes ranging from 17.5 to 35 µL were deposited on cotton surfaces. The minimum tilt angles sufficient to create water mobility are reported in Fig. 2.13f. For example, 17.5µL-volume droplets started to roll-off the sample surfaces at 52°, 53° and 58° tilt angles for S5, S2 and S3 fabrics, respectively. The 17.5µL-volume droplet was sticky onto S4 surface, there was water droplet mobility within the 90° of tilting. Then, staring from 20 µL, all samples demonstrated to promote droplet mobility, conferring self-cleaning properties to the fabrics. Overall, the best performances were demonstrated by micro-emulsion spray-coated (S5) sample, which promoted the water rolling off already at 30° for 35 µL droplet volume. This is a excellent result, especially considering that no fluoropolymers or nanoparticles are included in the polymeric coating. Same results were obtained for identical samples which did not udergo the 60°C curing fpr 24 hours. This is particularly interesting, especially considering that this formulation is proposed for Cultural Heritage objects.

a)

static contact angle (°)	
S1	n.a
S2	147° ± 4°
S3	145° ± 3°
S4	143° ± 2°
S5	145° ± 3°

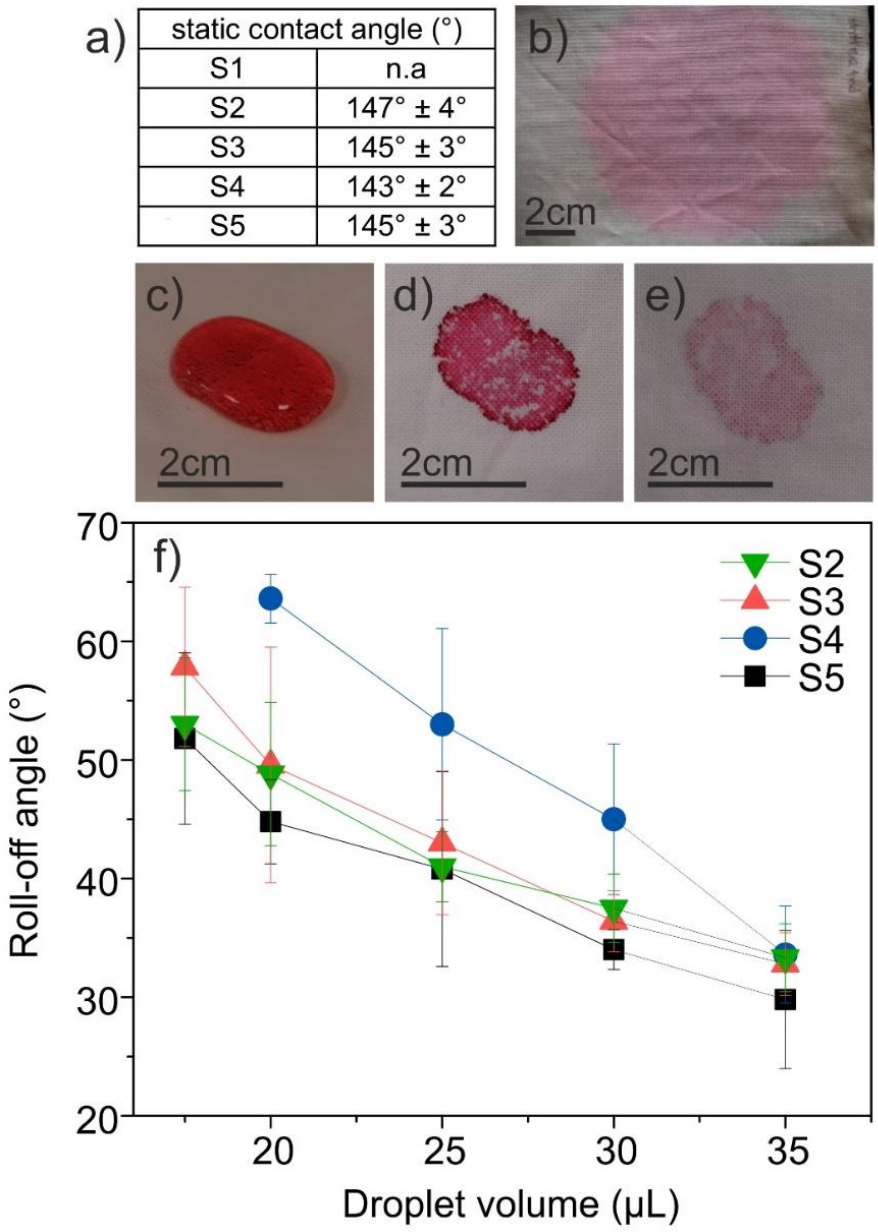

Fig. 2.13 . a) WCAs; b) 1 mL of colored water on S1 (untreated cotton), c) on S5 (micro-emulsion sprayed); d) on front side of S5 after 10 hours; (e) and back side of S5; f) water roll-off angles of different volume droplets on samples S2 (double layer dip coating), S3 (micro-emulsion dip coating), S4(double layer spray) and S5.

Zisman Plot method was then used to determine the micro-emulsion critical surface tension. The variation of Young's WCA as a function of different liquid surface tension was tested. Cos(Θ) of different liquids with well-known surface tensions were plotted versus γ_{LV} and, as demonstrated

by Dr. W.A. Zisman, a linear plot was obtained. The linear regression of the experimental data lead to the linear equation: y=1.52784-0.02756x, with R^2=0.9782, as shown in Fig. 2.14. The critical surface tension was obtained by extrapolating the γ value for which cos(Θ) corresponds to 1 [106]. The resulting polymeric micro-emulsion surface energy was 19.5 dyne/cm, which is a good result, especially if compared to silicone critical surface tensions reported in literature: 22.8mN/m [128], 24.7 mN/m [129], 20.4 dyne/cm [130], and 24 mN/m at 20°C [131]. Overall, we can state that the polymeric micro-emulsion with low surface energy coated a cotton surface with intrinsic micro-roughness and these two factors together contributed to confer high hydrophobicity to the surface.

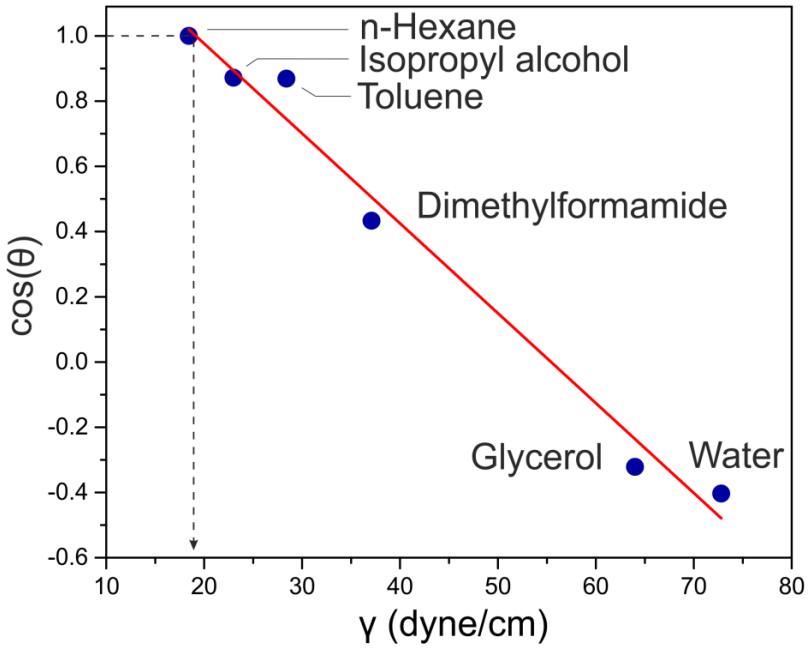

Fig. 2.14 Zisman plot obtained from solvents droplet placed on the polymeric film obtained from the PCU and siloxane micro-emulsion.

2.3.5 Water vapor permeability

Water vapor permeability (WVP) was monitored before and after polymeric treatment to assure that breathability of the cotton remained high, in order to avoid problems linked to the accumulation of humidity (*e.g.* condensation, dissolution of pollutants, formation of mold, moth infestations). The permeability can be maintained at high levels by maintaining opened the porosities between warp and weft or between the fibers in the treads. Moreover water vapour molecuse can diffuse though polymeric layers [132]. The measured WVP of untreated cotton (S1)

is $5.6\times10^{-4} \pm 0.7\times10^{-4}$, which corresponds to a high breathability value. All treated samples maintained a high WVP, in the same magnitude order: $5.7\times10^{-4} \pm 0.7\times10^{-4}$ for S2; $5.3\times10^{-4} \pm 0.1\times10^{-4}$ for S3; $5.7\times10^{-4} \pm 0.2\times10^{-4}$ for S4 and $5.7\times10^{-4} \pm 0.5\times10^{-4}$ for S5. Overall, there is not a significant difference among the applications. This could be due to the fact that porosity between warp and weft and still partially open (see Fig. 2.6), but also to the fact that PCU is known to promote the sorption-diffusion–desorption mechanism for water molecules [133]. According to this mechanism, water vapor molecules are absorbed by the PCU, diffused through the cellulose fiber bulk, transferred to the other side, and finally released to the environment though the rear hydrophilic PCU layer.

2.3.6 Stress-strain measurements

Fig. 2.15a shows the tensile stress-strain curves of samples S1, S2, S3, S4 and S5. This figure also shows a schematic representation of the tress-strain behavior of warp and weft. Warps extremities were constricted in between the instrument clamps, while wefts were free and their sections are represented. The part of the slopes included between 0 and 0.1 mm/mm is the crimp removal zone, which represents the movement of twisted fibers and yarns stretching while adapting to the starting stress. The second part of the slope, starting from 0.1 mm/mm, corresponds to the irreversible stretching of fibers, elongating within the woven network [72]. The Young Moduli associated to both slopes are reported in Fig. 2.15b. The initial elastic moduli are 19.5 ± 2.2 for samples S1, 23.7 ± 3.5 for sample S2, 16.4 ± 0.8 for sample S3, 38.5 ±6.1 for sample S4, and 18.6 ± 2.2 for sample S5. The final moduli are 264 ±28 for sample S1, 205 ±6 for samples S2, 217 ±11 for sample S3, 153 ±31 for sample S4 and 193 ±11 for sample S5. After treatments, the second moduli decreased so all treated samples had more plastic performances with respect to untreated cotton. When the micro-emulsion was applied (S3 and S5), the Young Modulus was maintained more similar to S1, with respect to the corresponding layer-by-layer applications. In Fig. 2.15c the stress at maximum load for all samples are reported: 45.1± 5.7 for S1, 39.1±1.9 for S2, 43.0 ± 4.5 for S3, 32.2 ± 5.1 for S4 and 38.5± 3.6 for S5. Again, samples treated with the micro-emulsion maintained properties more similar to untreated cotton, *i.e.* higher stress at maximum load. Finally, the elongations at break are reported in Fig. 2.15d: 35.6 ±5.0 for sample S1, 35.9 ± 5.2 for sample S2, 38.5 ±3.2 for sample S3, 34.6 ±5.6 for sample S4 and 38.6 ±2.8 for sample S5. So, micro-emulsion treatments conferred slightly higher elongation at break values. Overall, the treatments did not lead to high

variations in the mechanical properties of the fabrics and the best performances are ascribable to micro-emulsions applications.

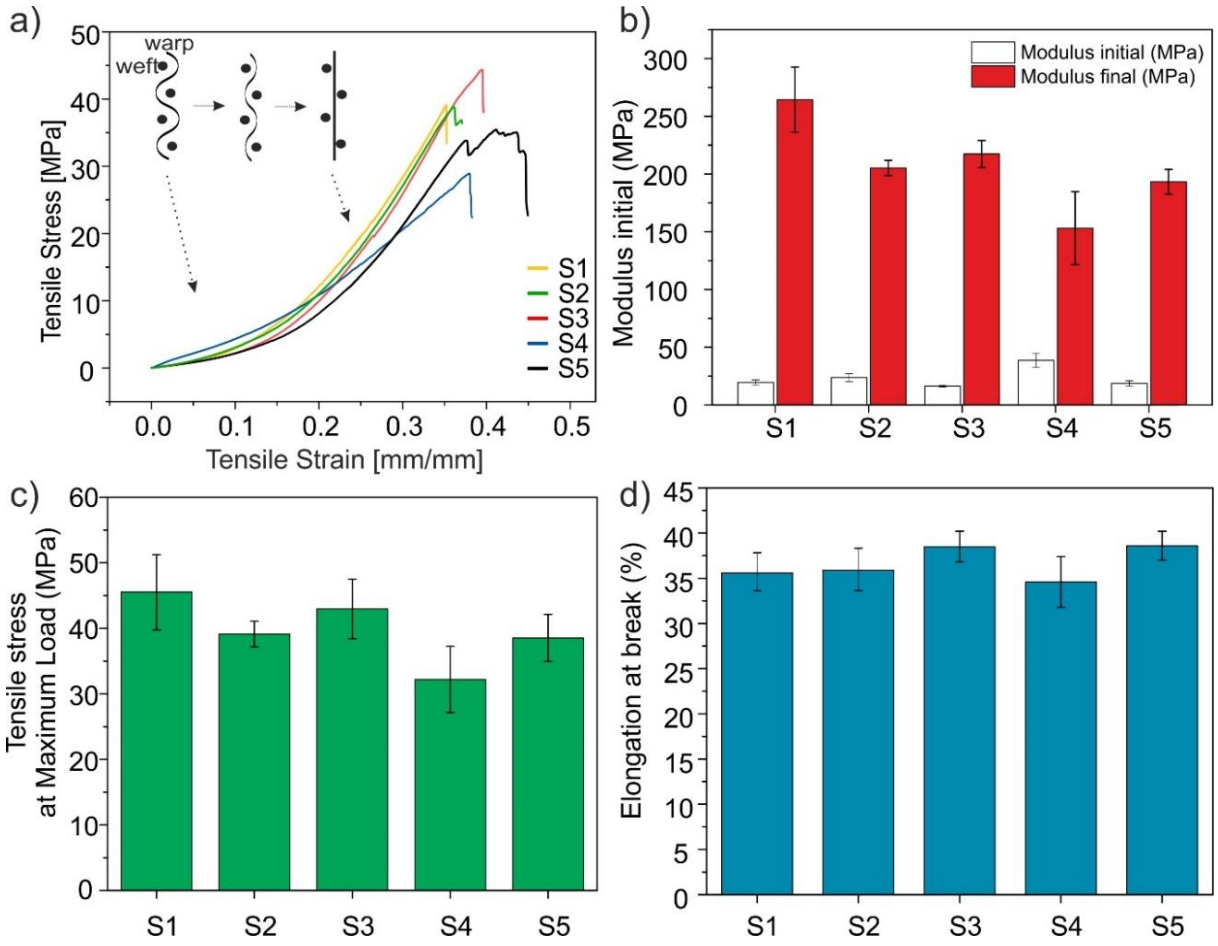

Fig. 2.15. Mechanical tests performed on samples S1, S2, S3, S4 and S5. (a) stress strain curves, (b) Young's modulus calculated on the first (0 to 0.1 mm/mm) and the second (0.1 mm/mm on) slopes, (c) tensile stress at maximum load, and (d) maximum elongation at breakpoint.

2.3.7 Flexural rigidity

Fabric drapability and handling were evaluated by measuring the bending stiffness of the fabric, before and after treatment. This property was very useful to quantify the resistance offered by fabrics while undergoing bending. The bending lengths were measured with the G.Pierce equipment, as shown in Fig. 2.16a for S1 sample, and the G.Pierce value was calculated. The longer the bending length, the stiffer the textile. Fig. 2.16a shows the flexural rigidity of all samples. The samples treated with the micro-emulsion, both by (S3) dip- and (S5) spray- coating,

are the ones showing the highest flexibility. In fact, when touching these samples, their behaviour is indistinguishable from the untreated cotton. Instead, samples treated first with PCU and then with aminosiloxane demonstrated a much higher bending stiffness. This analysis confirmed the behaviour observed stress-strain mechanical tests.

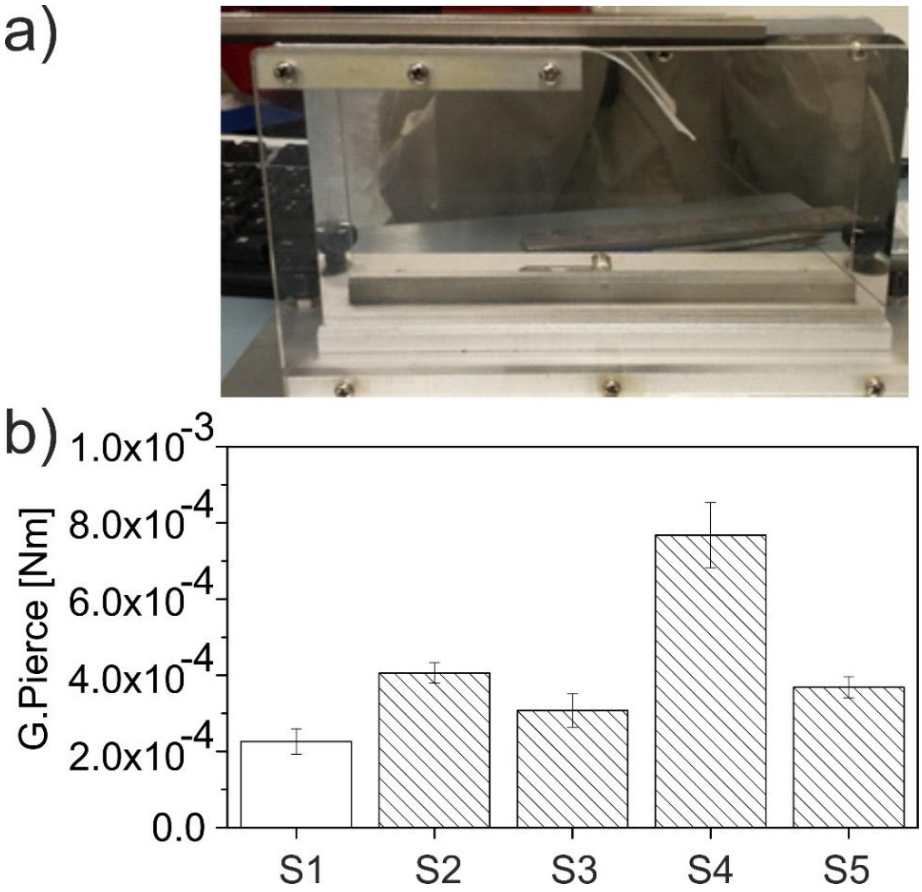

Fig. 2.16 a) S1 sample on G. Pierce equipment b) stiffness values calculated though G.Peirce cantilever test.

2.3.8 Determination of color variations

Checking the colorimetric variation is fundamental in order to evaluate whether the treatment and the aging have an aesthetical impact on the fabric. In fact, both after being treated and being aged, the fabrics should maintain the color variation under the limiting value of 3 in terms of ΔE.

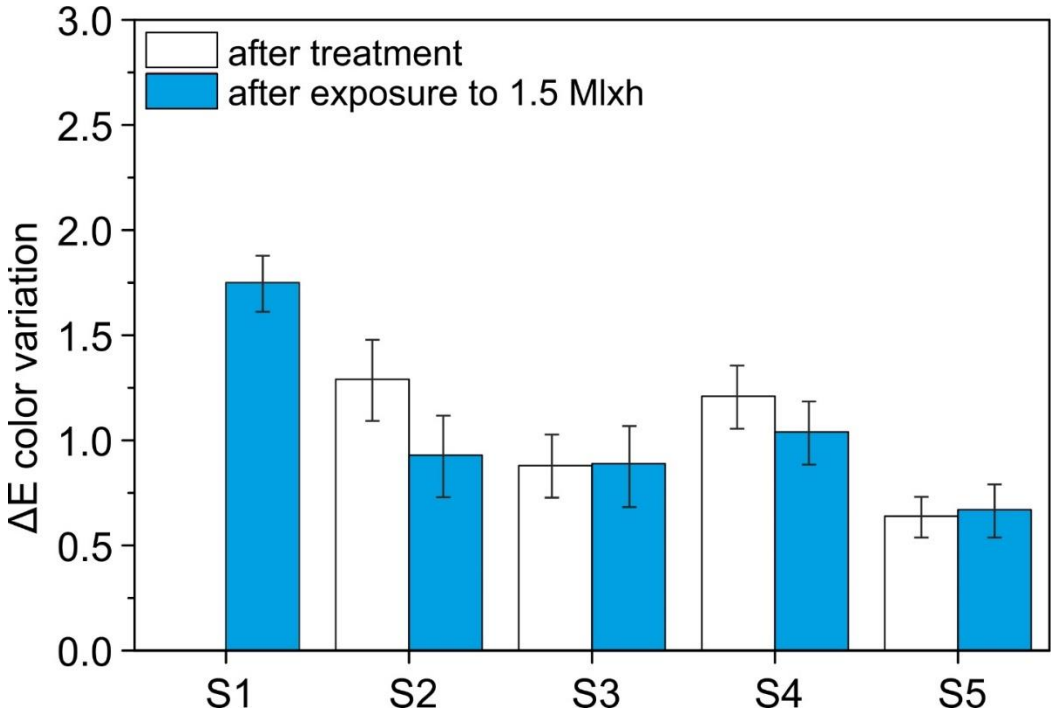

Fig. 2.17. ΔE colorimetric values of samples after treatment (white) and after aging (turquoise) with respect to untreated one.

Fig. 2.17 shows the color variation due to the PCU-aminosiloxane treatments and due to aging in the climatic chamber. All color changes after the polymeric application where much below 3. The best performances, in this sense, were given by PCU-aminosiloxane micro-emulsion applied by spray (S5), where the color change was approximately 0.6. Moreover, S1 sample had ΔE = 1.8 after accelerated aging, simulating 5 years in the museum conservation environment (1.5 million lux·hours of UV-Vis radiation). All treated samples had ΔE included between 0.9 and 1.4, this means that the protective polymers also active as a protective layers towards aging due to UV-Vis radiation. Pictures of the analyzed samples are reported in Fig. 2.18. Concluding, all the proposed treatments were beneficial for the conservation of Heritage-related fabrics.

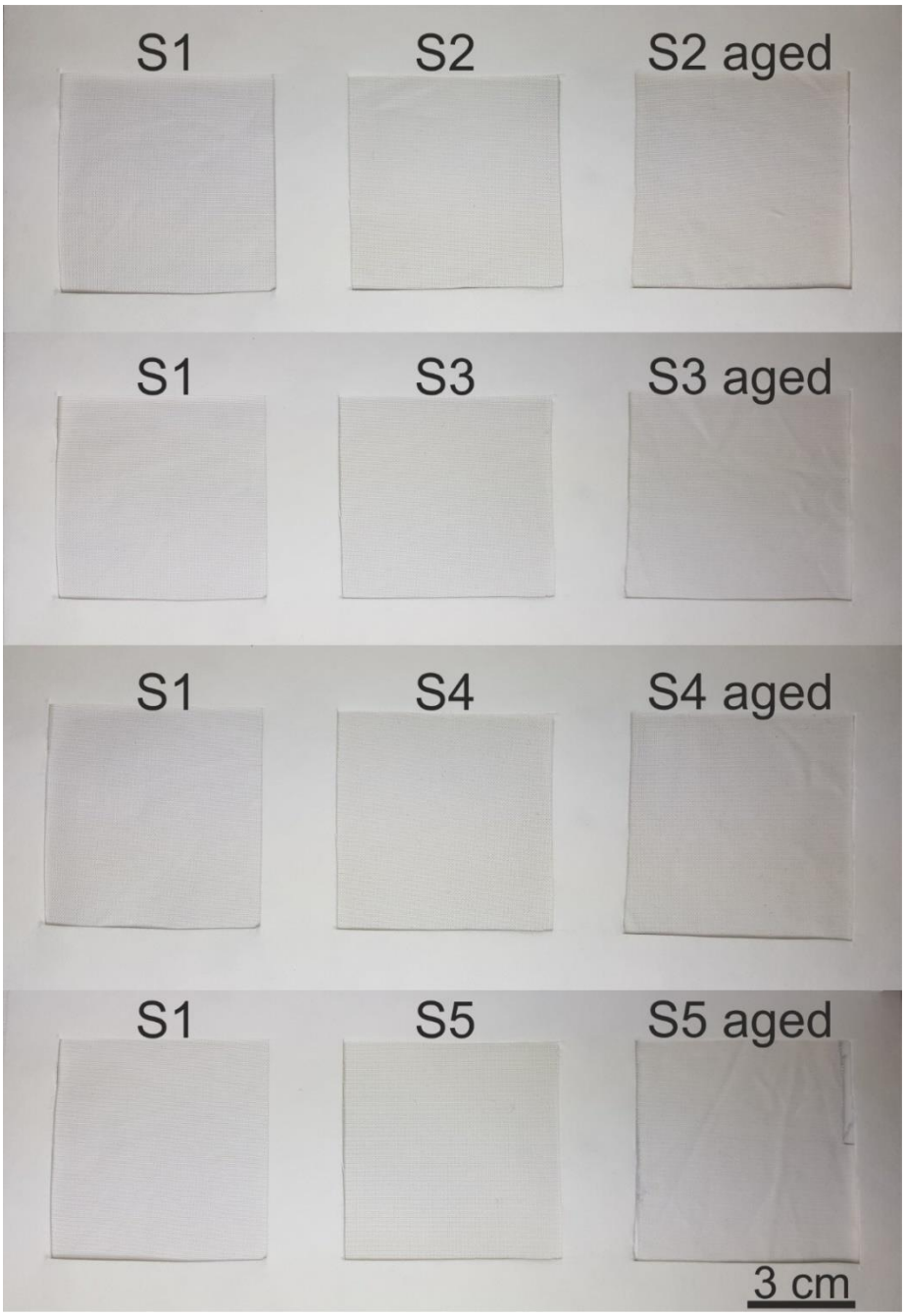

Fig. 2.18. Pictures of untreated cotton (S1) compared to treated cotton (S2, S3, S4 and S5) and to treated and aged cotton (S2 aged, S3 aged, S4 aged and S5 aged).

2.4 Conclusions

This chapter deals with the study of a fluorine free protective coating, focusing mainly on the protection of fabrics from water-linked degradation forms. For this purpose, a micro-emulsion based on aminosiloxane softener and polycarbonate diol polyurethane was created.

Summarizing, the most relevant strengths of this study are:

- The proposed polymers are fluorine-free and easy to purchase. The solvents used are water, ethanol and isopropyl alcohol, they have no environmental hazards. The dip- and spray-coating techniques are easy to apply at low cost;
- The emulsion was stable, with droplet diameters of approximately 1.5 μm and the micro-dimension allowed the polymers to penetrate in the core of the threads, this conferred bulk hydrophobicity to the fabric;
- This single fibers coating also mainlined the high vapor permeability of the fabrics, which in fact was unaltered;
- O-H and N-H bonds were found between the synthetic polymers and cellulose, indicating good compatibility of the polymers and suggesting resistance over time;
- The intrinsic roughness of pristine cotton, added a 19.5-dyne/cm-surface-energy emulsion, conferred high hydrophobicity to the fabrics;
- Water contact angles were always higher than 143°, with roll-off angles of less than 50° depending on the droplet volume; the fabrics could also withstand 1mL of liquid water, which fully evaporated before having the chance to penetrate the fabric;
- The mechanical properties of the pristine cotton fabrics were maintained, especially by the micro-emulsion applications;
- Color variation after polymeric application and accelerated aging are highly acceptable, according to Cultural Heritage conservation criteria.

3. Antioxidant and hydrophobic treatment for fabrics

3.1 Multi-functional coating: a 360-degree protection

In the previous chapter a hydrophobic coating was developed aiming at protecting woven fabrics of great cultural significance from those deterioration phenomena primarily governed by the presence of humidity, such as swelling or shrinkage, pollutants, formation of acids and hydrolysis, microbial/bacterial growth and proliferation. Besides humidity, oxidative degradation with ambient light and oxygen is another alarming source of textile deterioration. The presence of light is of fundamental importance, and storage in the dark is not a viable option for public display and museum profitability.

In literature, the proposal of coatings added with active substances such as UV absorbers[134] [135], antioxidants [80] [136], or oxidizing agent quenchers to reduce the fabrics deterioration [137] is reported. However, these coatings with additives were rarely developed for conservation purposed, so most of them lack of transparency or long term stability check.

Hence, for textile protection from oxidative processes and humidity induced deterioration, in this part of the thesis the use of multi-functional protective coatings is proposed, and, in particular, an antioxidant transparent fluorine-free hydrophobic treatment was in detail designed for the conservation of cotton-based heritage textiles [138].

Since a protocol for simulating peroxidative cotton ageing (relevant to long exposure to light and air) was not present in literature, an aggressive oxidative *ad hoc* protocol has been proposed and tested to simulate an accelerated exposure to harsh oxidation conditions.

3.2 Materials and Methods

3.2.1 Materials

The target of the conservation treatment was the same plain-woven and bleached 100% cotton fabric presented in the previous chapter. The fabric is characterized by a density of 24 threads/cm both in warp and weft direction.

All the following materials were taken into consideration for conservation treatments because of their transparency and no health or environmental danger.

More specifically, polycaprolactone (hereafter, PCL) was selected because of its enzymatic biodegradability but also its durability in aerobic conditions [139] and because of its good elongation and good compatibility with many types of polymers [140]. Powdered PCL was purchased from Polysciences, Inc. (USA).

Single component acetoxy moisture cured polydimethylsiloxane resin (hereafter PDMS) was selected for its hydrophobic properties, water vapour permeability and mechanical properties. The transparent silicone elastomer (ELASTOSIL®E43), was purchased from Wacker (Germany).

The antioxidant butylated hydroxytoluene ($C_{15}H_{24}O$, hereafter BHT) was selected as an antioxidant agent because of its solubility in benzyl alcohol, its transparency after solubilization, miscibility with PCL [141] and minor probability to generate chromophores, especially after undergoing oxidation, with respect to other antioxidants with more conjugated structures, such as ferulic acid [142], [143]. It was purchased from Sigma-Aldrich.

Hydrogen peroxide (H_2O_2) solution 30% (w/w) in water was selected as oxidizing agent. Together with UV light, H_2O_2 is expected to generate hydroxyl radical, which could simulate a natural oxidizing environment. H_2O_2 was purchased from Sigma-Aldrich.

3.2.2 Preparation of the active coatings

The antioxidant solution was created by dissolving 0.50 g of PCL in 25 mL of benzyl alcohol by stirring for 2 h at room temperature. When PCL was completely dissolved, the solution became transparent and 0.50 g of BHT were added to the polymeric solution and stirred for 30 more minutes. Then, 25 mL of acetone were added to the solution in enhance its volatility. This will be

beneficial for the applicability of the antioxidant treatment. Fig. 3.1a shows the proportions of the components used to prepare the antioxidant coating. The hydrophobic solution was instead obtained by stirring 1.00 g of PDMS in 50 mL of heptane for 24 hours. The components are represented in Fig. 3.1b and in this way a 2 % (w/v) homogeneous solution was reached.

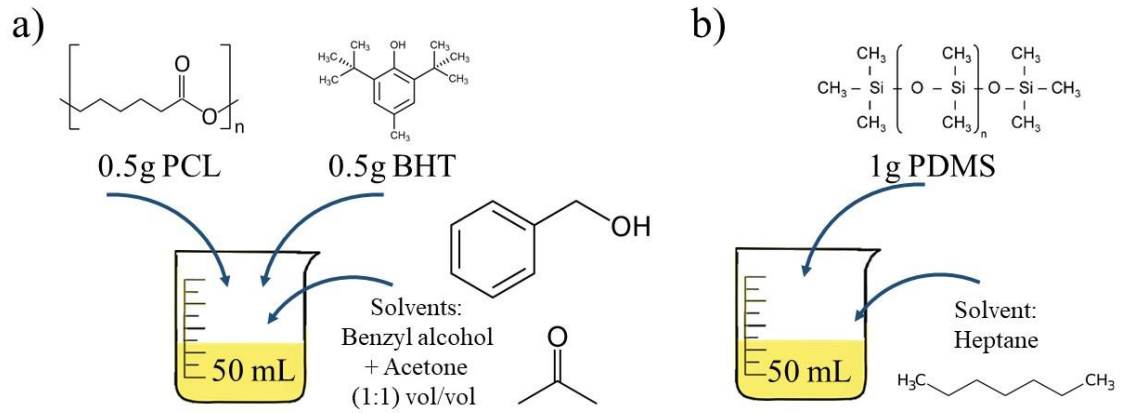

Fig. 3.1. Schematic representations of the preparation of (a) antioxidant and (b) hydrophobic coatings.

3.2.3 Application of the coatings

First of all, the cotton fabric was washed with delicate detergent to remove any possible form of dirt or pollutant, then it was rinsed and hanged to dry at room temperature. Cotton fabrics samples were cut into 5×15 cm^2 shape. Pure cotton samples were labeled as COT. Samples were dipped for 30 seconds into antioxidant solution (PCL-BHT 2% w/v) and immediately hanged to dry at 40°C for 24 hours. 40°C temperature was chosen as a compromise between the desired evaporation of benzyl alcohol, the glass transition temperature of PCL (≈60°C) [144] and caution with respect to real historical/ancient fabrics in Cultural Heritage field. The dip-dry process was repeated two more times and the resulting samples were named COT-AO, where AO stays for "antioxidant". For the additional hydrophobic function, COT-AO samples were immersed for 30 seconds in the PDMS (2% w/v in heptane) solution. Again, they were dried for 24 hours at 40°C. The 40°C curing parameter was chosen in accordance with literature [145], [146], [147] and in order not to compromise the PCL layer and the underneath cellulose. Here, the heating step was particularly important not only to dry the sample but also to accelerate silicone crosslinking process. The samples covered by both the antioxidant and the hydrophobic layers were labeled as COT-AOP, where P stays for "PDMS". All the procedure is schematically reported in Fig. 3.2 and samples

pictures are reported in Fig. 3.3. Moreover, a control sample was created by applying the PDMS solution directly onto cotton fabric. The sample was named COT-P.

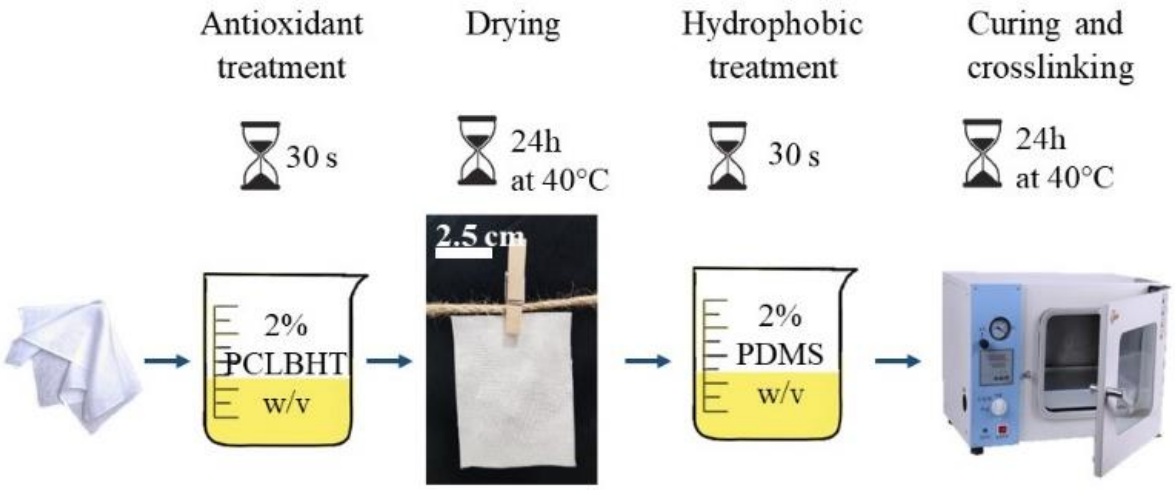

Fig. 3.2. Samples treatment procedure.

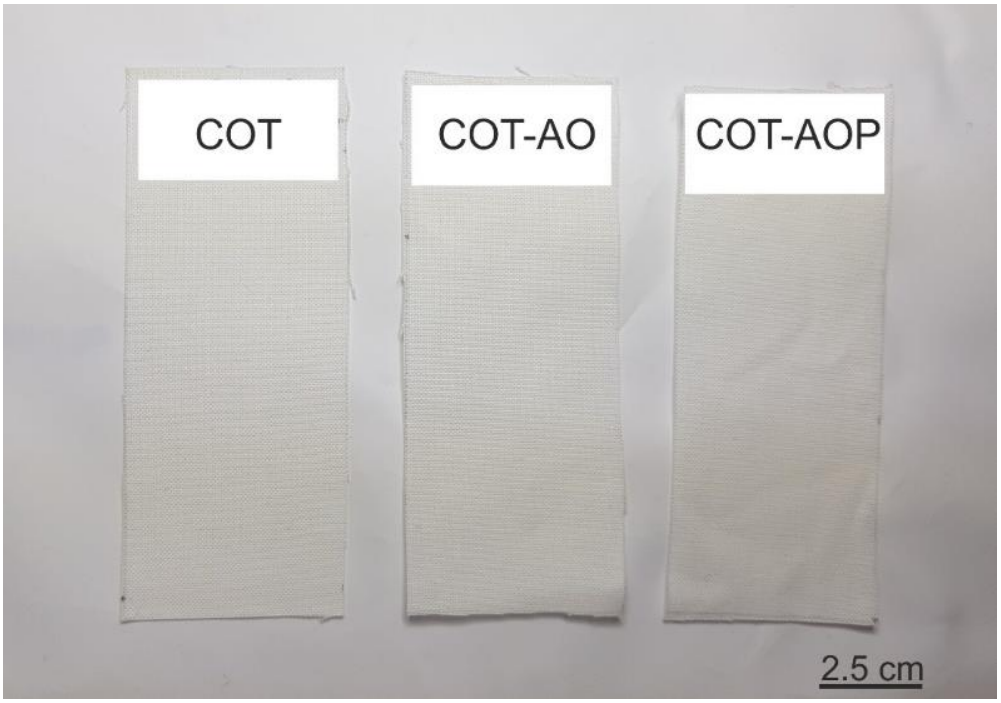

Fig. 3.3 Pictures of untreated cotton (COT), cotton treated with antioxidant coating (COT-AO) and cotton treated with antioxidant and hydrophobic coatings (COT-AOP).

3.2.4 Morphological characterization by SEM

The morphology of COT, COT-AO, COT-AOP samples was observed with SEM microscope. The aim of this analysis was to verify the presence of the coating, to observe how the polymers distributed and to monitor any changing in the porosity of the fabric. The instrument used is a JEOL JSM- 6490LA (Japan), with 10 kV acceleration voltage. Before analyzing the samples with SEM, the fabric surfaces were sputter-coated with a 10 nm thick film of gold (Cressington 208HR sputter coater, UK). Then, images where collected at ×50, ×1000, ×2000 magnifications.

3.2.5 Chemical characterization by Attenuated total reflection–Fourier transform infrared (ATR-FTIR) spectroscopy

The chemical characterization was performed with FTIR spectrometer (VERTEX 70v, FT-IR, Bruker) with a diamond crystal and coupled with (ATR) accessory (MIRacle ATR, PIKE Technologies). Analyses were performed onto COT, PCL, BHT, PDMS and their combinations: COT-AO, COT-P, COT-AOP, also after accelerated aging treatment. For each sample, three spectra of 128 scans each were collected in between 4000 to 600 cm^{-1} with a resolution of 4 cm^{-1}. All spectra were normalized to the maximum peak.

3.2.6 Surface wettability by water contact angle and water roll-off angle

Static water contact angle (WCA) and water roll-off angle were measured with a contact angle instrument (OCAH-200 DataPhysics, Germany). The static angle between a liquid drop and a solid surface is named Young's contact angle, as explained in the Materials and Methods section of the previous chapter. As the water droplets wets the surface, the contact angle approaches zero. Gastight 500 µL Hamilton precision syringe with blunt needle of 0.52 mm internal diameter was used to deposit 5 µL droplets onto surfaces. From each sample, a strip of 1×5 cm^2 was cut and attached to contact angle table with double sided adhesive tape to get a wrinkle free surface for WCA measurements. WCAs, as a function of droplet deposition time, were calculated by the software depending on the droplet shape in the video. The WCA was measured from video frames after 5, 10 and 60 seconds to compare surfaces wettability. Static WCAs at 10 different positions on each sample were measured and reported as mean values with standard deviations.

For roll-off angle measurements, different droplet volumes corresponding to 15 μL, 20 μL, 25 μL, and 30 μL were deposited and the substrate holder was tilted with an angular speed of 1.42°/sec. Side view videos of the rolling drops were captured and from the video the roll-off angle was extrapolated. Measurements were repeated 5 times [105].

3.2.7 Water vapor permeability

Water vapor permeability (WVP) of COT, COT-AO and COT-AOP was calculated at 25°C and 100% RH (%) according to the ASTM E96 standard method. 100%RH was reached by placing 400 μL of deionized water in the permeation chambers of 7 mm inner diameter and 10 mm height. Samples were cut and placed on the top of the permeation chamber, carefully closed with sealing rings, lid and screws. The chambers were then placed in a desiccator, maintained at 0% RH by anhydrous silica gel. The weights of the chambers were recorder every hour for 8 consecutive hours in order to register every weight change and to monitor the permeation of water vapor from the chamber, trough the porosity of the fabric, to the silica gel.

An electronic balance (with 0.0001 g accuracy) was used to weight the chambers containing water and fabric samples. The water mass loss versus time was plotted and the slope of the line was calculated by linear regression. Then, the water vapor transmission rate (WVTR) was determined as below:

Equation 9 $$WVTR(g(m^2d)^{-1}) = \frac{slope}{area\ of\ the\ sample}$$

The water vapor permeability (WVP) of the samples was calculated as follows:

Equation 10 $$WVP(g(mdPa)^{-1}) = \frac{WVTR \cdot L \cdot 100}{p_S \cdot \Delta RH}$$

where L(m) is the thickness of the sample, measured with a 0.001mm accuracy micrometer, ΔRH (%) is the percentage relative humidity gradient, and ps (Pa) is the saturation water vapor pressure at 25°C [107], [108], [109]. Every measurement was repeated 3 times. The graph in Fig. 3.8d shows the WVP values.

3.2.8 Water Uptake

Water uptake measurements were also performed onto untreated and treated fabrics to verify whether the coatings had a blocking effect with respect to the water moisture absorption. First, samples were placed for 24 hours in a dry chamber containing anhydrous silica gel. Then, dry samples were weighed on a sensitive electronic balance (0.0001 g accuracy) and placed in the humidity chamber at 100 % RH. From this moment, each sample was weighted every day at the same hour and the amount of adsorbed water was calculated with respect to the initial dry weight as the difference, according to the following formula:

Equation 11 $$\text{Water adsorption } (\%) = \frac{m_f - m_0}{m_0} \cdot 100$$

Where m_f is the sample weight at 100 % RH condition and m_0 is the sample at 0 % RH. The test proceeded until stabilization of the weight gain. The trend of mass increase over time is reported in Fig. 3.8c.

3.2.9 Stress-strain measurements

Mechanical strength and flexibility of the fabrics are major parameters in textiles conservation field, as explained in Chapter 1. Hence, it is crucial to achieve water-repellency and antioxidant properties without altering the mechanical characteristics of the fabric to a significant extent.

The mechanical properties of COT, COT-AO and COT-AOP samples were tested with 3365 Instron (USA) tensile tester. First, the samples were conditioned at room temperature. Specimens were cut in a dog-bone shaped, with standard dimension of 25 mm length along the axis of warp threads and 3.98 mm width. Samples were placed in between pneumatic clamps. The extension speed was maintained constant at 5 mm/min. in this study, the elastic modulus (MPa) was calculated using the initial slope of the curve, between the starting point 0 and 0.1 mm/mm. Elongation at maximum load was also calculated. The analyses were repeated 7 times for each specimen in order to calculate the averages and standard deviations of elastic moduli and elongation values [110], [111]. Moreover the samples were analyzed after undergoing 1,4 and 7 days of accelerated aging according to the protocol explained in “Accelerated aging and oxidation

treatments" section. Fig. 3.9 and Fig. 3.10 reports the data related to stress-strain measurements, before and after aging, respectively.

3.2.10 Flexural rigidity

The variation of tactile properties, such as bending properties and the drapability of fabrics after a hydrophobic treatment are very likely to happen and they can be quantified by measuring the flexural rigidity tough Peirce Cantilever test. COT, COT-AO and COT-AOP were cut in dimensions of 200mm × 25mm, they were placed on the horizontal board with a metal plate on them. The metal plate gradually slid, until the leading strip of the fabric made contact with the bending angle (Θ=41.5°) indicator. The flexural rigidity G_{Pierce} (Nm) was calculated according to the formula [114]:

Equation 12 $$G_{Pierce} = 9.81 \cdot 10^{-12} \cdot w \cdot l^3$$

where w (g/m^2) is the weight of the analyzed fabric and l (mm) is the bending length measured when the strip touched the Θ angle. So there is a proportion between the stiffness and the bending length of the fabric. A higher value of the bending length indicates higher fabric stiffness [104]. For each fabric, the front and rear side of both extremities were tested, leading to a total of four measurements per sample [114].

3.2.11 Accelerated aging and oxidation treatments

Accelerating aging is extremely important to test the efficiency of the antioxidant treatment onto cotton fabrics, but also to monitor the behavior of the polymers and their possible interactions with the supports.

To simulate an oxidative accelerated aging process, the samples COT, COT-AO, COT-AOP, and COT-P were immersed in a solution of 15% (w/w) H_2O_2 for 1 hour. Then, samples were extracted, the excess hydrogen peroxide was removed and the samples were placed into a climatic chamber (Memmert). The aging process consisted in 24 hours of exposition to three cold light fluorescent lamps (D65, 6500 K) and two UV lamps (320–400 nm) at 70% RH and 25°C.

After undergoing this accelerated aging process the samples are labeled COT(AG), COT-AO(AG), COT-AOP(AG), and COT-P(AG), respectively. A schematic representation of the whole process is shown in Fig. 3.4a.

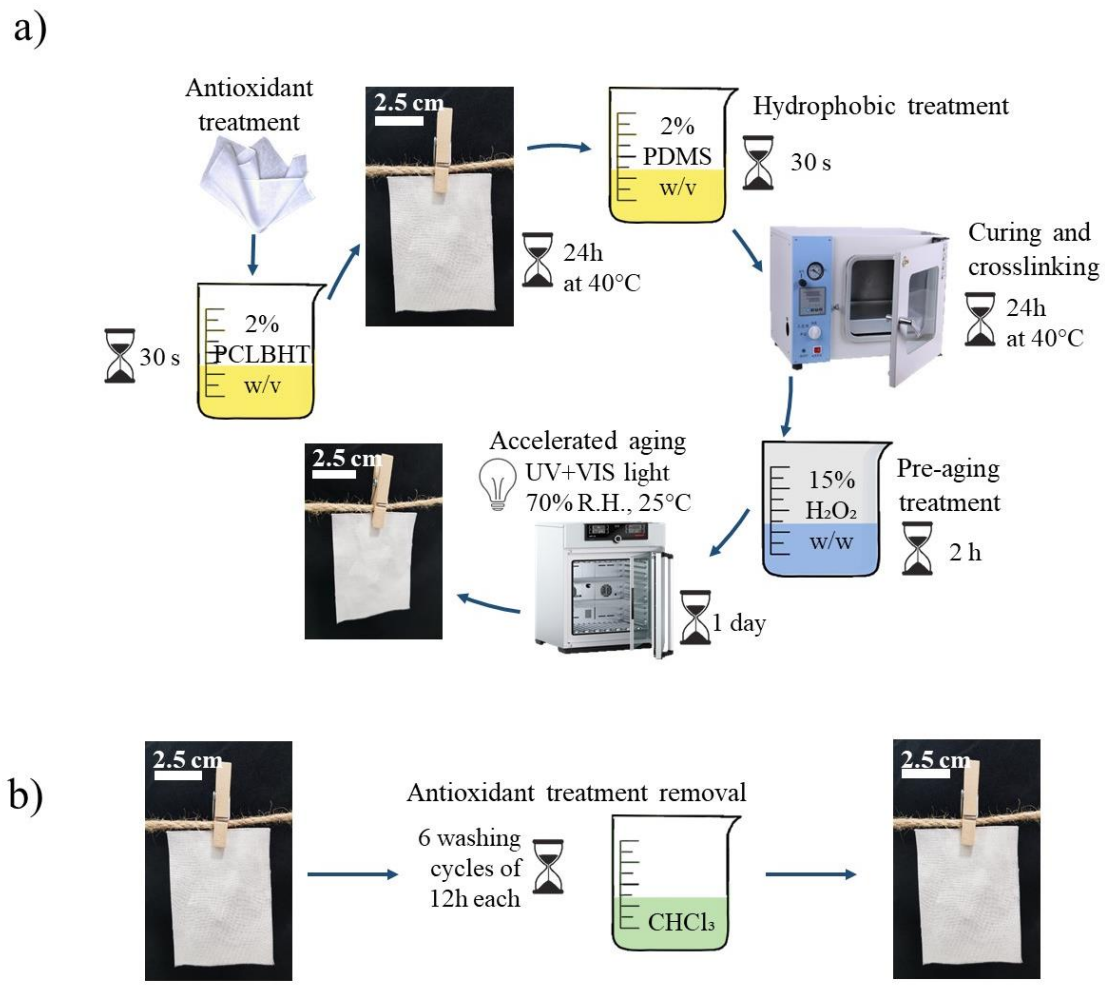

Fig. 3.4 A step-by-step representation of (a) coating, curing, and ageing processes for the fabric and (b) process for antioxidant polymeric layer removal.

Fig. 3.4b shows the steps representing the control of the treatment efficiency. The aged COT-AO samples were soaked in chloroform in order to remove the antioxidant coating (PCL). This would allow the analysis of chemical composition of the bare fabric after the ageing process, without havening any interference with PCL chemical structure. The samples were stirred in chloroform solution for 24 hours and then dried. This process was repeated 6 times to ensure full removal of PCL. The washed COT-AO(AG) samples are named as COT-AO(AG-W). The following **Table**

3.1 summarizes all the treatment and ageing procedures including the sample labels utilized for all the samples studied.

Table 3.1. Sample, treatment composition and labels.

Fabric composition	Treatment	Designation	Designation after ageing
cotton	none	COT	COT(AG)
cotton	PCL-BHT	COT-AO	COT-AO(AG)
cotton	PCL-BHT+PDMS	COT-AOP	COT-AOP(AG)
cotton	PDMS	COT-P	COT-P(AG)

3.2.12 Antioxidant properties

The antioxidant scavenging activity parameter is widely used to define the antioxidant capacity of the materials and, in this case, of the antioxidant coatings present onto the treated textiles [148], [149], [150]. The $ABTS^{\cdot+}$ radical solution was prepared following the standard method reported in the literature [151], [152]. Three replicates for each sample were cut into 1×4 cm^2 shape and were placed into 3 mL of the $ABTS^{\cdot+}$ radical solution. Caps for cuvettes were used to protect the solution from the air and to keep the cotton samples into the cuvettes, avoiding possible floating. This was particularly useful in the case of the hydrophobic samples, forcing them to go in contact with the radical solution. The measurements were collected after 24 hour of immersion by using a Varian Cary 6000i UV-Vis spectrophotometer. The variation of the characteristic absorption peak of $ABTS^{\cdot+}$ at 734 nm was used to calculate the percentage of radical inhibition following the equation

Equation 13 $$\text{Percentage of radical inhibition} = \frac{A_1 - A_2}{A_1} \text{x } 100$$

Where A_1 is $ABTS^{\cdot+}$ radical control solution and A_2 is the absorbance of the sample solution at the same wavelength.

3.2.13 Color variation

The evaluation of colorimetric parameter is of primary concern, especially in conservation science. The proposed treatment should guarantee the preservation of the original color and aesthetic properties of the object [112]. A portable spectrophotometer and colorimeter Konica Minolta CM 2600d was used to measure the color of fabrics before and after applying the protective coatings, also before and after performing accelerated aging tests. The surface area analysis was the small area view (SAV) of 3 mm, used with the 10° detector and the D65 primary source.

Reflectance measurements were analyzed according to the CIEL*a*b color parameters, which gave the Cartesian (L*a*b*) coordinates to identify any colorimetric variation produced by the polymers on the fabric.

The overall color variation, ΔE, represents the deviation from the original value due to the coating, and it is calculated from all the variations of L*, a* and b* parameters, as also reported in the previous chapter:

Equation 14 $$\Delta E^*_{ab} = \sqrt{(\Delta L^*)^2 + (\Delta a^*)^2 + (\Delta b^*)^2}$$

where L* stands for the brightness vector on a gray scale from 0 to 100, from black to white, respectively; a* stands for the red/green color vector with positive values and negative values corresponding to red and green respectively; b* stands for positive values and negative values corresponding to yellow and blue respectively.

3.3 Results and discussion

The samples were measured after both antioxidant and hydrophobic treatment and the overall changes are reported in Table 3.2. Most of the variations are due to the antioxidant treatment, which caused a thickness increase of 4.7% and a mass density increase of 5.3%. Minor is the contribution due to the hydrophobic layer, which, added to the previous PCL-BHT layer, caused a variation of 5.0% in thickness and 7.9% in mass density.

Table 3.2. Names, thickness and weight/area of samples

Sample name	**Thickness (µm)**	**Percent increase in thickness (Δµm%)**	**GSM (Grams per Square meter)**	**Percent increase in GSM (Δg/m²%)**
COT	297 ± 2	-	189 ± 1	-
COT-AO	311 ± 2	4.7%	199 ± 2	5.3%
COT-AOP	312 ± 3	5.0%	204 ± 2	7.9%

3.3.1 Morphological characterization by SEM

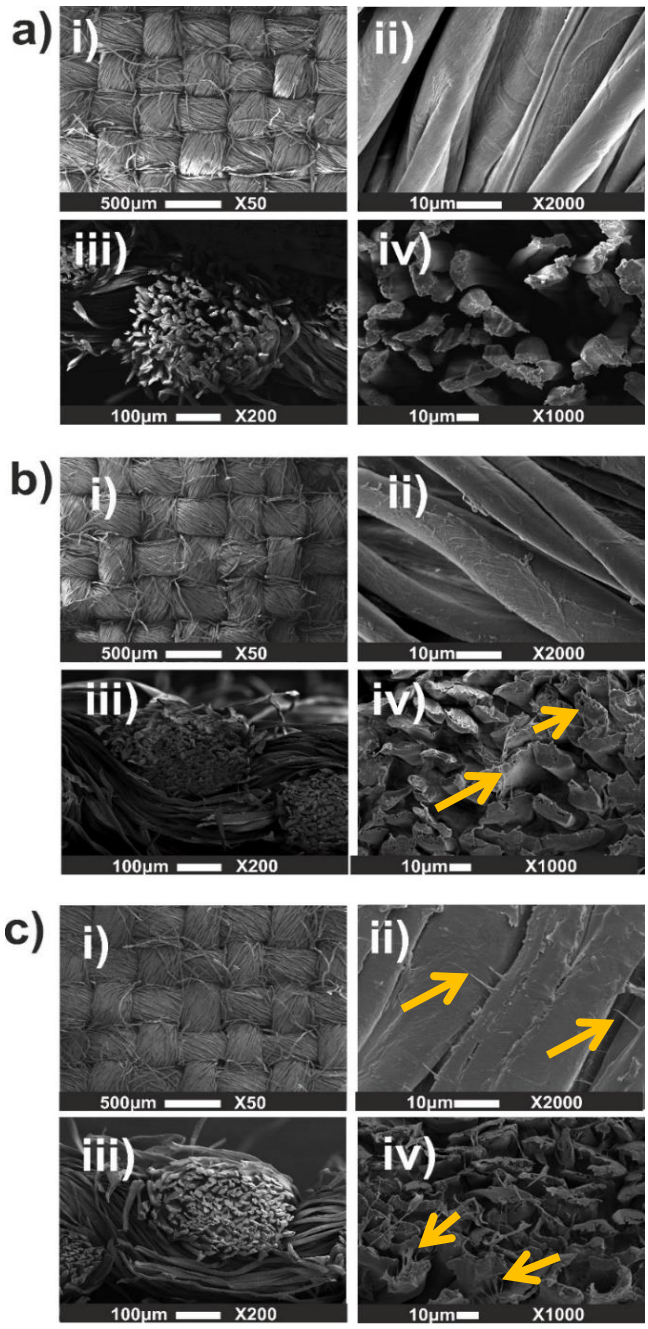

Fig. 3.5 SEM images of (a) COT: untreated sample, (b) COT-AO: cotton with the antioxidant treatment of PCL and BHT, (c) COT-AOP: cotton with the antioxidant treatment of PCL and BHT and hydrophobic treatment of PDMS. For each sample, there are SEM images of the top-view at ×50 (i) and ×2000 (ii) magnifications, and their corresponding cross-sectional images at ×200 (iii) and ×1000 magnification (iv). The arrows indicate the presence of polymeric materials.

Fig. 3.5a i) shows the warp and weft woven together to form the fabric structure, Fig. 3.5a ii) shows the typical wrinkle-like and longitudinal fibril structure [89], [153] of cotton fibres. Fig. 3.5a iii) shows the cross section of a thread at ×200 and, at higher magnification in Fig. 3.5a iv), there is the typical kidney-bean shape of the cotton fiber cross section.

Fig. 3.5b represents COT-AO at the same magnifications. In particular, Fig. 3.5b i) shows the same woven structure as Fig. 3.5a i). The presence of polymeric film is not detectable at ×50, warp and weft are unchanged and the porosity in between them was maintained. Some polymeric traces are visible on the fiber at ×2000 and some polymeric filaments are highlighted by the yellow arrows at ×1000 in Fig. 3.5b iv). These pictures suggests that the polymer is present and covers the fibers, adapting to their shape, leaving the macroscopic morphology of the woven structure unchanged.

Fig. 3.5c shows the morphology of COT-AOP, which is very similar to COT-AO. In fact, the presence of the polymeric layer is invisible at ×50 and ×200, in the top view and cross section respectively, while the presence of polymeric filaments is detectible at higher magnifications. The yellow arrows show at ×2000 and ×1000 the presence of the filaments. Especially at ×2000, the presence of polymeric filaments is more evident, probably because of the double layer of PCL and PDMS.

Although the antioxidant and hydrophobic treatment were not detectable to the naked eye, their presence was verified thanks to SEM observations at 2000 and 1000 enlargements.

As a consequence of the observed unchanged morphology, we expected to verify unchanged breathability of the woven textile, as it is reported in Fig. 3.8a.

3.3.2 Chemical characterization by Attenuated total reflection–Fourier transform infrared (ATR-FTIR) spectroscopy

Table 3.3. ATR-FTIR peak interpretation of Cotton, PDMS, BHT and PCL.

Cotton [38], [119], [120]		PDMS [121]	
Wave number (cm^{-1})	Functional group	Wave number (cm^{-1})	Functional group
3283	OH stretching	2963-2905	Asym. and sym CH_3 stretch.
2897-2866	Asym. and sym. CH_2 stretch.	1258	CH_3 symmetric bending
1643	O-H bending. Adsorbed H_2O	1074	Si-O-Si symmetric
1427	CH_2 scissoring	1007	Si-O-Si asymmetric
1364	CH bending	783	CH_3 rocking
1336	OH in-plane bending	BHT [154]	
1314	CH_2 rocking	3624	O-H stretching
1282	CH deformation stretch	3071	Aromatic C-H stretching
1201	C-O stretching	2953-2911	Asym. and sym. CH_2 stretch.
1159	Asym. bridge C-O-C stretch.	1431	C=C aromatic stretching
1105	Asym in-plane C-O-C stretch	1148	C-O stretching
1053	Asym. C-O stretching	PCL [155]	
1028	Sym. C-O stretching	2942-2866	Asym. and sym. CH_2 stretch.
986	ring stretching modes	1724	C=O stretching
897	Asym. out-of-phase ring stretch: C_1–O–C_4; b glucosidic bond	1238-1162	asym and symm C-O-C stretch.

The typical peaks of cotton are summed in Table 2.3. All the mentioned peaks are also visible in the spectrum named COT in Fig. 3.6a. As expected, there is no peak corresponding to C=O stretching in the spectral region 1800-1700 cm^{-1}.

All the characteristic peaks of PCL and BHT are described in Table 2.3 and represented in the spectra named PCL and BHT, respectively, in Fig. 3.6a.

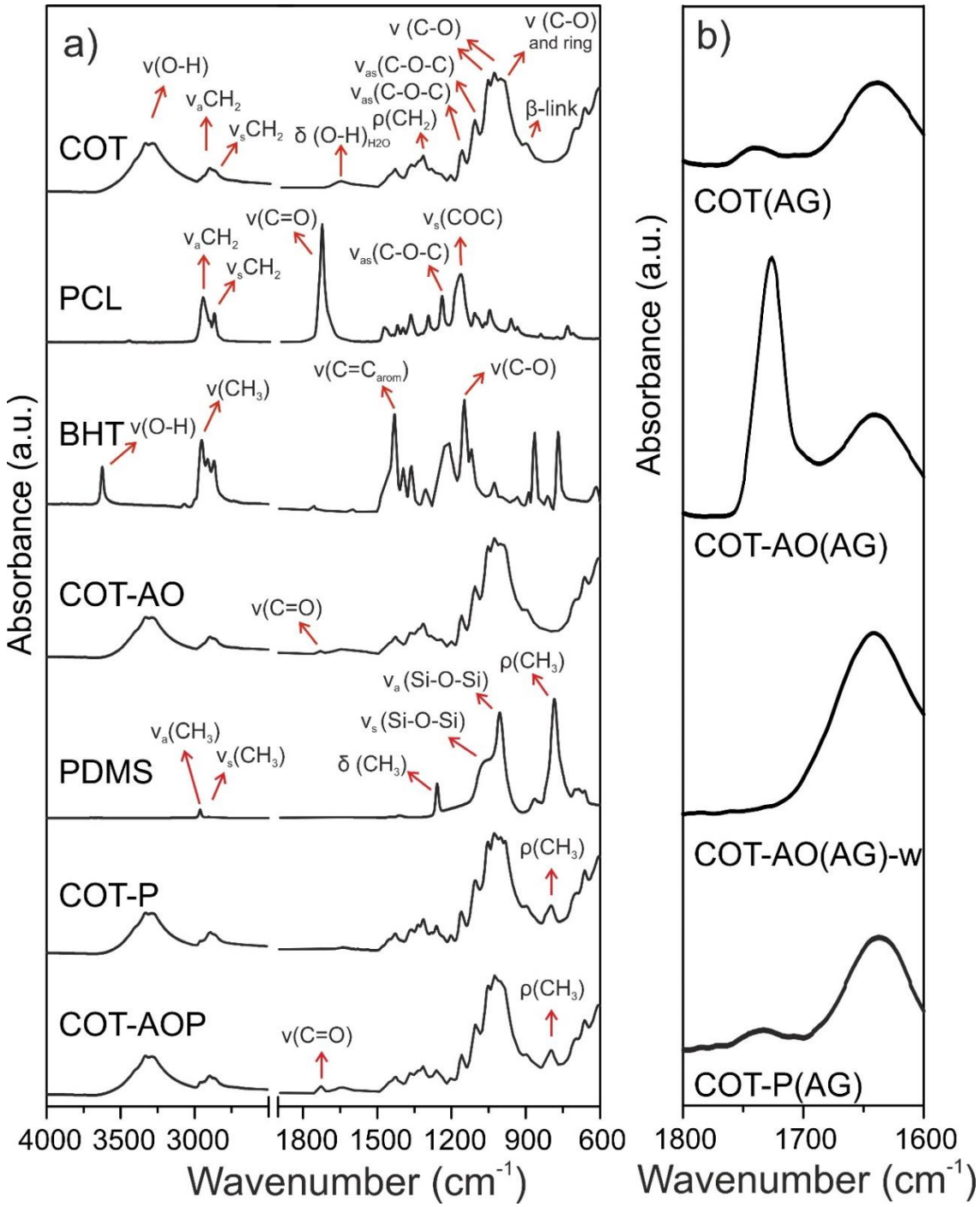

Fig. 3.6 (a) ATR-FTIR spectra of cotton fabric, PCL, BHT, COT-AO, PDMS, COT-P, and COT-AOP in the 4000 - 600 cm-1 region. The main assignments for cotton, BHT, PCL and PDMS are included. (b) The region at 1800 – 1600 cm-1 where the carbonyl band appears in the samples COT(AG), COT-AO(AG), and COT-P(AG), while it is not visible in the sample COT-AO(AG-W).

After dipping the cotton in the PCL-BHT solution, a spectrum of COT-AO was taken and it is reported in Fig. 3.6a. This spectrum is mainly characterized by cotton peaks, except for the C=O stretching peak typical of PCL, which appeared at 1724 cm^{-1}, confirming the presence of the polymeric coating.

PDMS main peaks are reported both in Table 2.3 and Fig. 3.6a. Moreover, a control sample of cotton dipped into PDMS was analysed and reported in Fig. 3.6a, with the name COT-P. This spectrum shows all the typical peaks of cellulose, as well as the increase in intensity of the peak at 1258 cm^{-1} and the appearance of CH_3 rocking mode at 795 cm^{-1}, characteristic of PDMS. Again, no bands were found in the area of 1750-1720 cm^{-1}, so, as expected, PDMS does not show any peak in the carbonyl area.

The presence of PCL and PDMS peaks onto cotton confirmed the presence of the antioxidant and hydrophobic layer, as it was also demonstrated by the SEM microscopic pictures.

As it was reported in the introduction chapter, the oxidative process is one of the natural aging processes of cellulose. Oxidation results in the rise of carbonyl groups along the polysaccharide backbones. This chemical change can be monitored by observing the characteristic peak in the spectral region 1750-1720 cm^{-1}, associated with the C=O stretching of the oxidation.

Before performing the oxidative aging, the C=O peak is not present in COT spectrum. After exposing the COT sample to 24 hours of oxidative environment an oxidation peak appeared at 1740 cm^{-1} appeared onto COT(AG), as shown in Fig. 3.6b. Hence, the new peak in the chemical structure of cellulose can be associated with an oxidative reaction. Fig. 3.7c shows a hypothetical oxidation reaction of C_6 of cellulose, where the CH_2OH group is oxidized to COOH.

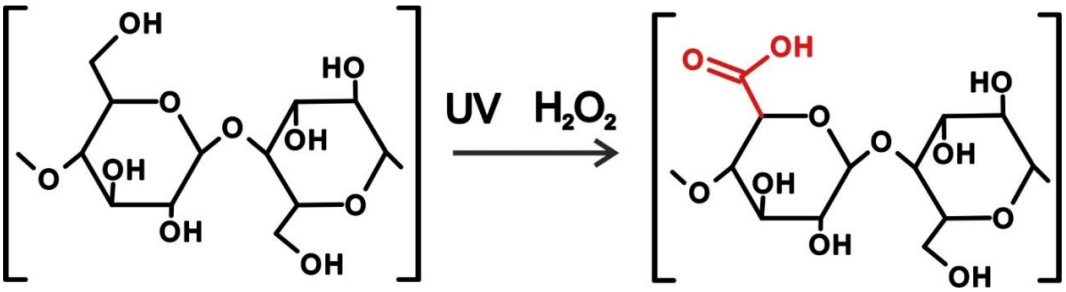

Fig. 3.7. A representative model of the chemical reaction occurring in cellulose through the accelerated ageing treatment.

Also COT-AO underwent the accelerated aging, to verify the efficiency of the PCL-BHT antioxidant later.

Unluckily, it was impossible to have an immediate feedback about the efficiently of the treatment, due to the presence in the same spectrum area of both the C=O group associated with the PCL (1724 cm^{-1}) and the C=O group associated with the cellulose oxidation. Hence, soaking the COT-AO(AG) sample in chloroform was the most efficient solution, in order to dissolve and remove the PCL from the fibers surfaces and observe the chemical composition of cotton fibres. The spectrum of sample COT-AO(AG) after PCL removal, named COT-AO(AG-W), is reported in Fig. 3.6b. After the PCL removal there was no peak at all in the spectral region 1750-1720 cm^{-1}. Thanks to this missing peak, two things were clear: all PCL was efficiently removed by chloroform and the antioxidant layer was demonstrated excellent efficacy in preventing oxidation.

To ensure that washing with chloroform did not alter or interfere with the oxidation peak of aged-cellulose, COT and COT(AG) were washed or soaked in chloroform six consecutive times; at the end of these washing cycles, the oxidation peak was still present. Hence, the chloroform did not interfere with the chemical structure of cellulose.

The control sample COT-P, also underwent accelerated aging and COT-P(AG) is reported in Fig. 3.6b. The peak at 1740 cm^{-1} is evident, indicating that cellulose was oxidized despite the presence of the silicone coating. In fact, PDMS is known to have poor gas and moisture barrier properties [156], [157] and it likely allowed the permeation of oxidizing agent to get in contact with cellulose. Hence, despite the excellent hydrophobicity of PDMS, it appeared to be ineffective in preventing oxidation of the underlying cellulose. This test confirmed the necessity to apply a specific coating to prevent oxidation, between cotton and the hydrophobic layer.

3.3.3 Water-linked properties: Surface wettability, Water vapor permeability and Water Uptake

Surfaces wettability was studied though static water contact angle (WCA) and water roll-off angle. WCA of pristine cotton was impossible to analyze. As expected, the droplets of water were immediately absorbed by the cotton, due to its high wettability and hygroscopicity The wettability of the fabric slightly decreased after the treatment with the PCL-based antioxidant treatment. In

fact, the droplets of water were not absorbed immediately, but after 10 seconds, as reported in Fig. 3.8a. High hydrophobicity was reached after applying the PDMS layer. Indeed, a contact angle of 144° was exhibited by COT-AOP, from which the water was never absorbed, it rather evaporated. The constant 144° WCA into COT-AOP is reported in Fig. 3.8a.

Roll off angles were then analysed to characterize the dynamic surface wettability of the cellulose surfaces covered by the double functional coatings (COT-AOP) and the control sample covered only by PDMS (COT-P). The tests were not performed onto COT and COT-AO, because of their high wettability, as shown Fig. 3.8a. Droplets of volumes ranging from 15 μL to 30 μL were deposited on the surfaces and the tilt angles were registered. COT-P showed water roll-off angles from 35° to 21°, while COT-AOP showed water roll-off angles from 52° to 26°. Overall, similar droplet mobility trends were found: the higher the water volume, the smaller the roll-off angle. This was due to the competition between gravitational and surface tension forces, as shown in Fig. 3.8b [105]. Moreover, a test with 100 μL of coloured water droplets onto COT-AOP was performed. The droplets were coloured to better detect the penetration of water in the fabrics. The double functional coating resisted this high volume of water, which fully evaporated without penetrating.

Then, water vapor uptake was monitored by placing all samples in 100 % RH, until their mass changes reached equilibrium. After 5 days, there was no significant variation, so the 5^{th} day was considered the point at which the maximum quantity of the water vapor was absorbed. The graph reported in Fig. 3.8c shows that water vapor uptake of COT increased 8.3 ± 0.2 % with respect to its initial weight. The weight increase after 5 days of the sample COT-P was 7.6 ± 0.2%, *i.e.* slightly lower than COT. This result was expected, in fact it is well known from literature that PDMS is quite permeable to water vapor [156] [157]. The polymeric antioxidant layer, instead, had a more remarkable effect in the prevention of moisture absorption. The samples COT-AO and COT-AOP exhibited a mass increase of 6.1 ± 0.1 % and 6.2 ± 0.1 %, respectively, as shown in Fig. 3.8c. Again, the presence of PDMS in COT-AOP did not substantially contribute to the protection from water vapor.

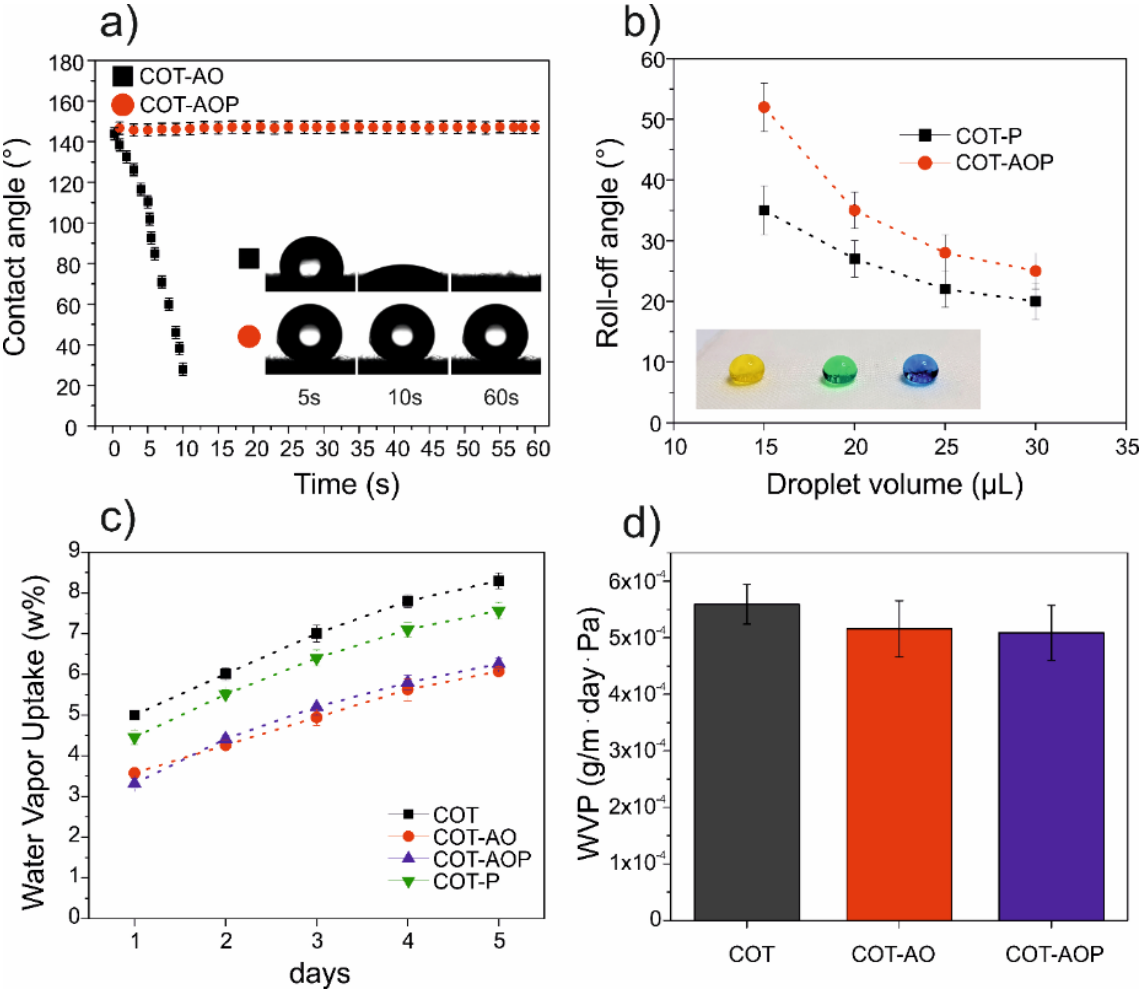

Fig. 3.8 (a) Water contact angles as a function of droplet deposition time. Static WCA are reported at 5s, 10s, 60s for the samples COT-AO and COT-AOP. (b) Water roll off angle of the samples COT-AOP and COT-P0; colored water droplets of 100 µL onto the sample COT-AOP. (c) Water vapor uptake of the samples COT, COT-AO, COT-AOP and COT-P kept at 100 % R.H. for 5 days. (d) Water vapor permeability of the samples COT, COT-AO and COT-AOP.

Finally, the breathability of the fabric samples was tested through water vapor permeability (WVP) test. The first (PCL-BHT) and the second (PDMS) polymeric treatments were meant to confer antioxidant and hydrophobic properties to the fibers, respectively. Moreover, the treatments are expected not to occlude the porosity between warp and weft or between the fibers in the threads, to prevent humidity accumulation and, consequently, all the deterioration forms liked to humidity and mentioned in Chapter 1. The average WVTR of the untreated cotton resulted to be ~ 5866 ($g/m^2 \cdot day$), which corresponds to WVP ~ $5.5 \cdot 10^{-4}$ g (m day Pa)$^{-1}$. These data matched with the high breathability exhibited by woven cotton. After applying the antioxidant and hydrophobic

layers, all analyzed samples exhibited WVP values similar to the original fabric ones. Fig. 3.8d shows that WVP decreased only by 8% for COT-AO and 9% for COT-AOP. This high breathability could be maintained after the protective coating applications thanks to the ability of the polymers to penetrate in the bulk and to cover every fiber, without occluding the porosities, as it was confirmed through the SEM images in Fig. 3.5.

Concluding, the protective treatments did not remarkably modify the breathability and the porosity of the fabrics, keeping the original structure and appearance of the fabric unchanged. They rather decreased the hygroscopicity of the samples, lowered the wettability and enhanced the mobility of liquid water on the surfaces. All these properties are beneficial for the conservation of fabrics in Cultural Heritage field, because they reduce the risk of swelling, shrinking, biological attack and biodeterioration.

3.3.4 Mechanical characterization

Fig. 3.9a represents the tensile stress-strain curves of COT, COT-AO and COT-AOP samples. The low strain behavior (from 0 to 0.1 mm/mm) in the stress-strain curves coincides with the crimp removal zone. The results concerning this part of the slope resulted from straightening crimped yarns. After crimp removal started the second part of the slope, which corresponded to the actual yarn behavior analysis. Here, individual fibers started elongating within the woven network [72].

The Young's modulus associated with both slopes is reported in Fig. 3.9b. it is evident that, after treatment, a slightly higher stress was required to strain the crimped yarns. Concerning the second part of the slopes, the elastic modulus was measured to be ~270 ± 25 MPa for the sample COT, ~287 ± 12 MPa for the sample COT-AO and ~228 ± 8 MPa for the sample COT-AOP, as reported in Fig. 3.9.

In Fig. 3.9c the values of stress at maximum load for each sample are shown. A diminished stress was found in treated samples: ~50 ± 3 MPa for the sample COT (pristine cotton fabric), ~39 ± 3 MPa and ~42 ± 2 MPa for the samples COT-AO and COT-AOP.

Finally, Fig. 3.9d shows the results of maximum elongation at break. The pristine cotton fabric (COT) exhibited a maximum elongation at break of ~37 ± 2 %. Treated samples COT-AO and COT-AOP, instead, reached an elongation of ~26 ± 2 % and ~31 ± 2 %, respectively.

The mechanical test was performed in order to verify that the treatment did not cause remarkable variations in the mechanical properties of the starting woven cotton fabric. The results show that the proposed antioxidant and hydrophobic treatments did not focus on enhancing the mechanical properties of the fabrics.

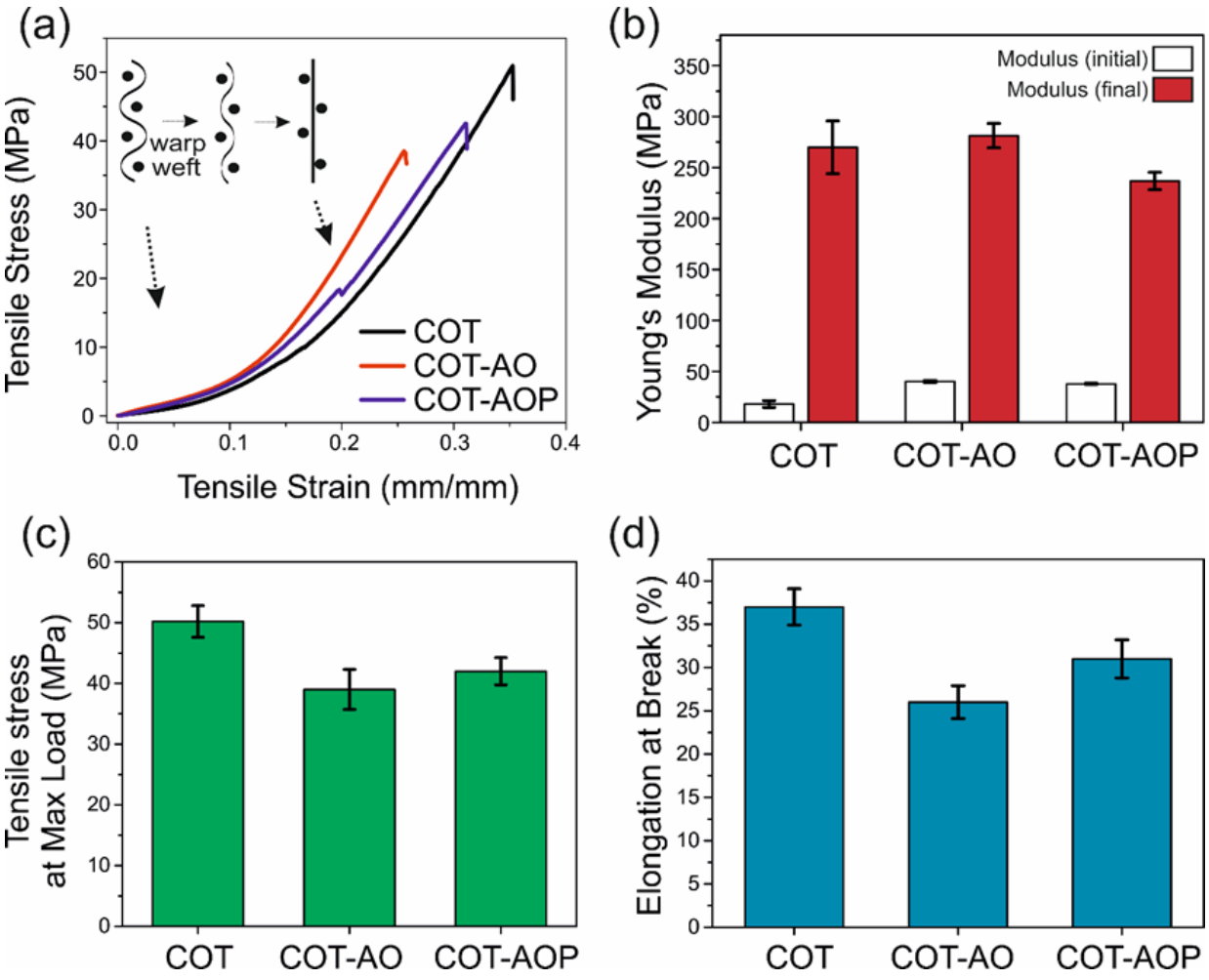

Fig. 3.9 Mechanical tests performed on the samples COT, COT-AO and COT-AOP. (a) stress strain curves, (b) Young's modulus calculated on the first (0 to 0.1 mm/mm) and the second (0.1 mm/mm on) slopes, (c) tensile stress at maximum load, and (d) maximum elongation at breakpoint.

The mechanical properties of untreated and treated fabrics were also tested after accelerated aging. According to the developed protocol, the accelerated aging procedure lasted 1 day. In order to stress the samples and observe the mechanical behaviors in extreme conditions the samples were aged also 4 and 7 days. The mechanical data of 0, 1, 4 and 7 days are compared in Fig. 3.10.

The first modulus, corresponding to the crimp removal zone, was basically unchanged for the different samples after aging: COT went from 28±3 to 9±1 MPa, COT-AO went from 30 ±2 to 15±1 MPa and COT-AOP went from 26±1 to 11±1 MPa. The Young's modulus concerning the second part of the slope drastically decreased for COT, as shown in Fig. 3.10a. It passed from 285 ±16 to 22±5 MPa. When the samples were coated with the protective treatment, the modulus decreased less drastically: COT-AO went from 274±20 to 57 ±2 MPa and COT-AOP went from 257±15 to 41±10. The trend was similar for stress at maximum load, as represented in Fig. 3.10b. COT could withstand a stress of 54 ±3 MPa at the beginning and only 2±1 MPa after 7 days. COT-AO passed from 45±5 to 5±1 MPa, COT-AOP passed from 47 ±2 to 3±1 MPa. Finally, the elongation a break (Fig. 3.10c) were calculated to pass from 31 ±1% to 11±1 % for COT, while COT-AO demonstrated 29±2 % before aging and 17 ±1% after 7 days of aging; COT-AOP passed from 31±1 % to 16 ± 1% in 7 days.

To sum up, the mechanical properties exhibited by untreated samples after 7 days of accelerated aging were very poor. The developed treatment, which mainly focused on hydrophobic and antioxidant properties, could partially slow down the mechanical deterioration of the underneath cotton yarns.

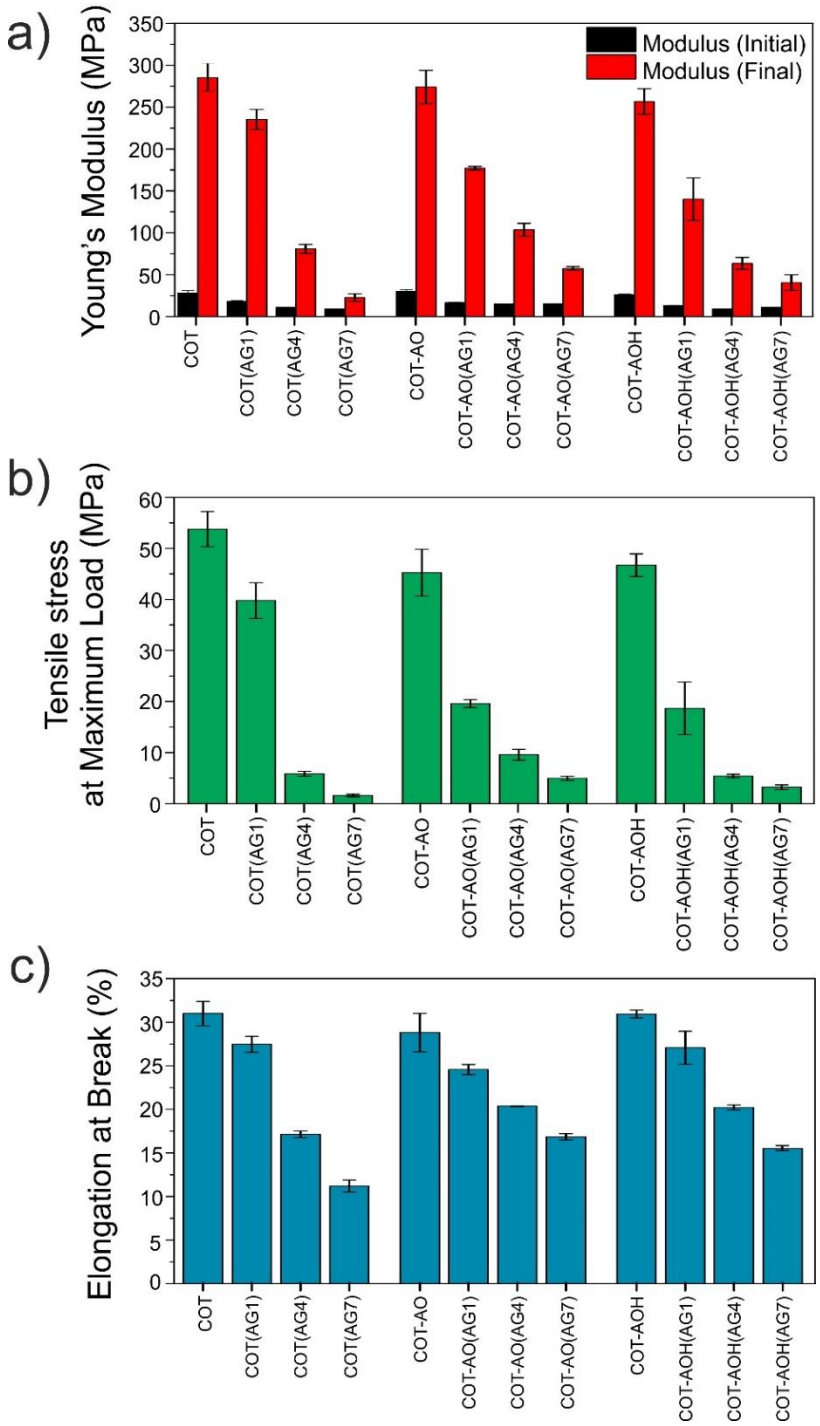

Fig. 3.10 Mechanical tests performed on the samples COT, COT-AO and COT-AOP before accelerated aging, and after 1, 4 and 7 days of accelerated aging. (a) Young's modulus calculated on the first (0 to 0.1 mm/mm) and the second (0.1 mm/mm on) slopes, (b) tensile stress at maximum load, and (c) maximum elongation at breakpoint.

3.3.5 Flexural rigidity

The bending length of COT, COT-AO and COT-AOP was measured with Peirce Cantilever test to verify their flexural rigidity. This property measured the draping quality of a fabric before and after treatments and it was useful to quantify the stiffness appreciated by the fingers. The COT had a G_{Peirce} equal to $2.26\times10^{-4} \pm 3.33\times10^{-5}$ Nm, while COT-AO had a value of $5.36\times10^{-3} \pm 5.73\times10^{-4}$ Nm and COT-AOP had a value of $5.15\times10^{-3} \pm 5.80\times10^{-4}$ Nm. These physical tests were useful to reflect the sensations felt by touching the fabrics, *i.e.* the increasing stiffness due to the antioxidant polymeric coating. The hydrophobic layer, instead, contributed to maintain the high flexibility of the original fabric.

3.3.6 Antioxidant properties

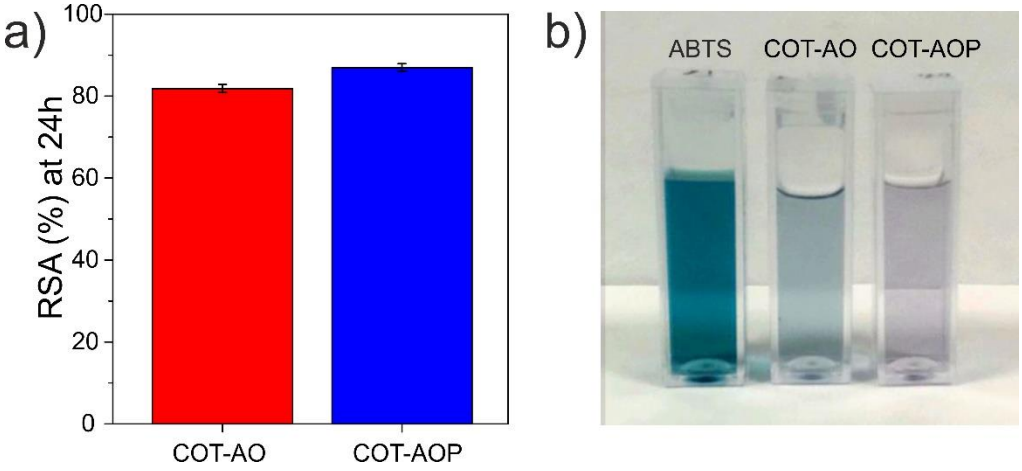

Fig. 3.11. (a) Radical scavenging activity. (b) Cuvettes containing the ABTS·+ radical solution without sample, the samples COT-AO and COT-AOP in the ABTS·+ radical solution after 24h.

$ABTS^{\cdot+}$ radical assay was performed to determine the free radical scavenging activity (RSA) of the antioxidant coating applied onto the cotton fabrics. The reaction between the radical and the radical inhibitor was evident thanks to $ABTS^{\cdot+}$ discoloration. The liquid gradually changed from an intense blue of the cation radical $ABTS^{\cdot+}$ to a colorless solution. In Fig. 3.11b the color loss of the $ABTS^{\cdot+}$ aqueous radical solution is represented after immersing the COT-AO and COT-AOP samples into radical solution for 24 h. The color fading demonstrated an effective antioxidant response of both samples.

Fig. 3.11a shows the RSA of the samples COT-AO and COT-AOP with respect to the radical cation $ABTS^{\cdot+}$ solution, after 24 hours of immersion in the radical solution. The samples COT-AO and COT-AOP reached 82 ± 1 % and 87 ± 1% inhibition level, respectively. PCL and PDMS do not show any antioxidant property [158], [125], so the obtained radical scavenging activity can be attributed to the presence of BHT in the cotton matrix, conferring a suitable antioxidant action.

This test gave complementary information to the ones collected via ATR-FTIR. The two analyses together contributed to verify that, whether exposed to an oxidative environment, the antioxidant treatment could interact with radicals to protect the underneath cellulose matrix. Hence, the proposed treatment seemed to have the adequate features to face long-term natural aging.

3.3.7 Color variation

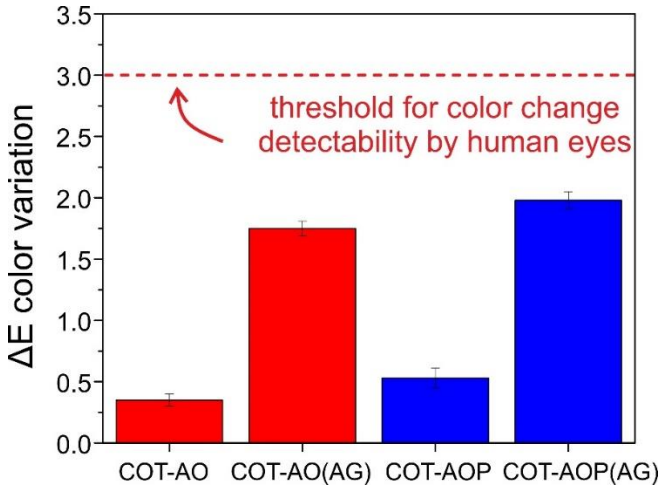

Fig. 3.12. ΔE color variation of treated and aged samples with respect to COT.

In order to propose this treatment for the conservation of Cultural Heritage, the aesthetical changes due to the polymeric solution and the accelerated aging were monitored. ΔE parameter, reported in Fig. 3.12, represents the overall colorimetric variations for each sample, with respect to the untreated and unaged cotton sample (COT). Both color variations after antioxidant and antioxidant plus hydrophobic treatments gave color variations much lower than ΔE values of 3. As for human perception, color determination depends on many factors, such as previous eye exposure, object and illuminant position with respect to the observer and to each other, and the color characteristics of the illuminant [159], [160]. Despite this, scientists and conservators defined a threshold value

below which color alteration cannot be detected by naked human eyes. This threshold value is generally accepted to be around ΔE = 2–3 [161], [157], [162], [163]. In this experiment, the values are: 0.35 ± 0.05 for the sample COT-AO and 0.53 ± 0.08 for COT-AOP. Higher ΔE colorimetric variation, but always lower than 3, were detected for samples after accelerated aging: 1.75 ± 0.06 for COT-AO(AG) and 1.98 ± 0.07 for COT-AOP(AG). These colorimetric data and the appearance of the fabrics (Fig. 3.13) gave one more confirmation that the proposed treatments can be applied onto Cultural Heritage object without altering their appearance, hence preserving the original forms in time.

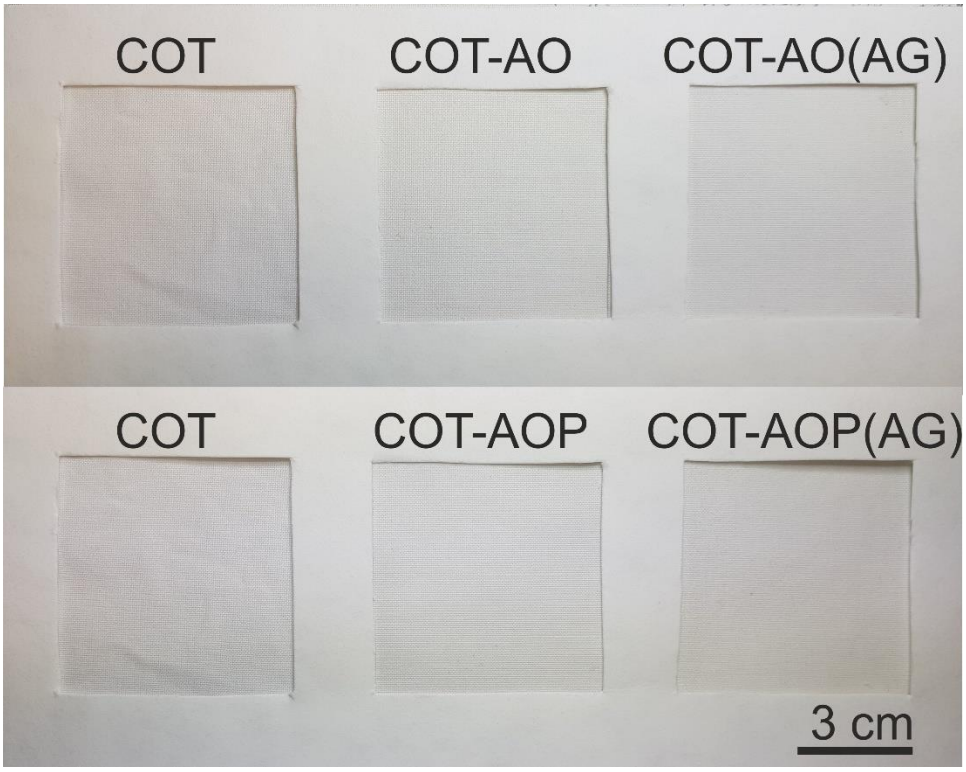

Fig. 3.13. Pictures of untreated cotton (COT), cotton with antioxidant treatment (COT-AO), cotton with antioxidant treatment after aging (COT-AO), cotton with antioxidant and hydrophobic treatment (COT-AOP), and cotton with antioxidant and hydrophobic treatment after aging (COT-AO).

3.4 Conclusions

This study focused on developing a new coating able to interfere with the natural aging process of woven cotton fabrics and protect them from several deterioration phenomena.

The milestones of this multi-functional coating are:

- An antioxidant layer was developed using BHT, which is a transparent antioxidant agent, maintaining its transparency also after reacting with radicals during the accelerated aging;
- PCL is a polymer, which is potentially biodegradable in anoxic conditions, but highly durable in aerobic conditions. Moreover, PCL demonstrated good compatibility with the overlapped polymer;
- A hydrophobic layer was developed without the use of fluorine chemistry, only by using PDMS; other than low wettability, PDMS demonstrated high water vapor permeability and excellent mechanical properties.
- The surface wettability was considerately decreased, and at the same time, the water vapor permeability was guaranteed. Moreover, the water uptake was halved. All these properties were efficiently modified to reduce the risk of water-linked deterioration phenomena;
- The protective treatments did not remarkably modify the breathability and the porosity of the fabrics, keeping the original structure and appearance of the fabric unchanged;
- Mechanical properties after treatment where almost unchanged, only flexural rigidity increased;
- An *ad hoc* protocol for simulating in only 24 hours the long-term cotton ageing under oxidative conditions had been proposed and tested. The developed protocol has been used to prove the efficiency of the presented protective treatment.
- After aging, the protected woven fabric demonstrated unchanged chemical structure, unchanged color and slowing down of the cotton yarns mechanical deterioration.

Overall, this work shows that textiles based on cellulose could be protected against oxidative ageing by a simple treatment using ecofriendly polymers and processes.

4. Conclusions & Future Perspectives

This study was born from the need to develop innovative treatments for the conservation of cellulose fabrics. Fabrics present in artworks are in fact prone to several degradation phenomena such as swelling ad shrinking due to humidity, loss of mechanical properties, biodeterioration and oxidation.

The literature investigation, presented in Chapter 1, revealed the presence of several natural and synthetic commercial products for protection and consolidation treatments. Moreover, the review revealed a lack of attention to conservation issues, such as esthetical problems, brittleness and color changes. In most of the researches, the study of mechanical properties was also absent, demonstrating insufficient concern about fabrics handling and museum installations for public fruition. Hence, this research focused on proposing innovative treatments, paying particular attention to conservation needs.

The development of a hydrophobic coating based on polycarbonate diol polyurethane combined with aminosiloxane was successfully tested onto fabrics in Chapter 2. Solvents with no environmental hazards were used and the selected application techniques (dip- and spray- coating) were easy to perform at low cost. The micro-emulsion of the two components was stable and demonstrated an excellent penetration in the bulk. Taking advantage of the intrinsic roughness of the cotton fibers and covering them with the low surface energy polymers, high hydrophobicity was conferred to the fabric bulk. The fluorine-free treatments also conferred high resistance to large volumes of water and, at the same time, maintained high water vapor permeability. The resulting high breathability of the fabrics was ideal to diminish the arise of degradation phenomena linked to condensation, such as mold, fungi, moth infestation, and swelling-shrinking behavior. In the attempt to respond to a literature lack of knowledge concerning mechanical data after conservation treatments, the stretching, strength, bendability and drapability of the fabrics were evaluated. These data confirmed that mechanical properties were unchanged, which was also noticeable thanks to the impossibility to distinguish treated and untreated samples by simple touching. The colorimetric properties were unaltered after the treatments and their stability to accelerated aging was also confirmed.

A multifunction coating have also been realized and presented in Chapter 3, aiming at protecting the fabrics, not only from water linked deterioration phenomena, but also from oxidation. For this

purpose, an *ad hoc* aging protocol was developed to bring pristine cotton to the same oxidation state of ancient fabrics reported in literature. The multifunctional coating, based on polycaprolactone, butylated hydroxytoluene, and polydimethylsiloxane was applied by dip-coating. Thanks to the coating, the surface wettability considerately decreased, the water uptake was halved, but the water vapor permeability and the porosity were maintained. These features conferred protection from liquid and vapor water, promoting the breathability and avoiding condensation phenomena. Moreover, color and mechanical properties after coating were maintained similar to untreated cotton fabrics. The arise of carbonyl groups in untreated cotton was verified trough spectroscopy after undergoing the accelerated oxidative treatment, while the chemical structure of coated cellulose was maintained unchanged. The ability of the antioxidant treatment to scavenge radicals in solution was also verified. In addition, after accelerated oxidation, the protective coating slowed down the mechanical deterioration and aesthetical properties were unchanged.

The developed technologies demonstrated to be highly suitable for fabrics of inestimable historical and cultural value. Thanks to their sustainability, hydrophobicity and breathability the proposed treatments may also be suitable for commercial fabrics used in modern design and fashion.

Future perspectives of this study should include the evaluation of proposed treatments reversibility. Removal procedures should be tested onto multi-component artworks, such as fabrics containing colorants, pigments, metal threads or protein-based fibers and artworks in compromised conservation states. It should be considered that fabrics mechanical properties benefitted from polymers application, especially after accelerated oxidative treatments. The removal of the coatings may be detrimental, making the object breakable and brittle. Hence, conservation scientist and restores may consider to verify the re-treatability of the coatings, rather than their reversibly.

Overall, the proposed treatments were found to fulfill conservation science requirements. Thanks to the promising results, the treatments could help to valorize ancient artworks, which are not exposed to the public due to the conservative issues described in this thesis.

Bibliography

[1] G. Scicolone, *Dipinti su tela - metodologie d'indagine per i supporti cellulosici*, Nardini Editore. Firenze, 2005.

[2] P. H. M. Association (HMA) and ICCROM, *Conserving textiles: studies in honour of Ágnes Timár-Balázsy*. 2009.

[3] K. Löbmann and A. J. Svagan, "Cellulose nanofibers as excipient for the delivery of poorly soluble drugs," *International Journal of Pharmaceutics*, vol. 533, no. 1, pp. 285–297, Nov. 2017, doi: 10.1016/j.ijpharm.2017.09.064.

[4] A. B. P. Rocky, "Comparison of Effectiveness Between Conventional Scouring & Bio-Scouring On Cotton Fabrics"," *International Journal of Scientific & Engineering Research Volume*, vol. 3, pp. 1–5, 2012.

[5] D. van der Reyden, "Recent Scientific Research in Paper Conservation," *Journal of the American Institute for Conservation*, vol. 31, no. 1, pp. 117–138, 1992, doi: 10.2307/3179619.

[6] J. M. Cardamone, "The Aging, Degradation, and Conservation of Historic Materials Made from Cellulosic Fibers," in *Historic Textiles, Papers, and Polymers in Museums*, vol. 779, J. M. Cardamone and M. T. Baker, Eds. Washington, DC: American Chemical Society, 2000, pp. 8–22.

[7] M. Börjesson and G. Westman, "Crystalline Nanocellulose — Preparation, Modification, and Properties | IntechOpen," *IntechOpen*, Dec. 2015, doi: 10.5772/61899.

[8] S. Park, J. O. Baker, M. E. Himmel, P. A. Parilla, and D. K. Johnson, "Cellulose crystallinity index: measurement techniques and their impact on interpreting cellulase performance," *Biotechnol Biofuels*, vol. 3, no. 1, p. 10, May 2010, doi: 10.1186/1754-6834-3-10.

[9] D. Halliday, R. Resnick, and J. Walker, *Fundamentals of physics*. John Wiley & Sons, 2013.

[10] C. Nave, "Young's Modulus," *HyperPhysics*. http://hyperphysics.phy-astr.gsu.edu/hbase/permot3.html.

[11] L. Hajji *et al.*, "Conservation of Moroccan manuscript papers aged 150, 200 and 800years. Analysis by infrared spectroscopy (ATR-FTIR), X-ray diffraction (XRD), and scanning electron microscopy energy dispersive spectrometry (SEM?EDS)," *Spectrochimica Acta Part A: Molecular and Biomolecular Spectroscopy*, vol. 136, pp. 1038–1046, Feb. 2015, doi: 10.1016/j.saa.2014.09.127.

[12] K. Kavkler and A. Demšar, "Application of FTIR and Raman Spectroscopy to Quantitative Analysis of Structural Changes in Cellulosic Fibres," *Application of FTIR and Raman Spectroscopy to Qualitative*, vol. 55, pp. 19–31, Feb. 2012.

[13] D. Bede, J. Robinson, and T. Pardoe, "An Illustrated Guide to the Care of Costume and Textile Collections," *Journal of the American Institute for Conservation*, vol. 40, no. 3, p. 267, 2001, doi: 10.2307/3179883.

[14] F. Ferrero, F. Testore, G. Malucelli, and C. Tonin, "Thermal Degradation of Linen Textiles: The Effects of Ageing and Cleaning," *Journal of the Textile Institute*, vol. 89, no. 3, pp. 562–569, Jan. 1998, doi: 10.1080/00405009808658642.

[15] G. S. Egerton, "The Mechanism of the Photochemical Degradation of Textile Material," *Journal of the Society of Dyers and Colourists*, vol. 65, no. 12, pp. 764–780, Oct. 2008, doi: 10.1111/j.1478-4408.1949.tb02558.x.

[16] A. M. Seves *et al.*, “Effect of thermal accelerated ageing on the properties of model canvas paintings,” *Journal of Cultural Heritage*, vol. 1, no. 3, pp. 315–322, Nov. 2000, doi: 10.1016/S1296-2074(00)01078-5.
[17] M. Oriola, G. Campo, C. Ruiz-Recasens, N. Pedragosa, and M. Strlič, “Collections care scenario appraisal for painting canvases at Museu Nacional d’Art de Catalunya, Barcelona, Spain,” *Studies in Conservation*, vol. 60, no. sup1, pp. S193–S199, Aug. 2015, doi: 10.1179/0039363015Z.000000000224.
[18] R. Hamilton, V. Kucera, J. Tidblad, and J. Watt, Eds., *The Effects of Air Pollution on Cultural Heritage*. Boston, MA: Springer US, 2009.
[19] G. Mazzon *et al.*, “Nanostructured coatings for the protection of textiles and paper,” *Ge-conservación/conservação*, no. 11, pp. 180–188, 2017.
[20] A. Timar-Balazsy and D. Eastop, *Chemical Principles of Textile Conservation*. London: Routledge, 1998.
[21] T. H. Mokhothu and M. J. John, “Review on hygroscopic aging of cellulose fibres and their biocomposites,” *Carbohydrate Polymers*, vol. 131, pp. 337–354, Oct. 2015, doi: 10.1016/j.carbpol.2015.06.027.
[22] M. F. Mecklenburg, *Micro climates and moisture induced damage to paintings*. 2007, pp. 19–25, ill.
[23] G. Capriotti and A. Iaccarino Idelson, *Tensionamento dei Dipinti su Tela. La ricerca del valore di tensionamento.*, Arte e Restauro. Nardini Editore, 2004.
[24] M. F. Mecklenburg, “Some aspects of the mechanical behavior of fabric supported paintings,” *The Mechanics of Art Materials and Its Future in Heritage Science*, p. 107, 1982.
[25] M. F. Mecklenburg, C. S. Tumosa, and D. Erhardt, “New Environmental Guidelines at the Smithsonian Institution,” 2004, Accessed: Nov. 09, 2020. [Online]. Available: http://repository.si.edu/xmlui/handle/10088/35931.
[26] D. Erhardt and M. Mecklenburg, “Relative humidity re-examined,” *null*, vol. 39, no. sup2, pp. 32–38, Jan. 1994, doi: 10.1179/sic.1994.39.Supplement-2.32.
[27] T. L. VIGO, “Preservation of Natural Textile Fibers—Historical Perspectives,” in *Preservation of Paper and Textiles of Historic and Artistic Value*, vol. 164, 0 vols., AMERICAN CHEMICAL SOCIETY, 1978, pp. 189–207.
[28] J. B. Upham and V. S. Salvin, “Effects of air pollutants on textile fibers and dyes. Final report,” North Carolina Univ., Greensboro (USA), PB-241507, Feb. 1975. [Online]. Available: https://www.osti.gov/biblio/7351204.
[29] R. D. Fagan, H. E. Grethlein, A. O. Converse, and A. Porteous, “Kinetics of the acid hydrolysis of cellulose found in paper refuse,” *Environmental Science & Technology*, vol. 5, no. 6, pp. 545–547, Jun. 1971, doi: 10.1021/es60053a006.
[30] C. Li and Z. K. Zhao, “Efficient Acid-Catalyzed Hydrolysis of Cellulose in Ionic Liquid,” *Advanced Synthesis & Catalysis*, vol. 349, no. 11–12, pp. 1847–1850, 2007, doi: https://doi.org/10.1002/adsc.200700259.
[31] S.-Y. Yoon, S.-H. Han, and S.-J. Shin, “The effect of hemicelluloses and lignin on acid hydrolysis of cellulose,” *Energy*, vol. 77, pp. 19–24, Dec. 2014, doi: 10.1016/j.energy.2014.01.104.
[32] L. Di Giorgio, L. Martín, P. R. Salgado, and A. N. Mauri, “Synthesis and conservation of cellulose nanocrystals,” *Carbohydrate Polymers*, vol. 238, p. 116187, Jun. 2020, doi: 10.1016/j.carbpol.2020.116187.

[33] S. Sankar Panda, S. Kumar Bisaria, and M. R. Singh, “The spectroscopic and microscopic evaluation of cellulose used in conservation of archival materials,” *Microchemical Journal*, vol. 160, p. 105707, Jan. 2021, doi: 10.1016/j.microc.2020.105707.
[34] L. Fras, L.-S. Johansson, P. Stenius, J. Laine, K. Stana-Kleinschek, and V. Ribitsch, “Analysis of the oxidation of cellulose fibres by titration and XPS,” *Colloids and Surfaces A: Physicochemical and Engineering Aspects*, vol. 260, no. 1–3, pp. 101–108, Jun. 2005, doi: 10.1016/j.colsurfa.2005.01.035.
[35] G. F. Davidson and T. P. Nevell, “The acidic properties of cotton cellulose and derived oxycelluloses. Part IV.,” *Journal of the Textile Institute Transactions*, vol. 39, no. 3, pp. T93–T101, Mar. 1948, doi: 10.1080/19447024808659405.
[36] S. Sözen, T. Olmez-Hanci, M. Hooshmand, and D. Orhon, “Fenton oxidation for effective removal of color and organic matter from denim cotton wastewater without biological treatment,” *Environ Chem Lett*, vol. 18, no. 1, pp. 207–213, Jan. 2020, doi: 10.1007/s10311-019-00923-8.
[37] J. M. Cardamone, J. M. Gould, and S. H. Gordon, “Characterizing Aged Textile Fibers by Fourier Transform Infrared Photoacoustic Spectroscopy: Part I: Comparison of Artificial and Natural Ageing in Cotton,” *Textile Research Journal*, vol. 57, no. 4, pp. 235–239, Apr. 1987, doi: 10.1177/004051758705700408.
[38] P. Garside and P. Wyeth, “Identification of Cellulosic Fibres by FTIR Spectroscopy - Thread and Single Fibre Analysis by Attenuated Total Reflectance,” *Studies in Conservation*, vol. 48, no. 4, pp. 269–275, Dec. 2003, doi: 10.1179/sic.2003.48.4.269.
[39] A. Boukir, I. Mehyaoui, S. Fellak, L. Asia, and P. Doumenq, “The effect of the natural degradation process on the cellulose structure of Moroccan hardwood fiber: a survey on spectroscopy and structural properties,” *Mediterranean Journal of Chemistry*, vol. 8, no. 3, p. 179, May 2019, doi: 10.13171/10.13171/mjc8319050801ab.
[40] V. Librando, Z. Minniti, and S. Lorusso, “Ancient and modern paper characterization by FTIR and Micro-Raman spectroscopy,” *Conservation Science in Cultural Heritage*, vol. 11, no. 1, pp. 249–268, Dec. 2011, doi: 10.6092/issn.1973-9494/2700.
[41] F. Nuttgens and Z. Tinker, “The conservation of rubberised textiles: Two case histories,” *The Conservator*, vol. 24, no. 1, pp. 24–38, Jan. 2000, doi: 10.1080/01410096.2000.9995147.
[42] M. Berkouwer, “Freezing to eradicate insect pests in textiles at Brodsworth Hall,” *The Conservator*, vol. 18, no. 1, pp. 15–22, Jan. 1994, doi: 10.1080/01410096.1994.9995080.
[43] S. Rowe, “The Effect of Insect Fumigation by Anoxia on Textiles Dyed with Prussian Blue,” *Studies in Conservation*, vol. 49, no. 4, pp. 259–270, Jan. 2004, doi: 10.1179/sic.2004.49.4.259.
[44] D. W. Grattan and M. Gilberg, “Ageless oxygen absorber: chemical and physical properties,” *Studies in Conservation*, vol. 39, no. 3, pp. 210–214, Aug. 1994, doi: 10.1179/sic.1994.39.3.210.
[45] J. Szostak-Kotowa, “Biodeterioration of textiles,” *International Biodeterioration & Biodegradation*, vol. 53, no. 3, pp. 165–170, Apr. 2004, doi: 10.1016/S0964-8305(03)00090-8.
[46] K. Kavkler, N. Gunde-Cimerman, P. Zalar, and A. Demšar, “FTIR spectroscopy of biodegraded historical textiles,” *Polymer Degradation and Stability*, vol. 96, no. 4, pp. 574–580, Apr. 2011, doi: 10.1016/j.polymdegradstab.2010.12.016.

[47] M. Zotti, A. Ferroni, and P. Calvini, "Mycological and FTIR analysis of biotic foxing on paper substrates," *International Biodeterioration & Biodegradation*, vol. 65, no. 4, pp. 569–578, Jul. 2011, doi: 10.1016/j.ibiod.2010.01.011.
[48] K. Kavkler, N. Gunde Cimerman, P. Zalar, and A. Demšar, "Deterioration of contemporary and artificially aged cotton by selected fungal species," *Polymer Degradation and Stability*, vol. 113, pp. 1–9, Mar. 2015, doi: 10.1016/j.polymdegradstab.2015.01.004.
[49] C. C. Institute, "Caring for textiles and costumes - Preventive conservation guidelines for collections," *aem*, May 11, 2018. https://www.canada.ca/en/conservation-institute/services/preventive-conservation/guidelines-collections/textiles-costumes.html (accessed Nov. 09, 2020).
[50] A. Timar-Balazsy, "Wet cleaning of historical textiles: surfactants and other wash bath additives," *Studies in Conservation*, vol. 45, no. 1, pp. 46–64, Mar. 2000, doi: 10.1179/sic.2000.45.1.46.
[51] G. O. Oyeleke, M. A. Salam, O. A. Adedayo, I. A. Abdulazeez, and A. A. Adebisi, "Storage Stability of Extracted Dye from the Surface of Polyester Fabric in Non Aqueous Cleaning Solvents," *Journal of Materials Science Research and Reviews*, pp. 11–17, Jul. 2020.
[52] A. R. Martin, "Dry Cleaning Museum Textiles," *Bulletin of the American Group. International Institute for Conservation of Historic and Artistic Works*, vol. 7, no. 2, pp. 9–13, 1967, doi: 10.2307/3178953.
[53] "Dust deposition on textile and its evolution in indoor cultural heritage | SpringerLink." https://link.springer.com/article/10.1140/epjp/i2019-12671-5 (accessed Nov. 17, 2020).
[54] O. Abdel-Kareem and M. A. Harith, "Evaluating the use of laser radiation in cleaning of copper embroidery threads on archaeological Egyptian textiles," *Applied Surface Science*, vol. 254, no. 18, pp. 5854–5860, Jul. 2008, doi: 10.1016/j.apsusc.2008.03.144.
[55] C. Degrigny, E. Tanguy, R. Le Gall, V. Zafiropulos, and G. Marakis, "Laser cleaning of tarnished silver and copper threads in museum textiles," *Journal of Cultural Heritage*, vol. 4, pp. 152–156, Jan. 2003, doi: 10.1016/S1296-2074(02)01191-3.
[56] M. Lassithiotaki, A. Athanassiou, D. Anglos, S. Georgiou, and C. Fotakis, "Photochemical effects in the UV laser ablation of polymers: Implications for laser restoration of painted artworks," *Appl Phys A*, vol. 69, no. 3, pp. 363–367, Sep. 1999, doi: 10.1007/s003390051015.
[57] J. L. Down, M. A. MacDonald, J. Tétreault, and R. S. Williams, "Adhesive Testing at the Canadian Conservation Institute: An Evaluation of Selected Poly(Vinyl Acetate) and Acrylic Adhesives," *Studies in Conservation*, vol. 41, no. 1, pp. 19–44, 1996, doi: 10.2307/1506550.
[58] M. Zahid, G. Mazzon, A. Athanassiou, and I. S. Bayer, "Environmentally benign non-wettable textile treatments: A review of recent state-of-the-art," *Advances in Colloid and Interface Science*, Jun. 2019, doi: 10.1016/j.cis.2019.06.001.
[59] M. Cocca *et al.*, "Water dispersed polymers for textile conservation: a molecular, thermal, structural, mechanical and optical characterisation," *Journal of Cultural Heritage*, vol. 7, no. 4, pp. 236–243, Oct. 2006, doi: 10.1016/j.culher.2005.11.002.
[60] L. D'Arienzo, G. Gentile, E. Martuscelli, C. Polcaro, and L. D'Orazio, "Acrylic and acetovinylic polymers for preserving and restoring cotton textiles," *Textile research journal*, vol. 74, no. 4, pp. 281–291, 2004.
[61] O. M. A. Abdel-Kareem, "The long-term effect of selected conservation materials used in the treatment of museum artefacts on some properties of textiles," *Polymer Degradation*

and Stability, vol. 87, no. 1, pp. 121–130, Jan. 2005, doi: 10.1016/j.polymdegradstab.2004.07.014.
[62] F. Cappitelli and C. Sorlini, "Microorganisms Attack Synthetic Polymers in Items Representing Our Cultural Heritage," *Applied and Environmental Microbiology*, vol. 74, no. 3, pp. 564–569, Feb. 2008, doi: 10.1128/AEM.01768-07.
[63] T. Bilson, "The conservation of a Roman Egyptian painted shroud fragment," *The Conservator*, vol. 16, no. 1, pp. 3–11, Jan. 1992, doi: 10.1080/01400096.1992.9635620.
[64] Q. Chen *et al.*, "Preparation and application of modified carboxymethyl cellulose Si/polyacrylate protective coating material for paper relics," *Chemical Papers*, vol. 70, no. 7, pp. 946–959, 2016, doi: 10.1515/chempap-2016-0029.
[65] G. Owen and S. Reidell, "Cast Composites: a system for texturing repair materials in book conservation," Milwaukee, Wisconsin, 2011, vol. 14, p. 12.
[66] E. Princi, S. Vicini, E. Pedemonte, V. Arrighi, and I. J. McEwen, "New polymeric materials for paper and textiles conservation. II. Grafting polymerization of ethyl acrylate/methyl methacrylate copolymers onto linen and cotton," *Journal of Applied Polymer Science*, vol. 103, no. 1, pp. 90–99, 2007, doi: 10.1002/app.24689.
[67] C. Johnson, B. Wills, T. Peacock, and G. Bott, *The conservation of an Egyptian mummy, cartonnage cover and mask*. 19950000, pp. 47–55.
[68] M. Zahid, J. A. Heredia-Guerrero, A. Athanassiou, and I. S. Bayer, "Robust water repellent treatment for woven cotton fabrics with eco-friendly polymers," *Chemical Engineering Journal*, vol. 319, pp. 321–332, Jul. 2017, doi: 10.1016/j.cej.2017.03.006.
[69] H. Zhou, H. Wang, H. Niu, A. Gestos, X. Wang, and T. Lin, "Fluoroalkyl Silane Modified Silicone Rubber/Nanoparticle Composite: A Super Durable, Robust Superhydrophobic Fabric Coating," *Advanced Materials*, vol. 24, no. 18, pp. 2409–2412, 2012, doi: 10.1002/adma.201200184.
[70] H. Zhou, H. Wang, H. Niu, A. Gestos, and T. Lin, "Robust, Self-Healing Superamphiphobic Fabrics Prepared by Two-Step Coating of Fluoro-Containing Polymer, Fluoroalkyl Silane, and Modified Silica Nanoparticles," *Advanced Functional Materials*, vol. 23, no. 13, pp. 1664–1670, 2013, doi: 10.1002/adfm.201202030.
[71] T. R. Kar, A. K. Samanta, M. Sajid, and R. Kaware, "UV protection and antimicrobial finish on cotton khadi fabric using a mixture of nanoparticles of zinc oxide and poly-hydroxy-amino methyl silicone," *Textile Research Journal*, vol. 89, no. 11, pp. 2260–2278, Jun. 2019, doi: 10.1177/0040517518790973.
[72] G. Mazzon *et al.*, "Hydrophobic treatment of woven cotton fabrics with polyurethane modified aminosilicone emulsions," *Applied Surface Science*, Jun. 2019, doi: 10.1016/j.apsusc.2019.06.069.
[73] L.-M. Ferreira, "Green composites from castor oil and renewable reinforcing materials: maleated castor oil-polystyrene matrix reinforced with greige fibre," University of Cape Town, South Africa, 2019.
[74] O. Nechyporchuk *et al.*, "On the potential of using nanocellulose for consolidation of painting canvases," *Carbohydrate Polymers*, vol. 194, pp. 161–169, Aug. 2018, doi: 10.1016/j.carbpol.2018.04.020.
[75] K. Kolman, O. Nechyporchuk, M. Persson, K. Holmberg, and R. Bordes, "Combined Nanocellulose/Nanosilica Approach for Multiscale Consolidation of Painting Canvases," *ACS Applied Nano Materials*, vol. 1, no. 5, pp. 2036–2040, May 2018, doi: 10.1021/acsanm.8b00262.

[76] A. Bridarolli *et al.*, “Evaluation of the Adhesion and Performance of Natural Consolidants for Cotton Canvas Conservation,” *ACS Applied Materials & Interfaces*, vol. 10, no. 39, pp. 33652–33661, Oct. 2018, doi: 10.1021/acsami.8b10727.
[77] N. Böhme, M. Anders, T. Reichelt, K. Schuhmann, A. Bridarolli, and A. Chevalier, “New treatments for canvas consolidation and conservation,” *Herit Sci*, vol. 8, no. 1, p. 16, Feb. 2020, doi: 10.1186/s40494-020-0362-y.
[78] Z. Zhao, M. Zhang, C. Hurren, L. Zhou, J. Wu, and L. Sun, “Effects of UV absorbers and reducing agents on light fastness of cotton fabrics pre-dyed with sodium copper chlorophyllin and gardenia yellow,” *Textile Research Journal*, vol. 90, no. 19–20, pp. 2245–2257, Oct. 2020, doi: 10.1177/0040517520911372.
[79] E. R. de la Rie, “Polymer Stabilizers. A Survey with Reference to Possible Applications in the Conservation Field,” *Studies in Conservation*, vol. 33, no. 1, pp. 9–22, 1988, doi: 10.2307/1506236.
[80] S. J. Hackney and G. A. Hedley, “The deterioration of linen canvas: accelerated aging tests to investigate the modes of deterioration and to assess retarding treatments,” *Studies in Conservation*, vol. 27, no. sup1, pp. 151–153, Jan. 1982, doi: 10.1179/sic.1982.27.Supplement-1.151.
[81] R. S. Orr, L. C. Weiss, G. C. Humphreys, T. Mares, and J. N. Grant, “Degradation of Cotton Fibers and Yarns by Heat and Moisture,” *Textile Research Journal*, vol. 24, no. 5, pp. 399–406, May 1954, doi: 10.1177/004051755402400502.
[82] O. Nechyporchuk, K. Kolman, M. Oriola, M. Persson, K. Holmberg, and R. Bordes, “Accelerated ageing of cotton canvas as a model for further consolidation practices,” *Journal of Cultural Heritage*, vol. 28, pp. 183–187, Nov. 2017, doi: 10.1016/j.culher.2017.05.010.
[83] A. Barański, A. Konieczna-Molenda, J. M. Łagan, and L. M. Proniewicz, “Catastrophic Room Temperature Degradation of Cotton Cellulose,” *Restaurator*, vol. 24, no. 1, Jan. 2003, doi: 10.1515/REST.2003.36.
[84] S. Zervos and A. Moropoulou, “Cotton Cellulose Ageing in Sealed Vessels. Kinetic Model of Autocatalytic Depolymerization,” *Cellulose*, vol. 12, no. 5, p. 485, Oct. 2005, doi: 10.1007/s10570-005-7131-7.
[85] C. Young, “Accelerated ageing of fabric supports: is it possible?,” in *AHRB Textile Conservation Centre Conference Post Prints*, Oct. 2020, pp. 111–117.
[86] H. Křížová, V. Tuček, J. Neoralová, and J. Wiener, “Buffering and Antibacterial Properties of Cotton Canvas with Dolomite/ZnO-Styrene-Acrylic Complex Coating and their Comparison with Properties after the Accelerated Aging,” *TEKSTILEC*, vol. 60, pp. 275–282, Dec. 2017, doi: 10.14502/Tekstilec2017.60.275-282.
[87] L. Bílková, “Application of infrared spectroscopy and thermal analysis to the examination of the degradation of cotton fibers,” *Polymer Degradation and Stability*, vol. 97, no. 1, pp. 35–39, Jan. 2012, doi: 10.1016/j.polymdegradstab.2011.10.018.
[88] M. Zhang, S. Wang, C. Wang, and J. Li, “A facile method to fabricate superhydrophobic cotton fabrics,” *Applied Surface Science*, vol. 261, pp. 561–566, Nov. 2012, doi: 10.1016/j.apsusc.2012.08.055.
[89] C.-H. Xue, S.-T. Jia, J. Zhang, and L.-Q. Tian, “Superhydrophobic surfaces on cotton textiles by complex coating of silica nanoparticles and hydrophobization,” *Thin Solid Films*, vol. 517, no. 16, pp. 4593–4598, Jun. 2009, doi: 10.1016/j.tsf.2009.03.185.

[90] S. Qiang, K. Chen, Y. Yin, and C. Wang, “Robust UV-cured superhydrophobic cotton fabric surfaces with self-healing ability,” *Materials & Design*, vol. 116, pp. 395–402, Feb. 2017, doi: 10.1016/j.matdes.2016.11.099.
[91] H. Liu *et al.*, “Multifunctional superamphiphobic fabrics with asymmetric wettability for one-way fluid transport and templated patterning,” *Cellulose*, vol. 24, no. 2, pp. 1129–1141, Feb. 2017, doi: 10.1007/s10570-016-1177-6.
[92] M.-J. Oh, S.-Y. Lee, and K.-H. Paik, “Preparation of hydrophobic self-assembled monolayers on paper surface with silanes,” *Journal of Industrial and Engineering Chemistry*, vol. 17, no. 1, pp. 149–153, Jan. 2011, doi: 10.1016/j.jiec.2010.12.014.
[93] F. Liu, M. Ma, D. Zang, Z. Gao, and C. Wang, “Fabrication of superhydrophobic/superoleophilic cotton for application in the field of water/oil separation,” *Carbohydrate Polymers*, vol. 103, pp. 480–487, Mar. 2014, doi: 10.1016/j.carbpol.2013.12.022.
[94] C.-H. Xue, P.-T. Ji, P. Zhang, Y.-R. Li, and S.-T. Jia, “Fabrication of superhydrophobic and superoleophilic textiles for oil–water separation,” *Applied Surface Science*, vol. 284, pp. 464–471, Nov. 2013, doi: 10.1016/j.apsusc.2013.07.120.
[95] M. E. Yazdanshenas and M. Shateri-Khalilabad, “One-Step Synthesis of Superhydrophobic Coating on Cotton Fabric by Ultrasound Irradiation,” *Industrial & Engineering Chemistry Research*, vol. 52, no. 36, pp. 12846–12854, Sep. 2013, doi: 10.1021/ie401133q.
[96] M. Aymerich, A. I. Gómez-Varela, E. Álvarez, and M. T. Flores-Arias, “Study of Different Sol-Gel Coatings to Enhance the Lifetime of PDMS Devices: Evaluation of Their Biocompatibility,” *Materials*, vol. 9, no. 9, p. 728, Sep. 2016, doi: 10.3390/ma9090728.
[97] S. Nagappan, D. B. Lee, D. J. Seo, S. S. Park, and C.-S. Ha, “Superhydrophobic mesoporous material as a pH-sensitive organic dye adsorbent,” *Journal of Industrial and Engineering Chemistry*, vol. 22, pp. 288–295, Feb. 2015, doi: 10.1016/j.jiec.2014.07.022.
[98] A. M. Ferrari, M. Pini, P. Neri, and F. Bondioli, “Nano-TiO2 Coatings for Limestone: Which Sustainability for Cultural Heritage?,” *Coatings*, vol. 5, no. 3, Art. no. 3, Sep. 2015, doi: 10.3390/coatings5030232.
[99] M. Frigione, M. Lettieri, A. Sarcinella, and J. L. Barroso de Aguiar, “Applications of Sustainable Polymer-Based Phase Change Materials in Mortars Composed by Different Binders,” *Materials*, vol. 12, no. 21, Art. no. 21, Jan. 2019, doi: 10.3390/ma12213502.
[100] C. Giuliani *et al.*, “Chitosan-based coatings for corrosion protection of copper-based alloys: A promising more sustainable approach for cultural heritage applications,” *Progress in Organic Coatings*, vol. 122, pp. 138–146, Sep. 2018, doi: 10.1016/j.porgcoat.2018.05.002.
[101] S. M. Cakić, M. Špírková, I. S. Ristić, J. K. B-Simendić, M. M-Cincović, and R. Poręba, “The waterborne polyurethane dispersions based on polycarbonate diol: Effect of ionic content,” *Materials Chemistry and Physics*, vol. 138, no. 1, pp. 277–285, Feb. 2013, doi: 10.1016/j.matchemphys.2012.11.057.
[102] V. García-Pacios, V. Costa, M. Colera, and J. M. Martín-Martínez, “Waterborne polyurethane dispersions obtained with polycarbonate of hexanediol intended for use as coatings,” *Progress in Organic Coatings*, vol. 71, no. 2, pp. 136–146, Jun. 2011, doi: 10.1016/j.porgcoat.2011.01.006.
[103] Z. Li, Y. Xing, and J. Dai, “Superhydrophobic surfaces prepared from water glass and non-fluorinated alkylsilane on cotton substrates,” *Applied Surface Science*, vol. 254, no. 7, pp. 2131–2135, Jan. 2008, doi: 10.1016/j.apsusc.2007.08.083.

[104] N. Ahmad, S. Kamal, Z. A. Raza, T. Hussain, and F. Anwar, “Multi-response optimization in the development of oleo-hydrophobic cotton fabric using Taguchi based grey relational analysis,” *Applied Surface Science*, vol. 367, pp. 370–381, Mar. 2016, doi: 10.1016/j.apsusc.2016.01.165.
[105] H. F. Hoefnagels, D. Wu, G. de With, and W. Ming, “Biomimetic Superhydrophobic and Highly Oleophobic Cotton Textiles,” *Langmuir*, vol. 23, no. 26, pp. 13158–13163, Dec. 2007, doi: 10.1021/la702174x.
[106] K. G. Kabza, J. E. Gestwicki, and J. L. McGrath, “Contact Angle Goniometry as a Tool for Surface Tension Measurements of Solids, Using Zisman Plot Method. A Physical Chemistry Experiment,” *Journal of Chemical Education*, vol. 77, no. 1, p. 63, Jan. 2000, doi: 10.1021/ed077p63.
[107] Y. Liu, J. H. Xin, and C.-H. Choi, “Cotton Fabrics with Single-Faced Superhydrophobicity,” *Langmuir*, vol. 28, no. 50, pp. 17426–17434, Dec. 2012, doi: 10.1021/la303714h.
[108] T. T. T. Ho, T. Zimmermann, S. Ohr, and W. R. Caseri, “Composites of Cationic Nanofibrillated Cellulose and Layered Silicates: Water Vapor Barrier and Mechanical Properties,” *ACS Applied Materials & Interfaces*, vol. 4, no. 9, pp. 4832–4840, Sep. 2012, doi: 10.1021/am3011737.
[109] J. Wu *et al.*, “Designing breathable superhydrophobic cotton fabrics,” *RSC Advances*, vol. 5, no. 35, pp. 27752–27758, 2015, doi: 10.1039/C5RA01028D.
[110] E. de Bilbao, D. Soulat, G. Hivet, and A. Gasser, “Experimental Study of Bending Behaviour of Reinforcements,” *Experimental Mechanics*, vol. 50, no. 3, pp. 333–351, Mar. 2010, doi: 10.1007/s11340-009-9234-9.
[111] A. Maziz, A. Concas, A. Khaldi, J. Stålhand, N.-K. Persson, and E. W. H. Jager, “Knitting and weaving artificial muscles,” *Science Advances*, vol. 3, no. 1, p. e1600327, Jan. 2017, doi: 10.1126/sciadv.1600327.
[112] J. Zimmermann, F. A. Reifler, G. Fortunato, L.-C. Gerhardt, and S. Seeger, “A Simple, One-Step Approach to Durable and Robust Superhydrophobic Textiles,” *Advanced Functional Materials*, vol. 18, no. 22, pp. 3662–3669, Nov. 2008, doi: 10.1002/adfm.200800755.
[113] B. Goetzendorf-Grabowska, A. Karaszewska, V. Vlasenko, and A. Arabuli, “Bending Stiffness of Knitted Fabrics,” *Fibres & Textiles in Eastern Europe*, vol. 22, no. 1(103), pp. 43–50, 2014.
[114] N. Lammens, M. Kersemans, G. Luyckx, W. Van Paepegem, and J. Degrieck, “Improved accuracy in the determination of flexural rigidity of textile fabrics by the Peirce cantilever test (ASTM D1388),” *Textile Research Journal*, vol. 84, no. 12, pp. 1307–1314, Jul. 2014, doi: 10.1177/0040517514523182.
[115] R. L. Feller, *Accelerated aging: photochemical and thermal aspects*. Marina del Rey, CA: Getty Conservation Institute, 1994.
[116] T. T. Schaeffer, *Effects of light on materials in collections: data on Photoflash and related sources*, 2nd printing. Los Angeles: Getty Conservation Institute, 2001.
[117] C. M. Kim, H. B. Lee, J. U. Kim, and G. M. Kim, “Fabrication of poly (lactic-co-glycolic acid) microcontainers using solvent evaporation with polydimethylsiloxane stencil,” *Journal of Micromechanics and Microengineering*, vol. 27, no. 12, p. 125018, Dec. 2017, doi: 10.1088/1361-6439/aa9591.
[118] D. Khang, S. Y. Kim, P. Liu-Snyder, G. T. R. Palmore, S. M. Durbin, and T. J. Webster, “Enhanced fibronectin adsorption on carbon nanotube/poly(carbonate) urethane:

Independent role of surface nano-roughness and associated surface energy," *Biomaterials*, vol. 28, no. 32, pp. 4756–4768, Nov. 2007, doi: 10.1016/j.biomaterials.2007.07.018.
[119] C. Chung, M. Lee, and E. Choe, "Characterization of cotton fabric scouring by FT-IR ATR spectroscopy," *Carbohydrate Polymers*, vol. 58, no. 4, pp. 417–420, Dec. 2004, doi: 10.1016/j.carbpol.2004.08.005.
[120] N. Abidi, L. Cabrales, and C. H. Haigler, "Changes in the cell wall and cellulose content of developing cotton fibers investigated by FTIR spectroscopy," *Carbohydrate Polymers*, vol. 100, pp. 9–16, Jan. 2014, doi: 10.1016/j.carbpol.2013.01.074.
[121] L. Ceseracciu, J. A. Heredia-Guerrero, S. Dante, A. Athanassiou, and I. S. Bayer, "Robust and Biodegradable Elastomers Based on Corn Starch and Polydimethylsiloxane (PDMS)," *ACS Appl. Mater. Interfaces*, vol. 7, no. 6, pp. 3742–3753, Feb. 2015, doi: 10.1021/am508515z.
[122] A. Szelest-Lewandowska, B. Masiulanis, M. Szymonowicz, S. Pielka, and D. Paluch, "Modified polycarbonate urethane: Synthesis, properties and biological investigation in vitro," *Journal of Biomedical Materials Research Part A*, vol. 82A, no. 2, pp. 509–520, Aug. 2007, doi: 10.1002/jbm.a.31357.
[123] L. J. Bellamy, *The Infrared Spectra of Complex Molecules*. New York: Chapman and Hall, 1975.
[124] T. N. Tran *et al.*, "Transparent and flexible amorphous cellulose-acrylic hybrids," *Chemical Engineering Journal*, vol. 287, pp. 196–204, Mar. 2016, doi: 10.1016/j.cej.2015.10.114.
[125] J. A. Heredia-Guerrero *et al.*, "Antimicrobial, antioxidant, and waterproof RTV silicone-ethyl cellulose composites containing clove essential oil," *Carbohydrate Polymers*, vol. 192, pp. 150–158, Jul. 2018, doi: 10.1016/j.carbpol.2018.03.050.
[126] M. Zahid *et al.*, "Fabrication of Visible Light-Induced Antibacterial and Self-Cleaning Cotton Fabrics Using Manganese Doped TiO2 Nanoparticles," *ACS Appl. Bio Mater.*, vol. 1, no. 4, pp. 1154–1164, Oct. 2018, doi: 10.1021/acsabm.8b00357.
[127] L. Gao and T. J. McCarthy, "A Perfectly Hydrophobic Surface (θA/θR = 180°/180°)," *J. Am. Chem. Soc.*, vol. 128, no. 28, pp. 9052–9053, Jul. 2006, doi: 10.1021/ja062943n.
[128] T. Métivier and P. Cassagnau, "Compatibilization of silicone/fluorosilicone blends by dynamic crosslinking and fumed silica addition," *Polymer*, vol. 147, pp. 20–29, Jul. 2018, doi: 10.1016/j.polymer.2018.05.070.
[129] S. M. Mirabedini, M. Mohseni, Sh. PazokiFard, and M. Esfandeh, "Effect of TiO2 on the mechanical and adhesion properties of RTV silicone elastomer coatings," *Colloids and Surfaces A: Physicochemical and Engineering Aspects*, vol. 317, no. 1–3, pp. 80–86, Mar. 2008, doi: 10.1016/j.colsurfa.2007.09.044.
[130] R.-J. Roe, "Surface Tension of Polymer Liquids," in *The Journal of Physical Chemistry*, vol. 72, 1968, pp. 2013–2017.
[131] M. J. Owen, "The Surface Activity of Silicones: A Short Review," *Industrial & Engineering Chemistry Product Research and Development*, vol. 19, no. 1, pp. 97–103, Mar. 1980, doi: 10.1021/i360073a023.
[132] A. A. Badr and A. El-Nahrawy, "Moisture properties of raised 3-thread fleece fabric knitted with different face and fleecy yarns," *Alexandria Engineering Journal*, vol. 55, no. 3, pp. 2881–2892, Sep. 2016, doi: 10.1016/j.aej.2016.06.021.
[133] S. Mondal and J. L. Hu, "Water vapor permeability of cotton fabrics coated with shape memory polyurethane," *Carbohydrate Polymers*, vol. 67, no. 3, pp. 282–287, Feb. 2007, doi: 10.1016/j.carbpol.2006.05.030.

[134] Ö. Altun and N. Becenen, “Antioxidant, Antibacterial and UV-Resistant Activities of Undyed and Dyed Wool Fabrics Treated with CuO Nanoparticles,” *j nanosci nanotechnol*, vol. 17, no. 6, pp. 4204–4209, Jun. 2017, doi: 10.1166/jnn.2017.13119.
[135] Th. I. Shaheen, M. E. El-Naggar, A. M. Abdelgawad, and A. Hebeish, “Durable antibacterial and UV protections of in situ synthesized zinc oxide nanoparticles onto cotton fabrics,” *International Journal of Biological Macromolecules*, vol. 83, pp. 426–432, Feb. 2016, doi: 10.1016/j.ijbiomac.2015.11.003.
[136] D. Coman, S. Oancea, and N. Vrînceanu, “Biofunctionalization of textile materials by antimicrobial treatments: a critical overview,” *Romanian Biotechnological Letters*, vol. 15, no. 1, p. 9.
[137] T. Koussoulou, “Photodegradation and photostabilization of historic silks in the museum environment – evaluation of a new conservation treatment.,” p. 14.
[138] G. Mazzon *et al.*, “Antioxidant and hydrophobic Cotton fabric resisting accelerated ageing,” *Colloids and Surfaces A: Physicochemical and Engineering Aspects*, vol. 613, p. 126061, Mar. 2021, doi: 10.1016/j.colsurfa.2020.126061.
[139] T. Narancic *et al.*, “Biodegradable Plastic Blends Create New Possibilities for End-of-Life Management of Plastics but They Are Not a Panacea for Plastic Pollution,” *Environmental Science & Technology*, vol. 52, no. 18, pp. 10441–10452, Sep. 2018, doi: 10.1021/acs.est.8b02963.
[140] L. Avérous and E. Pollet, “Environmental silicate nano-biocomposites,” 2012.
[141] C. E. Plazas Bonilla, S. Trujillo, B. Demirdögen, J. E. Perilla, Y. Murat Elcin, and J. L. Gómez Ribelles, “New porous polycaprolactone–silica composites for bone regeneration,” *Materials Science and Engineering: C*, vol. 40, pp. 418–426, Jul. 2014, doi: 10.1016/j.msec.2014.04.024.
[142] J. Ahn, I. Grun, and A. Mustapha, “Effects of plant extracts on microbial growth, color change, and lipid oxidation in cooked beef,” *Food Microbiology*, vol. 24, no. 1, pp. 7–14, Feb. 2007, doi: 10.1016/j.fm.2006.04.006.
[143] R. Kumarathasan, A. B. Rajkumar, N. R. Hunter, and H. D. Gesser, “Autoxidation and yellowing of methyl linolenate,” *Progress in Lipid Research*, vol. 31, no. 2, pp. 109–126, 1992, doi: 10.1016/0163-7827(92)90005-4.
[144] T. Patrício and P. Bártolo, “Thermal Stability of PCL/PLA Blends Produced by Physical Blending Process,” *Procedia Engineering*, vol. 59, pp. 292–297, 2013, doi: 10.1016/j.proeng.2013.05.124.
[145] Q. Dou, C. Wang, C. Cheng, W. Han, P. C. Thüne, and W. Ming, “PDMS-Modified Polyurethane Films with Low Water Contact Angle Hysteresis,” *Macromolecular Chemistry and Physics*, vol. 207, no. 23, pp. 2170–2179, 2006, doi: https://doi.org/10.1002/macp.200600375.
[146] M. A. Eddings, M. A. Johnson, and B. K. Gale, “Determining the optimal PDMS–PDMS bonding technique for microfluidic devices,” *J. Micromech. Microeng.*, vol. 18, no. 6, p. 067001, Jun. 2008, doi: 10.1088/0960-1317/18/6/067001.
[147] M. H. Madsen, N. A. Feidenhans’l, P.-E. Hansen, J. Garnæs, and K. Dirscherl, “Accounting for PDMS shrinkage when replicating structures,” *J. Micromech. Microeng.*, vol. 24, no. 12, p. 127002, Dec. 2014, doi: 10.1088/0960-1317/24/12/127002.
[148] M. Á. Bonet-Aracil, P. Díaz-García, E. Bou-Belda, N. Sebastiá, A. Montoro, and R. Rodrigo, “UV protection from cotton fabrics dyed with different tea extracts,” *Dyes and Pigments*, vol. 134, pp. 448–452, Nov. 2016, doi: 10.1016/j.dyepig.2016.07.045.

[149] M. Shabbir, L. J. Rather, and F. Mohammad, “Economically viable UV-protective and antioxidant finishing of wool fabric dyed with Tagetes erecta flower extract: Valorization of marigold,” *Industrial Crops and Products*, vol. 119, pp. 277–282, Sep. 2018, doi: 10.1016/j.indcrop.2018.04.016.
[150] L. F. Zemljič, J. Volmajer, T. Ristić, M. Bracic, O. Sauperl, and T. Kreže, “Antimicrobial and antioxidant functionalization of viscose fabric using chitosan–curcumin formulations,” *Textile Research Journal*, vol. 84, no. 8, pp. 819–830, May 2014, doi: 10.1177/0040517513512396.
[151] A. I. Quilez-Molina, J. A. Heredia-Guerrero, A. Armirotti, U. C. Paul, A. Athanassiou, and I. S. Bayer, “Comparison of physicochemical, mechanical and antioxidant properties of polyvinyl alcohol films containing green tealeaves waste extracts and discarded balsamic vinegar,” *Food Packaging and Shelf Life*, vol. 23, p. 100445, Mar. 2020, doi: 10.1016/j.fpsl.2019.100445.
[152] A. I. Quilez-Molina, L. Marini, A. Athanassiou, and I. S. Bayer, “UV-Blocking, Transparent, and Antioxidant Polycyanoacrylate Films,” *Polymers*, vol. 12, no. 9, Art. no. 9, Sep. 2020, doi: 10.3390/polym12092011.
[153] V. Trovato, G. Rosace, C. Colleoni, S. Sfameni, V. Migani, and M. R. Plutino, “Sol-gel based coatings for the protection of cultural heritage textiles,” *IOP Conf. Ser.: Mater. Sci. Eng.*, vol. 777, p. 012007, May 2020, doi: 10.1088/1757-899X/777/1/012007.
[154] M. K. Trivedi, A. Branton, D. Trivedi, G. Nayak, R. Singh, and S. Jana, “Physicochemical and Spectroscopic Characterization of Biofield Treated Butylated Hydroxytoluene,” *Journal of Food & Industrial Microbiology*, vol. 1, no. 1, Oct. 2015, doi: 10.4172/jfim.1000101.
[155] T. Elzein, M. Nasser-Eddine, C. Delaite, S. Bistac, and P. Dumas, “FTIR study of polycaprolactone chain organization at interfaces,” *Journal of Colloid and Interface Science*, vol. 273, no. 2, pp. 381–387, May 2004, doi: 10.1016/j.jcis.2004.02.001.
[156] S. Sato, M. Suzuki, S. Kanehashi, and K. Nagai, “Permeability, diffusivity, and solubility of benzene vapor and water vapor in high free volume silicon- or fluorine-containing polymer membranes,” *Journal of Membrane Science*, vol. 360, no. 1–2, pp. 352–362, Sep. 2010, doi: 10.1016/j.memsci.2010.05.029.
[157] C. Kapridaki and P. Maravelaki-Kalaitzaki, “TiO2–SiO2–PDMS nano-composite hydrophobic coating with self-cleaning properties for marble protection,” *Progress in Organic Coatings*, vol. 76, no. 2–3, pp. 400–410, Feb. 2013, doi: 10.1016/j.porgcoat.2012.10.006.
[158] M. Contardi *et al.*, “Low molecular weight ε-caprolactone-p-coumaric acid copolymers as potential biomaterials for skin regeneration applications,” *PLoS One*, vol. 14, no. 4, Apr. 2019, doi: 10.1371/journal.pone.0214956.
[159] F. W. Billmeyer and M. Saltzman, *Principles of color technology.*, II. New York: J. Wiley & Sons, 1981.
[160] G. Wyszecki and W. S. Stiles, *Color science: Concepts and methods, quantitative data and formulas*, XIV. New York: Wiley, 1967.
[161] A. M. Grancarić *et al.*, “Enhancement of acid dyestuff salt-free fixation by a cationizing sol-gel based coating for cotton fabric,” *Colloids and Surfaces A: Physicochemical and Engineering Aspects*, vol. 612, p. 125984, Mar. 2021, doi: 10.1016/j.colsurfa.2020.125984.

[162] Y. Ocak, A. Sofuoglu, F. Tihminlioglu, and H. Böke, “Protection of marble surfaces by using biodegradable polymers as coating agent,” *Progress in Organic Coatings*, vol. 66, no. 3, pp. 213–220, Nov. 2009, doi: 10.1016/j.porgcoat.2009.07.007.
[163] B. Sundqvist and T. Morén, “The influence of wood polymers and extractives on wood colour induced by hydrothermal treatment,” *Holz als Roh- und Werkstoff*, vol. 60, no. 5, pp. 375–376, Oct. 2002, doi: 10.1007/s00107-002-0320-2.